NTNU
Norwegian University of
Science and Technology

# Design, Numerical Modelling and Analysis of a Semi-submersible Floater Supporting the DTU 10MW Wind Turbine.

**Md Touhidul Islam**

Marine Technology
Submission date: June 2016
Supervisor: Zhen Gao, IMT

Norwegian University of Science and Technology
Department of Marine Technology

Md Touhidul Islam

# Design, Numerical Modelling and Analysis of a Semi-submersible Floater Supporting the DTU 10MW Wind Turbine

Supervisor: Prof. Zhen Gao

Trondheim, June 2016

Norwegian University of Science and Technology
Faculty of Engineering Science and Technology
Department of Marine Technology

NTNU
Innovation and Creativity

**NTNU Trondheim**
**Norwegian University of Science and Technology**
*Department of Marine Technology – Group of Marine Structures*

**MSC THESIS IN MARINE TECHNOLOGY**

**SPRING 2016**

**FOR**

**STUD.TECHN. Md Touhidul Islam**

**Design, Numerical Modeling and Analysis of a Semi-submersible Floater Supporting the DTU 10MW wind turbine**

**Background:**
Wind industry develops very fast in recent years, moving from onshore to offshore in shallow water and then in deep water. Cost reduction is one of the main challenges for offshore wind turbines, in particular for floating concepts. One way to reduce the cost of energy is to use a larger wind turbine, absorbing more wind power. This can potentially reduce the installation and maintenance costs since these activities per wind turbine will be reduced considering the same rated power. DTU has developed a 10MW reference wind turbine, which will be used in this thesis work.

In the project work, the candidate has already made a preliminary design of a semi-submersible floater supporting the 10MW wind turbine. This design was achieved by upscaling the 5MW WindFloat concept that satisfied the basic design requirements on hydrostatic stability and dynamic properties of the floating wind turbine. In the thesis work, the candidate should proceed with the time-domain numerical model of the developed concept and perform dynamic response analysis for selected wind and wave conditions. Moreover, in the other two parallel thesis work, a spar and a TLP floater will be designed and the candidate should do a comparative study on the dynamic responses of these three concepts.

The student will be provided the following information, the DTU 10MW wind turbine design and the WindFloat design for the NREL 5MW wind turbine.

**Assignment:**
The following tasks should be addressed in the thesis work:

1. Literature review on floating concepts for wind turbines, design criteria and design methods, and numerical modeling and dynamic analysis of floating wind turbines. Literature review on design based on upscaling of wind turbines and floaters.

2. Finalize the design of the semi-submersible floater. According to the stability requirement, design properly the location of the connection point between the floater and the wind turbine tower, which is typically a bolted connection. Comment on the conflicting design requirements in stability and in dynamic performance.

3. Finalize the hydrodynamic analysis in HydroD, with the heaving plates modeled properly.

4. Establish the SRA (Simo-Riflex-AeroDyn) model including the aerodynamic and structural model of the DTU 10MW wind turbine and the developed floater. Perform basic test analyses (static analysis and decay test) to verify the numerical model. The SRA model of the wind turbine will be provided. But modifications are necessary for the application to this floater.

5. Perform time domain analysis for selected sea states. Post-process the results and produce the statistical and spectral results.

6. Compare the dynamic responses of the three concepts (Spar, TLP and Semi-submersible).

7. Report and conclude on the investigation.

In the thesis the candidate shall present his personal contribution to the resolution of problem within the scope of the thesis work.

Theories and conclusions should be based on mathematical derivations and/or logic reasoning identifying the various steps in the deduction.

The candidate should utilize the existing possibilities for obtaining relevant literature.

The thesis should be organized in a rational manner to give a clear exposition of results, assessments, and conclusions. The text should be brief and to the point, with a clear language. Telegraphic language should be avoided.

The thesis shall contain the following elements: A text defining the scope, preface, list of contents, summary, main body of thesis, conclusions with recommendations for further work, list of symbols and acronyms, reference and (optional) appendices. All figures, tables and equations shall be numerated.

The supervisor may require that the candidate, in an early stage of the work, present a written plan for the completion of the work. The plan should include a budget for the use of computer and laboratory resources that will be charged to the department. Overruns shall be reported to the supervisor.

The original contribution of the candidate and material taken from other sources shall be clearly defined. Work from other sources shall be properly referenced using an acknowledged referencing system.

The thesis shall be submitted electronically in DAIM:

- Signed by the candidate
- The text defining the scope included
- Codes, drawings and/or computer prints which cannot be bound should be organized in a separate folder.

Zhen Gao
Supervisors

Deadline: 28.6.2016

# Abstract

In recent years, the demand for renewable energy has increased significantly because of its lower environmental impact than conventional energy technologies. Wind power is one of the most important sources of renewable energy produced nowadays. As land based turbines have reached their maximum potential, recent market trends are moving into deeper waters with higher capacity turbines.

The design of a floating offshore wind turbine (FOWT) foundation poses few technical challenges. Floating stability, favourable motion characteristics and introduction of cost effective solutions to name a few. Moreover, as deep water offshore designs are still at an early stage of development, numerical modelling of the coupled dynamic behaviour also remains one of the key issues.

This work presents the design of a semi-submersible floater that can support the generic, publicly available DTU 10MW RWT. The design is developed from NREL 5MW WindFloat and verified with detail stability analysis in GHS, rigid body motions and wave frequency loads are calculated using Wadam. The interaction between wind loads on the pitch controlled rotor and motions of the floating structure are captured by coupled aero-hydro-servo-elastic simulations in Simo-Riflex-AeroDyn (SRA). Platform and turbine responses are compared against a Spar and TLP supporting the same wind turbine for identical environmental conditions.

Based on simulation results, it is found that the semi-submersible platform has satisfactory responses in different operational and in extreme wind condition. The design is proved to have the lowest displacement (and draft) compare to the Spar and TLP which will allow the semi-submersible platform to employ equally in intermediate and deep water offshore.

# Acknowledgement

First of all, I would like to thank my supervisor, Prof. Zhen Gao with his guidance, care and supervision for the thesis work throughout the semester. The thesis work has finished within the stipulated time because of his careful planning of regular meetings. Prof. Gao shared a wealth of knowledge during discussions and his perspectives have always provided valuable input to the thesis work. At any time, if I am diverting from my course, He always points me to the right direction.

A very sincere thanks shall also be given to Mr. Chenyu Luan, PhD candidate at CeSOS, NTNU and co-supervisor of the thesis work. Especially with his guidance regarding Sesam GeniE, HydroD and NREL Turbsim software packages. A heartfelt thanks shall also be given to Dr. Erin Bachynski, Associate Professor at Department of Marine Technology in NTNU for her guidance regarding coupled numerical modelling in Simo-Riflex-AeroDyn. She was always there when her advice is needed. I would like to give my warmest thanks to Mr. Qiang Wang, MSc who generously answered all of my queries regarding floating wind turbine.

I am indebted to Mr. Muhammad Sirajul Islam, Naval Architect and Chairman of SST Marine Solutions Ltd., Bangladesh for allowing me to use their licensed copy of GHS (naval architectural software package) for stability calculations in my master thesis. I would also like to thank my classmates Wenfei Xue and Xiaoshuang Tian for sharing their ideas and comments during the thesis works.

I am very fortunate for the inspiration from my beloved wife, Jinnat and son, Junaid. It would be impossible to finish my master's education without their understanding, continuous support and unconditional love!

Trondheim, Norway
June 2016

Md Touhidul Islam

# Nomenclature

## Latin Symbols

| Symbol | Description |
|---|---|
| $a, a'$ | axial and rotational induction factor |
| $a_c$ | column centre to centre distance |
| $\mathbf{A}$ | added mass matrix |
| $\mathbf{A}(\omega)$ | frequency dependent part of added mass matrix |
| $A_w$ | water plane area |
| $\mathbf{B}$ | potential Damping matrix |
| $c$ | chord of an airfoil section |
| $\mathbf{C}$ | restoring matrix |
| $C_D$ | drag coefficient |
| $C_h$ | height coefficient |
| $C_l$ | lift coefficient |
| $C_n$ | normal force coefficient |
| $C_s$ | shape coefficient |
| $C_t$ | tangential force coefficient |
| $D$ | column diameter |
| $f$ | freeboard |
| $f_L$ | lift loads |
| $f_D$ | drag loads |
| $\overline{F}$ | mean drift force |
| $\mathbf{F}$ | force vector |
| $F^{FK}$ | froude-Krylov force |
| $F^D$ | diffraction forces |
| $g$ | acceleration due to gravity |
| $\mathbf{G}$ | centre of gravity |
| $\overline{GM}_L$ | longitudinal metacentric height |
| $\overline{GM}_T$ | transverse metacentric height |
| $h$ | water depth |
| $h(\tau)$ | retardation function |
| $H$ | column height |
| $k$ | wave number |

| | |
|---|---|
| $l$ | total length of mooring line |
| $l_{min}$ | minimum length of mooring line |
| $m$ | platform mass |
| $\mathbf{M}$ | mass matrix |
| $M_o$ | overturning moment on the platform |
| $M_y$ | bending moment about $y-$axis |
| $M_z$ | bending moment about $z-$axis |
| $\mathbf{n}$ | normal vector pointing toward fluid |
| $p$ | pressure |
| $r$ | radial distance along a blade |
| $R$ | rotor radius |
| $sd$ | standard deviation |
| $sf$ | scaling factor |
| $S_{0B}$ | mean wetted body surface |
| $S_B$ | instantaneous wetted body surface |
| $t_{eq}$ | equivalent thickness of plating |
| $T$ | tension along mooring lines |
| $T_c$ | draft of the platform |
| $T_d$ | damped period of oscillation |
| $T_H$ | horizontal tension in mooring lines |
| $T_n$ | natural period of oscillation |
| $T_R$ | rated thrust from turbine |
| $U_w$ | wind velocity at hub height |
| $\mathbf{V}$ | fluid velocity vector |
| $\mathbf{V_B}$ | body velocity |
| $V_{rel}$ | relative velocity |
| $w$ | unit weight of mooring line in water |
| $x$ | horizontal scope of mooring lines |
| $(x_b, y_b, z_b)$ | coordinate of centre of buoyancy |
| $(x_g, y_g, z_g)$ | coordinate of centre of gravity |
| $\mathbf{X}$ | horizontal distance between fairlead and anchor |

## Greek Symbols

| Symbol | Description |
|---|---|
| $\alpha$ | angle of attack |
| $\delta$ | logarithmic decrement |
| $\Delta$ | displaced in ton |
| $\boldsymbol{\eta}$ | body displacement vector |
| $\dot{\boldsymbol{\eta}}$ | body velocity vector |
| $\ddot{\boldsymbol{\eta}}$ | body acceleration vector |
| $\forall$ | displaced volume in $m^3$ |
| $\lambda$ | wave length |
| $\omega$ | angular velocity |
| $\omega_n$ | eigenfrequecy of a system |
| $\phi$ | inflow angle |

| | |
|---|---|
| $\varrho_w$ | density of sea water |
| $\varrho_a$ | density of air |
| $\sigma$ | solidity ratio |
| $\sigma_b$ | bending stress |
| $\theta$ | twist angle |
| $\zeta$ | damping ratio |

## Abbreviations

| | |
|---|---|
| 1P | Rotational frequency of turbine blade |
| 3P | Blade passing frequency for a three (3) bladed wind turbine |
| AOA | Angle of attack |
| ADAMS | Automatic Dynamic Analysis of Mechanical Systems (MSC software) |
| BEM | Blade Element Momentum |
| BM | Bending moment |
| CAE | Computer Aided Engineering |
| COB | Centre of buoyancy |
| COF | Centre of floatation |
| COG | Centre of gravity |
| CM | Centre of mass |
| DNV | Det Norske Veritas |
| dof | Degree of freedom |
| DOS | Disk Operating System |
| DTU | Technical University of Denmark |
| FAST | Fatigue, Aerodynamics, Sturctures and Turbulence |
| FEM | Finite element method |
| FF | Full field |
| FFT | Fast Fourier Transform |
| FOWT | Floating offshore wind turbine |
| GDW | Generalized dynamic wake |
| GL | Germanischer Lloyd |
| GM | Metacentric height |
| HAWC2 | Horizontal Axis Wind turbine simulation Code 2nd generation |
| HAWT | Horizontal axis wind turbine |
| HH | Hub height |
| JOHNSWAP | Joint North Sea Wave Project |
| LSS | Low speed shaft |
| NREL | National Renewable Energy Laboratory |
| QTF | Quadratic transfer function |
| RAO | Response amplitude operator |
| rpm | Revolutions per minute |
| RWT | Reference wind turbine |
| SRA | Simo-Riflex-AeroDyn |
| SWL | Still water level |
| TLP | Tension leg platform |
| TPC | Ton per centimeter immersion |

| | |
|---|---|
| ULS | Ultimate limit state |
| VAWT | Vertical axis wind turbine |
| VCB | Vertical centre of buoyancy |
| VCG | Vertical centre of gravity |

# Contents

# List of Tables

# List of Figures

# Chapter 1

# Introduction

The available power in a stream of wind varies to the third power of its speed. As offshore locations have strong and steady ocean winds in comparison to onshore locations, are more attractive in terms of wind power generation. Besides numerous technical challenges, cost reduction is one of the key issue for the offshore wind turbines. One way to reduce the cost of energy is to use a larger wind turbine to harness more wind power.

To support a floating offshore wind turbine, designing an efficient foundation is of utmost importance in order to make the offshore wind energy more competitive. Although, floating platforms are used with greater success in offshore oil and gas industry, but the same design cannot be used directly to support the floating wind turbines. For example, the weight supported by a floating platform in oil and gas industry are much higher than the weight it has to support for a offshore wind turbine. Moreover, wind turbines are highly dynamic systems with strong coupling effects due to imposed dynamic loading from environment. So, responses of a floating wind turbine will be much more complex than typical oil and gas platforms.

## 1.1 Floating offshore wind turbine concept

It is possible to design several types of floating platform which can support a wind turbine in offshore environment. These floating foundations shall be sufficiently stable while supporting a larger mass ($> 1000$ ton) with relatively high ($\sim 100$ m) centre of gravity. They can be classified based on their achievement of static stability, tanks and ballast arrangement and last but not the least mooring arrangement. Solutions of this problem fall into three (3) categories:

1. A deep draft Spar that obtains its restoring in pitch entirely by ballast.
2. Semi-submersible platform which achieves its stability by a combination of ballast and water plane stiffness.
3. TLP, (buoyancy is greater than displacement) obtains the pitch restoring moment from tension in tethers.

Figure 1.1 presents the three (3) Floating Offshore Wind Turbine (FOWT) concepts, Spar (left), Semi-submersible (middle) and TLP (right) with their relative draft and necessary mooring arrangement.

**Figure 1.1:** Floating offshore wind turbine concepts.
(DNV GL - Energy)

The use of semi-submersibles as the floating foundation for offshore wind turbine was proposed independently by Fulton and Zambrano [1]. But WindFloat type semi-submersible design was presented by Fulton. Figure 1.2 represents the concept design of the semi-submersible platform which will be designed to support the DTU 10MW RWT.

**Figure 1.2:** Concept design of the semi-submersible platform for the DTU 10MW RWT.

The initial design of the semi-submersible concept will be based on upscaling of NREL 5MW WindFloat [1]. Hence it is appropriate to describe the scaling procedure.

## 1.2 Upscaling of wind turbine and floater

The purpose is to design a semi-submersible floater that can support the DTU 10MW RWT. The scaling law considered for rotor and floater are different.

### 1.2.1 Scaling of wind turbine rotor

The scaling procedure of the DTU 10MW RWT is described by Bak et al. [2]. The DTU 10MW rotor is upscaled from NREL 5MW reference turbine [3] by applying classical similarity rules which is based on the assumptions of geometrical similarities. In simple words, if we doubled the swept area of the rotor, the power output will also be doubled. Thus, the geometrical scaling factor, $sf = \sqrt{(10/5)} = \sqrt{2}$. The upscaling factor is not applied for the blades. Turbine blades are designed to check the computational tools and designed methods. They are neither lightest nor the best performing rotor. Scaling factors of various rotor parameters are listed in Table 1.1.

**Table 1.1:** Scaling of rotor parameter.

| Design parameter | Scaling factor |
|---|---|
| Linear dimensions<br>(rotor diameter, blade length and chord length etc.) | $sf$ |
| Rated power | $sf^2$ |
| Thrust force at rated wind | $sf^2$ |
| Rotor mass | $sf^3$ |
| Moment of inertia of blade | $sf^5$ |
| Bending stiffness of blade | $sf^4$ |
| Natural periods of blade bending modes | $\sqrt{sf}$ |

### 1.2.2 Scaling of semi-submersible floater

The same geometrical scaling factor, $sf = \sqrt{2}$ is used for upscaling the floater and for hydrodynamic loads and induced responses Froude scaling law is used.

#### Stability requirements

The overturning moment due to the thrust is scaled by $sf^3$ and is given by $M_o = T_R * L$. Where $L$ is the vertical distance between rotation centre to the centre of buoyancy (COB). Therefore, the righting moment can be scaled by $sf^4$.

$$\begin{aligned} M_R &= \varrho_w g \forall \overline{GZ} \\ &= \varrho_w g \forall \overline{GM} \sin(\theta) \\ &= \varrho_w g \forall \overline{BM}\ \theta \\ &= \varrho_w g I \theta \end{aligned} \tag{1.1}$$

#### Hydrodynamic performance

The Froude scaling law is considered for hydrodynamic loads and their effects. A summary of scaling factors for the floating platform is shown in Table 1.2.

## 1.3 Numerical modelling and dynamic analysis of FOWT

Tools for developing numerical model of FOWT are studied extensively by Kvittem [4] and Jonkman, [5]. It is found that the numerical tools for dynamic analysis of FOWT are originated

**Table 1.2:** Scaling of floater parameters.

| Design parameter | Scaling factor |
|---|---|
| Linear dimensions (diameter and height of columns, plate thickness etc.) | $sf$ |
| Mass and displacement | $sf^3$ |
| Moment of inertia | $sf^5$ |
| Natural period of rigid body motion (heave, roll and pitch) | $\sqrt{sf}$ |
| Force | $sf^3$ |
| Righting moment | $sf^4$ |
| Stress | $sf$ |

either from fixed, land based wind turbine codes (FAST and HAWC2) or from offshore structural analysis software (Simo-Riflex-Aerodyn). Description about the software are discussed below:

### 1.3.1 Tools for coupled dynamic analysis

#### FAST

FAST [6] is a open source, state-of-the-art, computer aided engineering (CAE) tool developed by National Renewable Energy Laboratory (NREL) for aero-hydro-servo-elastic coupled simulation in the time domain. It can be used for the analysis of a wide range of wind turbine configurations. FAST can only be used for horizontal axis wind turbines (HAWT).

FAST uses AeroDyn [7] and HydroDyn [8] to calculate aerodynamic and hydrodynamic loadings on FOWT in the time domain. A typical flowchart in FAST among external loads, applied loads and wind turbine control are presented in Figure 1.3.

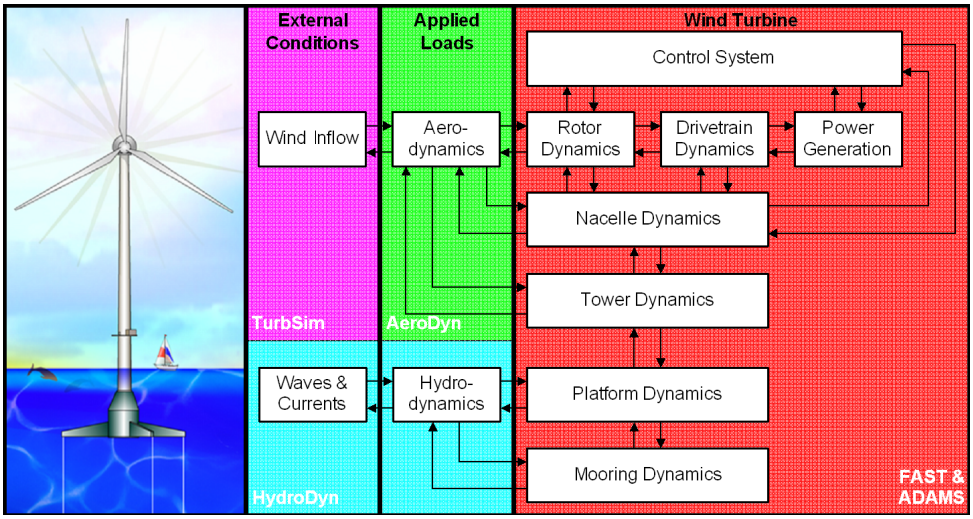


**Figure 1.3:** Interface between the modules in the FAST code for FOWT. (Jonkman [5])

### HAWC2

HAWC2 [9] is an aeroelastic code used for the calculation of wind turbine responses in the time domain. It is a standalone, proprietary (closed source) code developed and marketed by DTU Wind Energy. In addition to HAWT, HAWC2 can be used for dynamic analysis of vertical axis wind turbine (VAWT).

The code use its own aerodynamic codes based on blade element momentum theory (BEM). Structures are modeled using finite element beam formulations. Hydrodynamic model is based on Morison equation, WAMIT or McCamy & Fuchs. Shallow water hydrodynamics can be taken into account as the code accounts for stream function wave. Pre-generated wave kinematics can be used as input too.

### Simo-Riflex-AeroDyn

Simo-Riflex is a proprietary, closed source, coupled simulation code developed by MARINTEK when combined with AeroDyn, creates a powerful platform for coupled dynamic analysis of fixed or floating wind turbines. It can be used to read TurbSim [10] wind input files and user defined external control logic.

SIMO [11] is a computer program for simulation of motions and station-keeping behaviour of a complex system of floating vessels and suspended loads.

Riflex [12] is a riser system analysis program but it has the capability to conduct static and dynamic analysis of slender marine structures. Finite element formulation in Riflex are based on non-linear beam model and allow large displacement and large rotations.

For coupled dynamic analysis of the semi-submersible platform, Simo-Riflex-AeroDyn (SRA) is used extensively. An overview of numerical modelling and coupled dynamic analysis is presented in chapter 6 (see Figure 6.1).

## 1.4 Scope

The purpose of this thesis is to design a semi-submersible floater which can support the DTU 10MW RWT. The thesis work is divided into two parts: design and analysis. Design refers to the initial design of the floater and preliminary design of the mooring system. Analysis includes numerical modelling and coupled time domain simulations. The report is organized as follows:

**Chapter 1** introduces the background of offshore wind energy, different floating wind turbine concepts, upscaling method, code review of coupled dynamic analysis software.

**Chapter 2** describes aerodynamic (BEM) theory, linear hydrodynamic theory, second-order (drift forces) hydrodynamics, non-linear finite element formulations of beam element and coupled dynamic analysis.

**Chapter 3** presents design data comparison, floater upscaling and initial design calculation.

**Chapter 4** deals with modification of the tower, estimation of lightship and wind heeling moment, stability requirements accompanied with detail stability analysis.

**Chapter 5** compares the effect of circular and hexagonal heave plates, analysis of rigid body motions and frequency domain hydrodynamic analysis.

**Chapter 6** describes coupled numerical modelling in Simo-Riflex-Aerodyn (SRA).

**Chapter 7** discusses catenary theory, mooring configuration and preliminary design of the catenary spread mooring system.

**Chapter 8** numerical model of the platform and turbine are verified by free decay test and constant wind test. Coupled time domain simulation have been performed to determine the response characteristic of the platform and turbine.

**Chapter 9** compare dynamic responses of three (3) FOWT concepts, namely Spar, Semi-submersible and TLP.

**Chapter 10** Conclusions about the thesis work and recommendations for future study.

**NOTE:** work presented in **Chapter 3** is taken from the master project work (TMR4500: Marine Structures, Specialization Project). It has to be there for completeness of the report.

# Chapter 2

# Theory

Wind turbines convert the kinetic energy in the wind into usable form of energy, for example, electricity. When a stream of wind passes through the blades of a rotor, it generates lift force in the rotor plane and introduce spin in a low speed shaft. The shaft is connected to a generator by means of gear mechanisms which can increase the rotational speed of the generator shaft and thus generates electricity. Although, there are many concepts of wind turbines, all of them are based on different energy extraction principles.

## 2.1 Aerodynamics of wind turbine

Aerodynamic computation models for wind turbines are found from 1D Blade Element Momentum theory (BEM) to 3D Navier-Stokes solutions. The simplest yet widely used theory applicable to Horizontal Axis Wind Turbine (HAWT) is the BEM. Any elementary aerodynamic text book, for example, Hansen [13] describes a detail derivation of BEM theory. Almost all coupled dynamic simulation software (see section 1.3) uses BEM to compute the aerodynamic loads on the wind wind turbine including tower.

### 2.1.1 Blade Element Momentum theory

Blade element momentum (BEM) theory combines both the blade element theory and momentum theory. However, BEM model is based on following assumptions:

- no interaction is considered between annuli.
- force from the blades on the flow is constant in each annular element which means infinite number of blades in the rotor plane.

Figure 2.1 shows in an annular ring of width $\delta r$ at a radial distance $r$ from rotor centre. Now we may begin writing the equation of thrust and torque for the annular ring based on momentum theory:

$$dT = 4a(1-a)\frac{1}{2}\varrho_a v_0^2 2\pi r dr \tag{2.1}$$

$$dQ = 4a'(1-a)\frac{1}{2}\varrho_a v_0 \Omega r^2 2\pi r dr \tag{2.2}$$

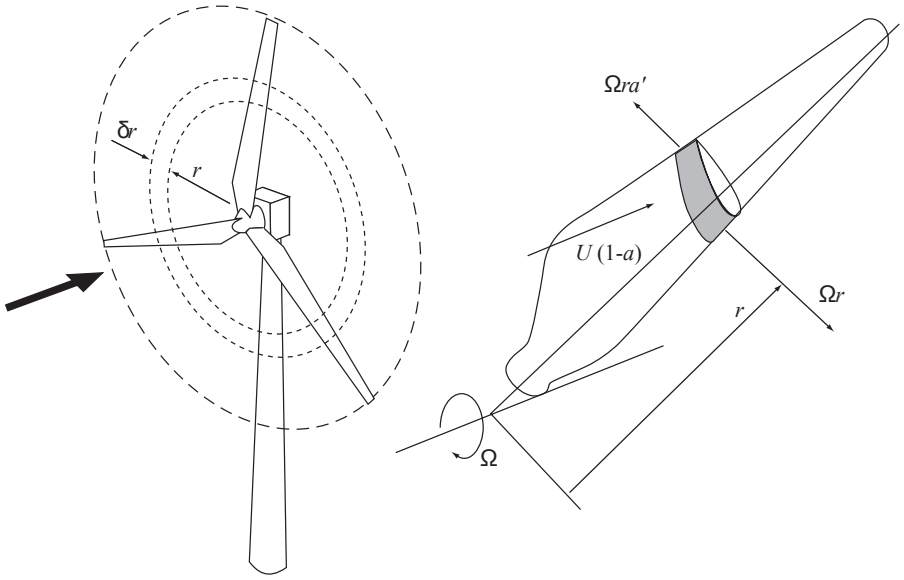


**Figure 2.1:** Blade element momentum. (Burton et al. [14, p. 60])

Let us consider an airfoil section as shown in Figure 2.2. Forces normal and tangential to the rotor plane can be identified as $p_N$ and $p_T$ respectively. The inflow velocity $V_{rel}$ includes the incoming wind, the velocity of the blade due to rotor rotation, induced axial and tangential velocity. The angle $\phi$ accounts for the angle of attack, $\alpha$ and the blade pitch angle. The blade pitch angle can results from the actual blade pitch and twist in the geometry.

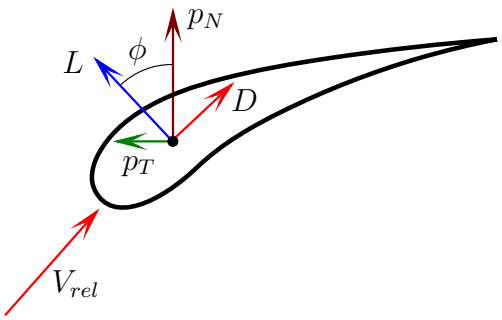


**Figure 2.2:** Airfoil section in the rotor plane with aerodynamic forces.
(redrawn from [15])

Using trigonometry, it is straightforward to establish the following relationship:

$$p_N = L\cos\phi + D\sin\phi \tag{2.3}$$
$$dT = Bp_N dr \tag{2.4}$$
$$dT = B(L\cos\phi + D\sin\phi)dr \tag{2.5}$$

Where, $B$ is the number of blades. The normal coefficient, $C_n$ and solidity ratio, $\sigma$ can be introduced as:

$$C_n = C_l \cos\phi + C_d \sin\phi \tag{2.6}$$

$$\sigma = \frac{Bc}{2\pi r} \tag{2.7}$$

By combining equation Equation 2.1 and Equation 2.5, it is possible to obtain an expression for axial induction factor, $a$ :

$$a = \left[1 + \frac{4\sin^2\phi}{\sigma C_n}\right]^{-1} \tag{2.8}$$

A similar approach can be used for torque to obtain an expression for rotational induction factor, $a'$:

$$dQ = 4a'(1-a)\frac{1}{2}\varrho_a v_0 \Omega r^2 2\pi r dr \tag{2.9}$$

$$dQ = Brp_T dr = Br(L\sin\phi - D\cos\phi)dr \tag{2.10}$$

$$C_t = C_l \sin\phi - C_d \cos\phi \tag{2.11}$$

$$a' = \left[1 + \frac{4\sin\phi\cos\phi}{\sigma C_t}\right]^{-1} \tag{2.12}$$

An iterative solution technique is required to find the value of axial induction factor, $a$ (see Equation 2.8) and rotational induction factor, $a'$ (see Equation 2.12) involve following steps:

1. guess starting values of $a$ and $a'$
2. calculate $\phi$ and consequently $\alpha$, $C_l$ and $C_d$
3. update $a$ and $a'$ using Equation 2.8 and Equation 2.12
4. check for convergence within a given tolerance, if convergence criteria is not fulfilled, the steps will be repeated.

### 2.1.2 Prandtl correction

In reality, due to finite number of blades, air tends to flow around the tip of a blade from lower to upper side (follow pressure gradient) which introduce a rotation in the wake. As a result, there is a net loss in the aerodynamic forces also known as Prandtl's tip loss correction factor. The correction factor is taken into account by Equation 2.13

$$F = \frac{2}{\pi}\cos^{-1}\left[\exp\left(-\frac{B(1-r/R)}{2r\sin(\phi)/R}\right)\right] \tag{2.13}$$

### 2.1.3 Glauert correction

BEM theory is not valid for values of induction factor greater than 0.5, since the wind velocity in the far wake would be negative. This is solved by Glauert correction factor. For values of $a > 0.4$ Glauert correction can be taken into account by using Equation 2.14 which is recommended by Burton et al. [14].

$$a = \frac{(C_T/F - C_{T1})}{C_{T2} - C_{T1}}(a_2 - a_1) + a_1 \tag{2.14}$$

## 2.2 Linear hydrodynamics

In order to evaluate sea loads and motions on the platform, linear hydrodynamic theory is used. By linear theory we mean the response of the floater will be proportional to the excitation at the same frequency but a phase difference between them.

### 2.2.1 Governing equations

Free surface fluid flow is based on potential theory. In potential theory, flow is assumed to be incompressible, inviscid (frictionless) and irrotational. Incompressible flow ensures that fluid particle will satisfy Equation 2.16 which in turn forces velocity potential to satisfy the Laplace equation (Equation 2.18). These assumptions in combination with linear wave theory gives a body interaction problem, when solved, the velocity potential $\phi$ is obtained. It is a continuous function of space and time i.e. $\phi = f(x, y, z, t)$ which satisfies the basic laws of fluid mechanics: conservation of mass and momentum. A velocity potential $\phi$ can be used to describe the fluid velocity vector $\mathbf{V}(x, y, z, t) = (u, v, w)$ at any instant $t$ at a particular point $\mathbf{X} = (x, y, z)$ in a Cartesian coordinate system, fixed in space. Fluid particle velocity components at any instant can be obtained by:

$$u = \frac{\partial \phi}{\partial x},\ v = \frac{\partial \phi}{\partial y},\ w = \frac{\partial \phi}{\partial z} \tag{2.15}$$

Governing equations are as follows:

$$\boldsymbol{\nabla} \cdot \mathbf{V} = 0 \tag{2.16}$$

The fluid is irrotational when the vorticity vector $\boldsymbol{\omega} = 0$ every where in fluid domain $\Omega_0$

$$\boldsymbol{\omega} = \boldsymbol{\nabla} \times \mathbf{V} \tag{2.17}$$

Laplace equation (in $\Omega_0$):

$$\frac{\partial^2 \phi}{\partial x^2} + \frac{\partial^2 \phi}{\partial y^2} + \frac{\partial^2 \phi}{\partial z^2} = \boldsymbol{\nabla}^2 \phi = 0 \tag{2.18}$$

Sea bottom boundary condition (on $S_{SB}$):

$$\frac{\partial \phi}{\partial n} = 0 \tag{2.19}$$

Body boundary condition (on $S_{0B}$):

$$\frac{\partial \phi}{\partial n} = \boldsymbol{V_B n} \tag{2.20}$$

Combined free surface condition:

$$\frac{\partial^2 \phi}{\partial t^2} + g\frac{\partial \phi}{\partial z} = 0 \tag{2.21}$$

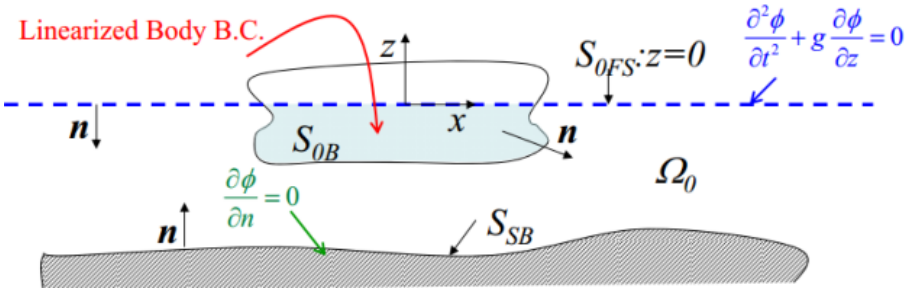


**Figure 2.3:** Kinematic boundary conditions in linear wave theory. [16]

### 2.2.2 The equations of motions

The equations of rigid body motions for a floating body can be written as:

$$\sum_{k=1}^{k=6}[(M_{jk} + A_{jk})\ddot{\eta}_k + B_{jk}\dot{\eta}_k + C_{jk}\eta_k] = F_j e^{-i\omega_e t} \quad (j = 1, \ldots, 6) \tag{2.22}$$

In matrix form Equation 2.22 can be written as:

$$[\mathbf{M} + \mathbf{A}(\omega)]\,\ddot{\boldsymbol{\eta}} + \mathbf{B}(\omega)\dot{\boldsymbol{\eta}} + \mathbf{C}(\omega)\boldsymbol{\eta} = \mathbf{F}(\omega) \tag{2.23}$$

### 2.2.3 Eigenvalue analysis

For eigenvalue problems, there is no external force or moments acting on the body ($\mathbf{F} = 0$) and no damping ($\mathbf{B} = 0$). So, Equation 2.23 can be written in following form:

$$\left[-\omega^2(\mathbf{M} + \mathbf{A}(\omega)) + \mathbf{C}(\omega)\right]\boldsymbol{\eta_a} = 0 \tag{2.24}$$

Non-trivial solution of Equation 2.24 can be obtained by setting

$$det\left[-\omega^2(\mathbf{M}+\mathbf{A}(\omega))+\mathbf{C}\right]=0 \tag{2.25}$$

Thus, explicit expression for natural period of rigid body motion of the platform can be obtained from Equation 2.26. No coupling is considered between motions ($i = j$).

$$T_{nj}=2\pi\left(\frac{M_{jj}+A_{jj}(\omega)}{C_{jj}}\right)^{\frac{1}{2}} \quad (j=1,\ldots,6) \tag{2.26}$$

Natural periods in heave, roll and pitch of the platform can be found from Equation 2.27, Equation 2.28 and Equation 2.29 respectively.

$$T_{n3}=2\pi\left(\frac{M+A_{33}}{\varrho_w g A_w}\right)^{\frac{1}{2}} \tag{2.27}$$

$$T_{n4}=2\pi\left(\frac{Mr_{44}^2+A_{44}}{\varrho_w g\forall\overline{GM_T}}\right)^{\frac{1}{2}} \tag{2.28}$$

$$T_{n5}=2\pi\left(\frac{Mr_{55}^2+A_{55}}{\varrho_w g\forall\overline{GM_L}}\right)^{\frac{1}{2}} \tag{2.29}$$

### 2.2.4 Viscous damping

The damping term, $\mathbf{B}(\omega)$ in Equation 2.23 includes only potential or radiation damping, associated with the wave generation ability of the body. For long waves, the generation of wave from body-structure interaction is negligible, which means that the potential damping associated with long waves can be ignored. For the case of large amplification of motion may be expected at resonance the viscous forces will become important.

One of the main sources of viscous damping is the drag force, acting on the structure which is neglected in potential theory. The drag force on the slender structures, for instance, columns of the semi-submersible platform can be taken into account by using Morison's equation. The drag force for a fixed cylinder with a diameter, $D$ can be written as:

$$dF_{drag}=\frac{1}{2}\varrho_w C_D D(u-\dot{\eta})\,|u-\dot{\eta}| \tag{2.30}$$

It can be seen from Equation 2.30 that the drag force is a quadratic function of the relative velocity of the wave particle ($u$) and the structure ($\dot{\eta}$). Therefore, quadratic drag force shall be linearized so that it can be added to linear frequency domain Analysis.

The viscous damping coefficient from linearized drag force can be taken into account by Equation 2.31.

$$B_v=\frac{4\varrho_w C_D D A}{3\pi} \tag{2.31}$$

## 2.3 Second-order hydrodynamics

Frequency domain representation of a wave is considered as the resultant of $N$ components of different circular frequencies and phases. As second order theory allowed each component to interact with others, loads result from second-order theory may excite with following three (3) frequencies:

- sum-frequency ($2\omega_j$, $2\omega_k$ and $(\omega_j + \omega_k)$) loads
- difference-frequency ($|\omega_j - \omega_k|$) loads
- mean (wave) drift loads

For the semi-submersible platform, drift forces are taken into account by means of Newman's approximation which only requires first order solutions. The transfer functions can be computed using Equation 2.32a.

$$T_{jk}^{ic} = T_{kj}^{ic} = \frac{1}{2}\left(T_{jj}^{ic} + T_{kk}^{ic}\right) \tag{2.32a}$$

$$T_{jk}^{is} = T_{kj}^{is} = 0 \tag{2.32b}$$

The second-order force $\mathbf{F}^{(2)}$ integrates the pressure from sea floor to the instantaneous wave elevation, proportional to the square of the wave amplitudes. Second order wave-excitation forces are responsible for producing significant slow-drift motion of the platform.

The effect of second-order hydrodynamics on FOWT (Spar and TLP only) are studied by Roald et al. [17] and suggest that the effect of second-order hydrodynamics is relatively small on Spar as sum and difference frequency responses are largely dependent on turbine aerodynamics. But for TLP, the effect of second-order hydrodynamics are relatively large with response in heave dominated by sum-frequency effect.

Recent study on Semi-submersible platform shows second-order loads dominate the response or at least same order of magnitude of the first-order wave loads [18]. Second-order wave loads become important for low wind conditions [18].

## 2.4 Non-linear FEM

Finite Element Analysis (FEM) is a numerical solution technique largely adopted in the field of structural mechanics. Using FEM, strong form (differential equation) formulations of a problem is approximated and solved using weak form construction. Weak form method uses three (3) principles: equilibrium, compatibility (strain-displacement relationship) and material law (Hook's law). It satisfies the equilibrium in an average sense.

Non-linear FEM refers to the solution methods that take the effects of large displacements, large rotations, non-linear material behaviour and change of boundary conditions into account. In FOWT, the non-linearities are related to the effects of large displacements and higher order load formulations from thrust and drag. Thus, both geometric and material non-linearity shall be taken into account.

The non-linear equation for dynamic equilibrium of a system of finite elements can be expressed by global matrices that contain the mass, damping and stiffness properties of the finite elements. External forces like buoyancy, weight, eccentricity and prescribed displacements shall be considered.

The non-linear FEM equilibrium equation (Equation 2.33) is discussed detail in [12].

$$\left(\mathbf{M}^H + \mathbf{M}^S\right)\ddot{\boldsymbol{r}}(t) + \mathbf{C}^S\dot{\boldsymbol{r}}(t) + \mathbf{K}(\boldsymbol{r})\boldsymbol{r}(\boldsymbol{t}) = \mathbf{R}^{ext}\left(\dot{\boldsymbol{r}}(t), \boldsymbol{r}(t)\right) \tag{2.33}$$

Geometric non-linearities are associated with large deflection of the blades and in mooring lines. The non-linear dynamic solver applies implicit integration for each time increment. Newmark-$\beta$ method is used to find the dynamic equilibrium at every time steps. This displacement driven method allows unlimited displacements and rotations but assumes small strains.

## 2.5 Coupled dynamic analysis

### 2.5.1 Equation of motion in time domain

According to potential theory, the frequency domain equation of motion for a rigid body submerged in fluid can be expressed using Equation 2.34 [19]

$$\left(\mathbf{M} + \mathbf{A}(\omega)\right)\ddot{\boldsymbol{\eta}}(\omega) + \mathbf{B}(\omega)\dot{\boldsymbol{\eta}}(\omega) + \mathbf{C}(\omega)\boldsymbol{\eta}(\omega) = \mathbf{F}(\omega) \tag{2.34}$$

Where, $\mathbf{F}(\omega)$ can represent environmental forces, mooring forces or other external forces.

For a non-linear system, solution of the equation of motion have to be solved by iterative procedure in the time domain. Equation 2.34 can be transformed into a non-linear time domain model Equation 2.35 by using the Cummins equation, which introduces a convolution integral (Duhamel integral), known as retardation function (see subsection 6.1.5).

$$\left(\mathbf{M} + \mathbf{A}_\infty\right)\ddot{\boldsymbol{\eta}}(t) + \int_0^\infty h(t-\tau)\dot{\eta}(t) + \mathbf{C}\boldsymbol{\eta}(t) = \boldsymbol{F}(t) \tag{2.35}$$

$\mathbf{F}$(t) in Equation 2.35 can be expressed as the sum of environmental forces (wind and wave), non-linear restoring, inertia and damping from the mooring lines and inertia and damping forces from the turbine.

$$\mathbf{F}(t) = \mathbf{F}^{(1)} + \mathbf{F}^{(2)} + \mathbf{F}^{drag}(t) + \mathbf{F}^{mooring}(t) + \mathbf{F}^{wind}(t) \tag{2.36}$$

All forces are functions of motions (restoring), velocities (damping), acceleration (inertia) of the platform and time.

### 2.5.2 Solution procedure

The first order wave excitation loads $\mathbf{F}^{(1)}$ can be found from radiation-diffraction analysis based on Panel Method in Wadam. The second order wave loads $\mathbf{F}^{(2)}$ can also be obtained using Wadam by solving the QTF functions with a free surface model which has not taken into account for the semi-submersible platform.

For time domain simulation, these wave loads are transformed into first order and second order transfer functions in Simo. The non-linear quadratic drag forces are taken into account by using Morison equation. The relative velocity of water particles and the platform motion are considered for calculating the viscous forces. Mooring line forces and aerodynamic forces are taken into account using Riflex and AeroDyn.

The solution of Equation 2.35 is based on an incremental procedure using the dynamic time integration algorithm. The Newton-Raphson iteration is used to achieve equilibrium at every time steps between external and internal forces. The coupling of Simo, Riflex and AeroDyn in the integrated dynamic analysis is discussed in chapter 6.

# Chapter 3

# Design data comparison, upscaling and initial design of the platform

A detail comparison of various rotor parameters between NREL 5MW and DTU 10MW RWT is presented in Table 3.1. The values of parameters are collected from [3] and [2] respectively.

**Table 3.1:** Design data comparison of the NREL 5MW and DTU 10MW wind turbine.

| Parameter | NREL 5MW | DTU 10MW RWT |
|---|---|---|
| Wind regime | IEC Class 1B | IEC Class 1A |
| Rotor orientation | Clockwise, upwind | Clockwise, upwind |
| Control | Variable speed, collective pitch | Variable speed, collective pitch |
| Cut-in wind speed | 3 m/s | 4.0 m/s |
| Cut-out wind speed | 25 m/s | 25 m/s |
| Rated wind speed | 11.4 m/s | 11.4 m/s |
| Rated power | 5 MW | 10 MW |
| Rated thrust | 750 kN | 1500 kN |
| Number of blades | 3 | 3 |
| Rotor diameter, Hub diameter | 126 m, 3 m | 178.3 m, 5.6 m |
| Hub height | 90 m | 119 m |
| Drivetrain | High speed | Medium speed |
| Cut-in, Rated rotor speed | 6.9 rpm, 12.1 rpm | 6 rpm, 9.6 rpm |
| Rated generator speed | 1173.7 rpm | 480.0 rpm |
| Gearbox ratio | 97 : 1 | 50 : 1 |
| Rated tip speed | 80 m/s | 90 m/s |
| Hub overhang, Shaft tilt, Precone | 5.0 m, $5^{\circ}$, $-2.5^{\circ}$ | 7.07 m, $5^{\circ}$, $-2.5^{\circ}$ |
| Blade prebend | 0.000 m | 3.332 m |
| Rotor mass | 110.0 t | 229.0 t |
| Nacelle mass | 240.0 t | 446.0 t |
| Tower mass | 347.5 t | 628.4 t |
| Total mass | 697.5 t | 1305.1 t |
| Centre of mass (CM) | (-0.2 m, 0.0 m, 64.0 m) | (-0.3 m, 0.0 m, 85.5 m) |

From Table 3.1 it can be shown that the DTU 10MW RWT is a direct upscale of NREL 5MW wind turbine except for the blades. Scaling factors of different rotor parameters are already described in Table 1.1. Actually, 10MW turbine shows an improvement in terms of the ratio of rotor mass (2.1), which is less than the upscaled value (2.8).

One of the task for this thesis (continued from master project) is to upscale the semi-submersible floater and make an initial design. For upscaling the floater, dynamic similarity, also known as Froude scaling is used. Froude scaling is a widely accepted and successfully applied scaling method in the marine industry for sea loads. NREL 5MW WindFloat platform described in [1] is taken as a basis for upscaling the floater in order to support the DTU 10MW RWT. The scaling factors are already shown in Table 1.2.

**Table 3.2:** Upscaled dimensions of 10MW Semi-submersible floater.

| Design parameter | 5MW WindFloat | 10MW Semi-sub. |
|---|---|---|
| Column diameter, $D$ [m] | 10 | 14.1 |
| Column height, $H$ [m] | 27 | 38.2 |
| Column centre to centre, $a_c$ [m] | 46 | 65.1 |
| Draft, $T_c$ [m] | 17 | 24 |
| Airgap, $f$ [m] | 10 | 14.1 |
| Displacement, $\Delta$ [t] | 4640 | 13125 |
| Overturning moment, $M_0$ [kNm] | 81375 | 230130 |
| **Natural periods:** | | |
| Heave, $T_{n3}$ [s] | 19.9 | 23.7 |
| Roll, $T_{n4}$ [s] | 43.3 | 51.5 |
| Pitch, $T_{n5}$ [s] | 43.2 | 51.4 |

Upscaled dimensions from Table 3.2 can be used as preliminary input for the initial design of the semi-submersible platform. However, it is interesting to note that the upscaled displacement for 10MW floater has increased approx. 3 times than 5MW WindFloat platform, which is considered an overestimation.

A similar study of 7-10MW WindFloat by Roddier et al. [20] suggests lower displacement value of approx. 7105 ton. Similarly, distance between column centres and height of the columns also shows conservative estimate from the Froude scaling. Column diameter and column centre to centre distance shall be adjusted in such a way that the platform is sufficiently stable and can counteract the overturning moment from thrust at rated wind speed.

During initial design calculation, an effort has taken to find the optimum value of column diameter and distance between column centre which is shown in Figure 3.1. It is based on maximum allowable static heel angle of the platform at the rated wind speed.

## 3.1 Initial design formulation

The initial design of the platform has to fulfill following two conditions which can be described by Equation 3.1.

1. floating foundation of the turbine shall ensure sufficient floating stability and

2. maximum allowable static pitch inclination must not exceed 10°

$$\varrho_w \forall = W_{turbine} + W_{platform} \tag{3.1a}$$

$$\varrho_w g \forall (Z_B - Z_G) + \varrho_w g \iint_{A_{wp}} x^2 \, ds \geq \frac{M_o}{\eta_5} \tag{3.1b}$$

## 3.2 Standards and guidelines

The standards for designing floating offshore wind turbine available today is limited in number. According to Johan Sandberg, the business development leader for wind at DNV

> Floating wind turbines introduce new risks and technological challenges related to stability, stationkeeping, power transmission and structural strength. In addition, economic aspects are likely to be challenging in the early phases. One barrier to the growth and development of this industry has been the lack of a design standard.

However, DNV-OS-J103: Design of Floating Wind Turbine Structures, is one of the mostly used standard today is released by DNV in 2013. The standard is the outcome of a joint industry project. For the design of floating offshore wind turbine following standards and recommended practices have been used extensively.

- DNV-OS-J101 Design of Offshore Wind Turbine Structures, May 2014.
- DNV-OS-J103 Design of Floating Wind Turbine Structures, June 2013.
- DNV-OS-C301 Stability and Watertight Integrity, April 2011.
- DNV-RP-C205 Environmental Conditions and Environmental loads, October 2010.
- DNV-RP-C203 Fatigue Strength Analysis of Offshore Steel Structures.
- IEC 61400-1:2005 Wind turbines - Part 1: Design requirements.
- IEC 61400-2:2013 Wind turbines - Part 2: Small wind turbines.
- IEC 61400-3:2009 Wind turbines - Part 3: Design requirements for offshore wind turbines.

## 3.3 Design parameters

The initial design parameters for a WindFloat type of semi-submersible can be listed as follows:

- Column diameter, $D$
- Column height, $H$
- Column centre to centre, $a_c$

- Operating draft, $T_c$
- Ballast water in operation, $W_{\text{b,op}}$

Although, the required ballast may vary based on different loading conditions, however, it is sufficient to determine the ballast only in operation condition during initial stage of design. For other load cases, ballast will be determined during detail stability analysis in (see chapter 4) using GHS.

## 3.4 Design philosophy

During initial design phase, design parameters were determined using laws of floatation, equilibrium of forces and moments and various empirical formulas. Motion characteristics like natural periods in heave, roll and pitch also play an important role. To make the task simple, a spreadsheet was prepared to investigate the effect of various design parameters.

In order to estimate the mass of the platform, a constant equivalent thickness of column plating is assumed. The equivalent thickness includes contribution from beams, girders and smeared stiffeners. The platform and turbine mass were used as a point mass for all initial calculations.

### Column diameter

Column diameter mostly contributes to the water plane inertia of the platform which counteracts the overturning moment. Overturning moment may arise from the distribution of weight and buoyancy and a resultant of thrust. Moreover, wind and waves loads will also create overturning moment on the platform.

The area moment of inertia of a circular cross section with diameter, $D$ about an axis passing through its centre is given by $I_c = \pi D^4/64$. At any draft, total area moment of inertia about centre of floatation (COF) can be found using parallel axis theorem.

From hydrodynamic point of view, consideration is given to keep the diameter of the columns as smaller as possible to reduce the loads on and response of the platform due to wind, waves and currents.

### Column height

Column height shall be chosen to provide required buoyancy and sufficient space for ballast, especially in the aft columns and to create a safe airgap. Increase in column height also increases the draft, thus stability of the platform improves. However, at the initial stage, it is not advised to increase the column height beyond 35 m. Because it may create problems for production inside a dock and quayside. Moreover, float-out and towing operations will face bigger challenge which may include increased resistance in towing operation. Moreover, increase in column height has the highest impact on steel weight of the platform.

### Column centre to centre

Distance between column centres has higher influence than column diameter while resolving the overturning moment. Increase in distance between column centre will make the platform more stiffer which may reduce natural periods in roll ($T_{n4}$) and pitch ($T_{n5}$). Moreover, increased

distance between column centre will increase the span of main beam and bracing, which are more prone to fatigue. During initial design study, the distance between column centre tried to keep as small as possible and closer to 5MW WindFloat value.

## Operating draft

One of the biggest advantage of a semi-submersible platform is it's higher flexibility to be operated within broader range of depth depending on it's mode of operation. Neither TLP nor SPAR shows such flexibility in terms of water depth. Ton per centimeter immersion (TPC) value of a semi-submersible is much higher than TLP and SPAR, so the platform can support much higher weight even in shallow water depth. Which makes semi-submersible an ideal choice to support 10MW DTU RWT. The drafts at which a semi-submersible platform can be operated are as follows:

- Transit draft
- Operation draft
- Survival draft

## Ballast

Ballast can be used as a means to obtain suitable draft, to improve stability by lowering the VCG of the platform and to obtain favourable motion characteristics by adjusting mass of the platform. Moreover, ballast is used to control trim of a platform which is a common practice in the marine industry. In addition, during storm, ballast may also be used to achieve even higher draft to ensure the safety of the platform which is a proven technique for semi-submersibles operating in deep water offshore.

## Static heeling angle

A smaller static heel angle of the platform is crucial for the wind turbine to maintain its high efficiency. The objective here is to keep the rotor plane perpendicular to the wind directions.

$$\begin{aligned} M_o &= T_R \cdot (Z_{hub} - Z_B) + M_{tower} \\ &= 1500 \cdot 125 + 3360 \ \text{[kNm]} \\ &= 188330 \ \text{[kNm]} \end{aligned}$$

Restoring coefficient in pitch due to pitch motion, $C_{55}$ can be written as [21]

$$\begin{aligned} C_{55} &= \varrho_w g \forall (Z_B - Z_G) + \varrho_w g \iint_{A_{wp}} x^2 \, ds \\ &= \varrho_w g \forall \overline{GM_L} \end{aligned} \tag{3.2}$$

At operation draft, $\Delta = 7295$ [t] and $\overline{GM_L} = 16.4$ [m]. Which gives $C_{55} = 1175820$ [kNm]. So static heeling angle at operation draft reads:

$$\eta_{5\,static} = \frac{M_o}{C_{55}} = \left(\frac{188330}{1175820}\right) \cdot \left(\frac{180}{\pi}\right) = 9.2^\circ$$

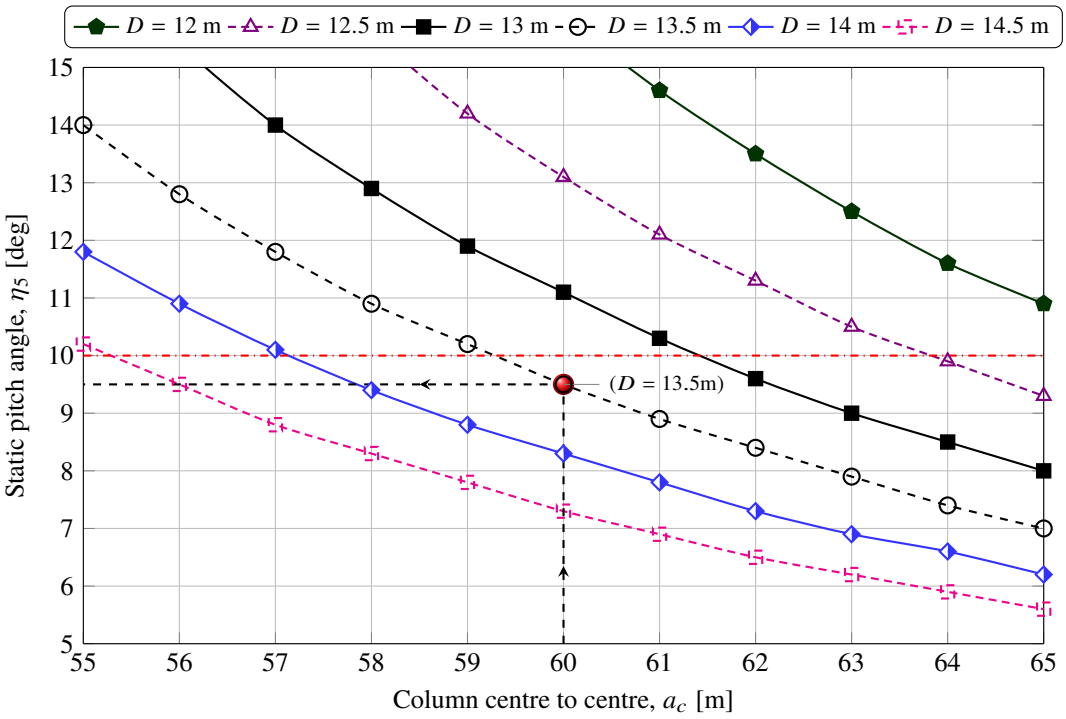


**Figure 3.1:** Variation of static heeling angle $\eta_{5\,static}$ for different column centre to centre $a_c$ and column diameter, $D$.

Figure 3.1 shows variation of static heel angle with the change of distance between column centres. To maintain a static heel angle below $10^\circ$, it is possible to select a diameter in the range of 13 m to 14.5 m. During selection of column diameter, emphasis is given to keep the distance between column centre below 60 m. As increasing distance between column centre will increase the span of bracing and loads at joint. The joint between bracing and column is also highly sensitive to fatigue. A diameter of 13.250 m and 60 m of column distance is selected for detail stability and analysis of rigid body motions.

## 3.5 Initial design algorithm

- A set of initial design parameters, for instance, column diameter ($D$), column height ($H$) and column centre to centre distance ($a_c$) can be chosen from Table 3.2. Equivalent plate thickness of ($t_{eq} = 30$) mm is used. So, hydrostatic properties and steel weight of the platform is known. Using TPC value, parallel sinkage due to platform weight is sorted out.

- Then the turbine is placed at the centre of floatation of the platform. As turbine weight and VCG are known quantity, parallel sinkage due to turbine weight is also known.

- Next, the turbine is moved on top of forward column (column2). Due to the movement, the platform trims forward. To make the platform upright, necessary ballast is filled equally in the aft two columns (column1, SB and column3, PS).

- Finally, to achieve required stability and motion characteristics, minimum ballast is distributed to all columns equally. A check shall be made so that filling volume in aft columns shall not exceed 50% of its capacity.

- Above steps can be repeated to find a optimum set of initial design parameters.

Algorithm described in section 3.5 is implemented in a spread sheet environment. A typical calculation is shown in Figure 3.2 and the results are listed in Table 3.3.

**Colour code:**

initial design input =>  constant input =>  calculated value =>

| | | | | | | | | |
|---|---|---|---|---|---|---|---|---|
| **Design parameters:** | | | | | | **Hydrostatic properties:** | | |
| column_diameter, D = | 13.250 | [m] | n_col = | 3 | [-] | TPC = | 4.2 | [t] |
| column_height, H = | 32.000 | [m] | rho_sw = | 1.025 | [t/m3] | | | |
| column_centre_to_centre, a = | 60.000 | [m] | rho_st = | 7.850 | [t/m3] | **Parallel sinkage:** | | |
| equivalent_plate_thickness, t = | 30 | [mm] | hub_height = | 119 | [m] | draft_for_platform_wt = | 2.966 | [m] |
| freeboard, f = | 14.800 | [m] | turbine_vcg = | 85.5 | [m] | draft_for_turbine_wt = | 3.078 | [m] |
| | | | rated_thrust = | 1500 | [kN] | draft_for_trim_ballast_aft = | 6.156 | [m] |
| **Column properties (single):** | | | thrust_arm = | 123 | [m] | draft_for_ballast_3col = | 5.000 | [m] |
| wp_area_col = | 137.9 | [$m^2$] | thrust_moment = | 184970 | [kN.m] | draft@LCF = | 17.200 | [m] |
| wp_inertia_col = | 1513.0 | [$m^4$] | wind_loads_tower = | 3359 | [kN.m] | | | |
| dx_col = | 52.0 | [m] | total_overturning_moment = | 188329 | [kN.m] | **Stability characteristics:** | | |
| dx_col_fwd = | 34.6 | [m] | | | | KB = | 8.600 | [m] |
| dx_col_aft = | 17.3 | [m] | | | | $BM_L$ = | 35.522 | [m] |
| | | | | | | $KM_L$ = | 44.122 | [m] |
| **WP area properties (platform):** | | | | | | $GM0_L$ = | 16.435 | [m] |
| wp_area_total = | 414 | [$m^2$] | trim_ballast_aft_2col = | 2546 | [m3] | | | |
| wp_inertia_total_$I_T$ = | 252735 | [$m^4$] | trim_ballast_ht_2col = | 9.2 | [m] | **Motion characteristics:** | | |
| wp_inertia_total_$I_L$ = | 252735 | [$m^4$] | equal_filling_3col = | 2068.3 | [m3] | C33 = | 4159 | [t/s2] |
| | | | | | | C55 = | 1175817 | [kN.m] |
| **Weight data:** | | | **VCG data:** | | | T_n3 = | 19 | [s] |
| platform_wt = | 1258 | [t] | kg_platform = | 14.4 | [m] | theta_5 = | 9.2 | [deg] |
| turbine_wt = | 1305 | [t] | kg_turbine = | 117.5 | [m] | | | |
| trim_ballast_aft2col = | 2610 | [t] | kg_trim_ballast_aft2col = | 4.6 | [m] | | | |
| ballast_wt_3col = | 2120 | [t] | kg_ballast_equal_fill_3col = | 8.7 | [m] | | | |
| **Displacement, Δ =** | 7293 | [t] | **KG =** | 27.7 | [m] | | | |

**Weight breakdown:**

| item | [t] | [m] | | | |
|---|---|---|---|---|---|
| cap_top_mass = | 97.4 | 32.015 | vol_each_column = | 4412.4 | [$m^3$] |
| cylinder_mass = | 941.1 | 16.000 | disp_vol_3col = | 7115 | [$m^3$] |
| cap_bottom_mass = | 219.2 | -0.015 | disp_vol_1col = | 2371.6 | [$m^3$] |
| **platform_mass =** | 1257.7 | **14.449** | steel_wt _1col = | 419.2 | [t] |

**Figure 3.2:** A typical initial design calculation in spreadsheet environment.

## 3.6 Initial design dimension and ballast requirement

A set of initial design dimensions of 10MW semi-submersible platform and required ballast in operation condition shown in Table 3.3.

**Table 3.3:** Initial design dimension and required ballast.

| Item | Value | Unit |
|---|---|---|
| Column diameter, $D$ | 13.25 | [m] |
| Column height, $H$ | 32 | [m] |
| Column centre to centre, $a_c$ | 60 | [m] |
| Equivalent plate thickness, $t_{eq}$ | 30 | [mm] |
| Freeboard, $f$ | 14.8 | [m] |
| Platform mass, $m$ | 1258 | [t] |
| Displacement, $\Delta$ | 7293 | [t] |
| **Ballast distribution:** | **volume** [m3] | **filling** [%] |
| Column1 [SB, AFT] | 1963 | 44% |
| Column2 [CL, FWD] | 689 | 16% |
| Column3 [PS, AFT] | 1963 | 44% |

A comparison of turbine weight and corresponding platform displacement are listed in Table 3.4. The ratio of turbine weight to displacement has lower value for the 10MW semi-submersible floater than 5MW WindFloat platform and can be considered as an improvement in terms of floater design.

**Table 3.4:** Ratio of turbine weight and displacement for 5MW and 10MW WindFloat.

| Turbine spec. | Turbine wt. [t] | Displacement [t] | Ratio [-] |
|---|---|---|---|
| 5MW NREL [1] | 698 | 4640 | 6.6 |
| 10MW DTU RWT | 1305 | 7295 | 5.6 |

# Chapter 4

# Stability analysis

To begin with the stability analysis, lightship weight and centre of gravity of the platform are estimated from the initial dimensions. Then, an approximation is made to the value of heeling moment due to the rated thrust from turbine. Next, a set of stability criteria are established based on DNV-GL classification guidelines and operational requirements. Using these information, analysis of maximum VCG is performed to check the allowable locations of maximum VCG for a series of displacement (or drafts). Next, the load cases (mainly distribution of ballast water in tanks) are prepared such a way that the final VCG of the platform is lower than that obtained from maximum VCG analysis. The design dimensions obtained from stability analysis are used as input for hydrodynamic analysis.

To investigate the stability of the floater in detail, GHS (General HydroStatics) from Creative Systems, Inc. (www.ghsport.com) is used exclusively. GHS is a widely used naval architectural software package for it's reliability.

## 4.1 Stability model

A typical sketch for stability model is shown in Figure 4.1 where origin, $\mathbf{O}(0, 0)$ is marked with axis directions and all symbols have their usual meanings.

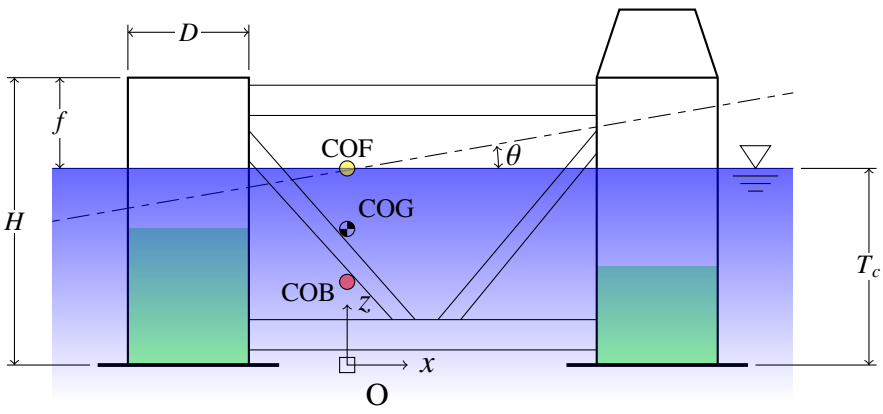


**Figure 4.1:** Stability model with design parameters and coordinate system.

## 4.2 Coordinate system

In order to perform the detail stability analysis of the platform, a coordinate system with following sign convention is followed.

The coordinate system is presented in Figure 4.1.

**LCG**: +ve forward of origin
**TCG**: +ve towards port side
**VCG**: +ve above base line

## 4.3 Modification of tower height

Structural design of the tower is described in DTU Wind Energy Report [2, pp. 57-62]. Loads and boundary conditions considered for tower design are as follows:

- A total concentrated force of 676000 $kg$ at tower top consist of nacelle mass (446000 $kg$), hub mass (105000 $kg$) and mass of three (3) blades altogether ($3 \times 41667 = 125000\ kg$).
- Self weight of the tower is considered as a distributed force and applied at element level.
- Bending moment of 17850 $kNm$ at tower bottom corresponding to maximum thrust at tower top.

As no hydrostatic pressure has been considered in tower design so the tower must not go under water during operation. Thus, for a floating wind turbine it is not possible to use the same tower of DTU 10MW RWT without necessary modifications. Most manufacturers offer a range of tower heights to be used with a particular wind turbine model in order to satisfy a specific hub height requirement for each site.

## 4.4 Lightship estimation

A complete breakdown of platform's lightship is shown in Table 4.1. Total lightship is composed of platform's lightship and turbine weight. The lightship and COG values are used as input for detail stability analysis.

## 4.5 Wind heeling moment

To evaluate sufficient floating stability, it is essential to estimate the wind loads on the turbine and its supporting structures. The total wind loads on a floating wind turbine is a combination of rotor-filtered wind load also known as thrust, wind loads on the tower and loads on wind exposed support structures.

Although, similar study was done by Qiang Wang [22] but the heeling moment due to wind loads on the tower and wind exposed support structures were not taken into account. So, an attempt has been made to estimate wind heeling moment on the tower and supports structures so that it can be used for initial stability calculation in addition to rated thrust force from the rotor. During final stability calculation wind heeling moment used in preliminary calculation can be replaced with wind tunnel data to obtain more accurate result which is a common, state of the art industry practice nowadays.

**Table 4.1:** Breakdown of lightship items.

| Lightship item | Weight [t] | LCG [m] | TCG [m] | VCG [m] |
|---|---|---|---|---|
| Heave plates | 671.4 | 0.000 | 0.000 | 0.000 |
| Columns | 963.9 | -1.074 | 0.000 | 16.992 |
| Connection piece | 54.0 | 34.640 | 0.000 | 35.070 |
| Platform lightship[a] | 1689.3 | 0.495 | 0.000 | 10.817 |
| Tower[b] | 474.4 | 34.641 | 0.000 | 79.198 |
| Blades | 125.2 | 26.429 | 0.000 | 138.243 |
| Nacelle | 446.0 | 37.327 | 0.000 | 137.230 |
| Hubmass | 105.5 | 27.567 | 0.000 | 138.150 |
| Turbine weight[c] | 1151.0 | 34.140 | 0.000 | 113.513 |
| **Total lightship** | 2840.0 | 14.129 | 0.000 | 52.433 |

[a] Weight of platform items are based on equivalent plate thickness, $t_{eq} = 30\ mm$ and material density of steel, $\rho_{steel} = 7850\ kg/m^3$.
[b] Tower weight is adjusted due to reduction in tower height.
[c] Turbine weight [2, p. 13] is composed of rotor mass, nacelle mass and tower mass.

### 4.5.1 Wind loads on the tower

Wind loads on the tower is a function of it's cross-section, corresponding wind speed at the section which will vary along the height of the tower. Variations of wind speed may also occur due to topographic location. Wind loads on a cylindrical structure can be calculated using Equation 4.1 of [23]

$$F = 0.5\ C_s \cdot C_h \cdot \varrho_a \cdot A \cdot V^2 \tag{4.1}$$

**Table 4.2:** Wind loads on turbine tower for operation and survival condition.

| $H_{mid}$ [m] | Δh [m] | $d_{mean}$ [m] | A [$m^2$] | $C_s$ [-] | $C_h$ [-] | $V_{op}$ [m/s] | $V_{sur}$ [m/s] | $F_{op}$ [kN] | $F_{sur}$ [kN] | arm [m] |
|---|---|---|---|---|---|---|---|---|---|---|
| 21.3 | 3.5 | 7.8 | 27.1 | 0.5 | 1.05 | 11.2 | 51.5 | 1.1 | 22.9 | 30.9 |
| 28.8 | 11.5 | 7.6 | 87.4 | 0.5 | 1.10 | 11.2 | 51.5 | 3.7 | 78.0 | 38.4 |
| 40.3 | 11.5 | 7.3 | 84.2 | 0.5 | 1.18 | 11.2 | 51.5 | 3.8 | 80.4 | 49.9 |
| 51.8 | 11.5 | 7.0 | 81.0 | 0.5 | 1.25 | 11.2 | 51.5 | 3.9 | 82.0 | 61.4 |
| 63.3 | 11.5 | 6.8 | 77.8 | 0.5 | 1.31 | 11.2 | 51.5 | 3.9 | 82.9 | 72.9 |
| 74.8 | 11.5 | 6.5 | 74.6 | 0.5 | 1.37 | 11.2 | 51.5 | 3.9 | 83.0 | 84.4 |
| 86.3 | 11.5 | 6.2 | 71.4 | 0.5 | 1.43 | 11.2 | 51.5 | 3.9 | 82.6 | 95.9 |
| 97.8 | 11.5 | 5.9 | 68.2 | 0.5 | 1.48 | 11.2 | 51.5 | 3.9 | 81.7 | 107.4 |
| 109.6 | 12.1 | 5.6 | 68.5 | 0.5 | 1.52 | 11.2 | 51.5 | 4.0 | 84.6 | 119.2 |
| | | | | | | | Total = | 32.1 | 678.2 | 77.6 |

It can be seen from Table 4.2 that at rated wind speed of 11.4 m/s, wind loads on the tower, $F_{op}$ have smaller value and it may further be reduced due to shadow effect of turbine blades. But

during survival condition, the turbine is not in operation and wind loads on tower could have very high value. However, it will never exceed the rated thrust of the turbine. So thrust value at rated wind speed govern the design of floating wind turbine.

### 4.5.2 Total wind heeling moment

The total wind heeling moment used for stability calculation is given by Equation 4.2. The moment kept constant irrespective of the heeling of the platform.

$$\begin{aligned} M_{heel} &= Thrust_{rated} \cdot (Z_{hub} + Draft - VCB) + M_{tower} \\ &= 1500 \cdot (119 + 19.150 - 9.574) + 32.1 \cdot 77.6 \; [kN \cdot m] \\ &= 195355 \; [kN \cdot m] \\ &= 19915 \; [MT \cdot m] \end{aligned} \tag{4.2}$$

## 4.6 Stability requirement

During early stages of design only floating stability shall be addressed properly. By floating stability we mean maximum value of KG, often refers to as limiting KG, shall be defined adequately so that the floating unit is in stable equilibrium. In other words, values of meta-centric height shall have positive value i.e. $\overline{GM} > 0$. While determining the stability criteria, it is assumed that the platform will remain unmanned during operation which considerably simplify the stability requirements.

### 4.6.1 Intact stability requirement

Stability criteria for various types of floating wind turbine are discussed in DNV offshore standard, DNV-OS-J103, Sec. 10. Intact stability requirements for a column-stabilized unit like WindFloat is given in Sec. 10.2.3 are listed as follows:

- The area under the righting moment curve to the angle of down-flooding shall be equal to or greater than 130% of the area under the wind heeling moment curve to the same limiting angle.
- The righting moment curve shall be positive over the entire range of angles from upright to second intercept.

To satisfy the area ratio requirement, the value of $k$ shown in Figure 4.2 shall be greater than or equal to 1.3.

### 4.6.2 Damage stability requirement

For unmanned units in damaged condition, sufficient floating stability is not a regulatory requirement, but an option. As the platform will be unmanned throughout its life, floating stability in damaged condition is not considered during initial stage of design. According to DNV stability standard

> For unmanned floating wind turbine units, i.e. for units which are unmanned during extreme environmental conditions and during normal operation of the wind turbine,

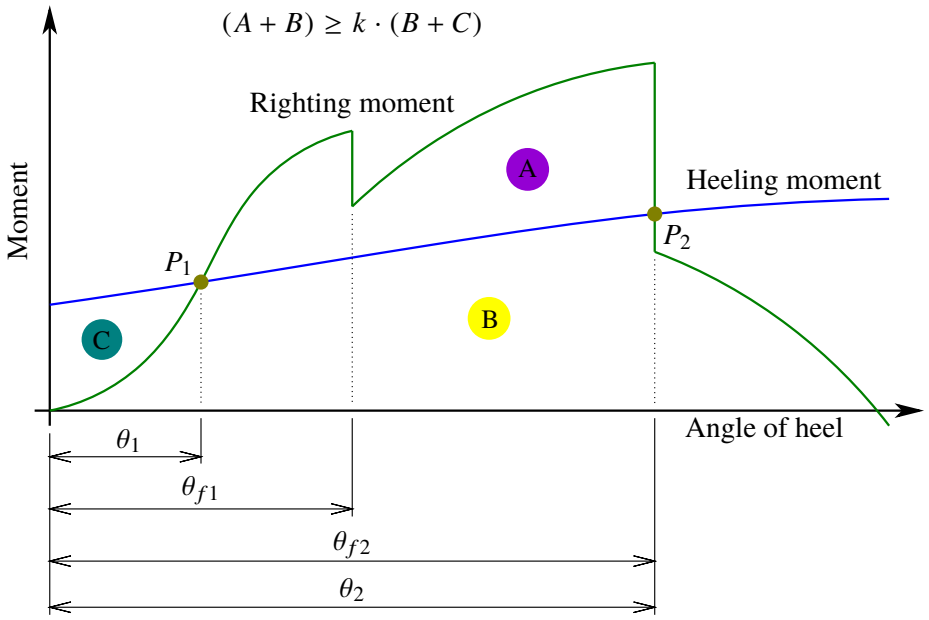


**Figure 4.2:** Righting moment and wind heeling moment curve.

sufficient floating stability is an absolute requirement in the intact condition. This applies to the operational phase as well as any temporary phases.

## 4.7 Critical axes orientation

A critical-axis is defined as the axis of least stability for a platform. It is not necessarily in the transverse direction or where trim becomes large when the platform is heeled. An arbitrary orientation of critical-axis, $C-C$ is shown in Figure 4.3 which makes an angle $\beta$ with longitudinal axis.

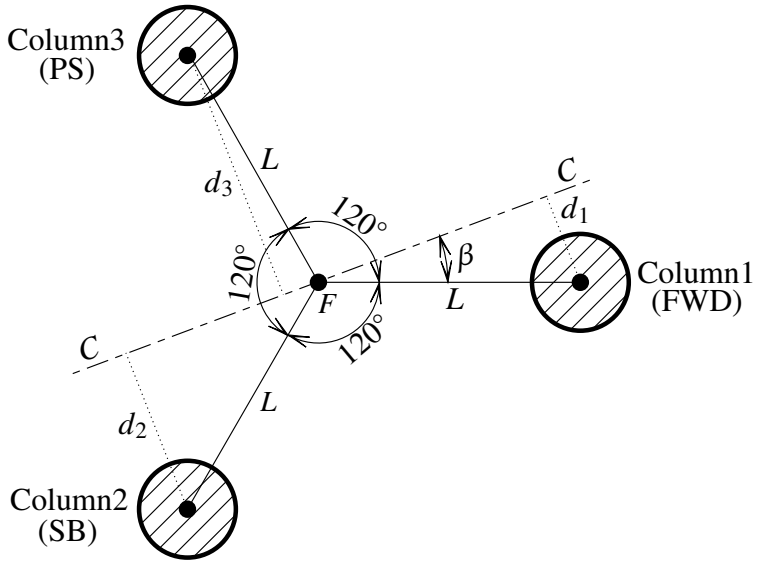


**Figure 4.3:** Critical axis orientation for intact stability analysis.

To determine the orientation of critical-axis, a hand calculation has been made and presented using Equation 4.3. It is obvious that the water plane inertia about any arbitrary axis is constant and free from its orientation angle, $\beta$. So, for intact stability analysis, any axis can be taken as critical-axis. For rest of the analysis, $y-$axis is taken as critical-axis.

$$
\begin{aligned}
I_T &= \sum_{i=1}^{i=3} I_{c_i} + A_i d_i^2 \\
&= I_{c_1} + A_1 d_1^2 + I_{c_2} + A_2 d_2^2 + I_{c_3} + A_3 d_3^2 \\
&= I_c + A d_1^2 + I_c + A d_2^2 + I_c + A d_3^2 \\
&= I_c A (d_1^2 + d_2^2 + d_3^2) \\
&= I_c A [(L \sin(60^\circ - \beta))^2 + (L \sin(\beta))^2 + (L \sin(120^\circ - \beta))^2] \\
&= I_c A L^2 [\sin^2(60^\circ - \beta) + \sin^2(\beta) + \sin^2(120^\circ - \beta)] \\
&= (\frac{\pi D^4}{64})(\frac{\pi D^2}{4})(\frac{\sqrt{3}a}{2})^2 [\sin^2(60^\circ - \beta) + \sin^2(\beta) + \sin^2(120^\circ - \beta)] \\
&= (\frac{3\pi^2 D^6 a^2}{2^{10}}) [\sin^2(60^\circ - \beta) + \sin^2(\beta) + \sin^2(120^\circ - \beta)] \\
&= (\frac{3\pi^2 D^6 a^2}{2^{10}}) [\sin^2(\beta) + \cos^2(\beta) + \frac{1}{2}\sin^2(\beta) + \cos^2(\beta)] \\
&= \frac{9\pi^2 D^6 a^2}{2^{11}}
\end{aligned}
\tag{4.3}
$$

## 4.8 Analysis of maximum VCG

Analysis of maximum VCG also known as limiting KG curves produce a series of maximum allowable VCG locations for a particular vessel corresponding to a series of drafts (or displacements) while satisfying certain stability criteria. The objective of this analysis is to provide a boundary within which all VCG values must lie for any operations throughout vessel's lifetime. So during preparation of loading conditions, deadweight items shall be placed in such a way that the VCG of the platform is lower than the value obtained from maximum VCG analysis. A list of required input for maximum VCG analysis are given below:

- underwater geometry of the platform
- location of downflooding points
- initial heel or trim of the platform
- heeling moment and
- stability criteria

Figure 4.4 presents curves of maximum VCG which satisfies the intact stability requirements described in subsection 4.6.1 and following operational criteria in addition. These operational criteria are not the part of regulatory requirement but essential for smooth operation of the turbine.

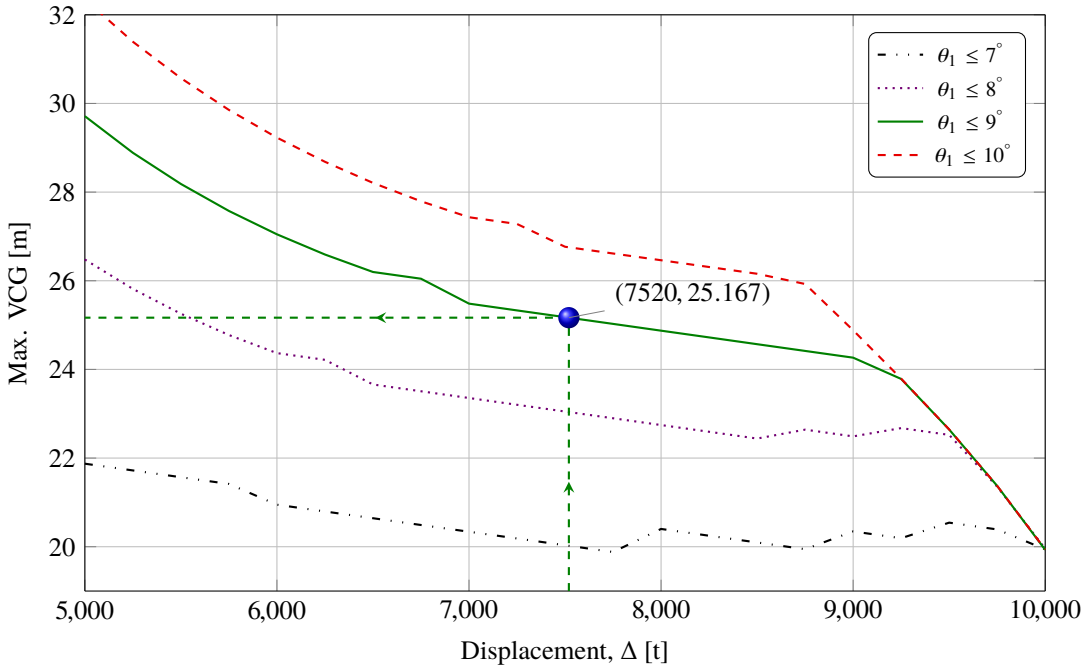


**Figure 4.4:** Comparison of MaxVCG curves.

- maximum static angle of heel at equilibrium or first intercept $\leq 10°$
- metacentric height in upright condition, $\overline{GM}_{upright} > 0.5$
- angle of downflooding occurs after first intercept, $\theta_1$ (see Figure 4.2)

During determination of initial design parameters of the platform, the effect of each parameters have been investigated thoroughly. Usually, increase in column diameter can raise the MaxVCG value of a platform at a certain displacement for similar stability criteria. But increase in column height has no influence on MaxVCG. Although increase in column height can increase the stability of the platform by providing larger freeboard but during detail stability calculation no improvement is noticed. Actually, increased column height will raise the VCG of the platform and in addition the overturning moment due to thrust from turbine will also increase. So, it is not suggested to increase the column height above 35 m, instead the diameter of the columns can be increased.

## 4.9 Stability load cases

Two (2) stability load cases are prepared as a guideline for safe operation of the platform. One in operation condition and another in free-floating condition. For free-floating load case, the turbine may remain idle or parked. There shall be no thrust force from the rotor. To be conservative 25% of rated thrust is assumed to account the heeling moment on the floater.

### 4.9.1 Load case - 1 (operation)

A load case is a detail report about the platform lightship, ballast and deadweight items including their centre of gravity. It may also presents a summary of the stability of the platform.

Figure 4.5 presents a load case of the platform in operation condition. By operation condition we mean the turbine is in power production mode. The term 'FIXED WEIGHT' refer to the lightship of the platform. A complete breakdown of lightship items are shown in Table 4.1. Total amount of ballast water is 4678 ton and distributed in three (3) tanks. BWT1.C refers to the forward ballast tank. It contains 19% of total ballast. BWT2.S and BWT3.P are the aft ballast tank in starboard and port side. Each of them contains identical share of ballast water of 47.2%. Total Weight 7518 ton is the sum of platform lightship and the total weight of ballast water. Total weight of the platform is balanced by the buoyancy force of the platform which is indicated as HULL.

```
                    WEIGHT and DISPLACEMENT STATUS
              Baseline draft: 19.107 @ 34.64f, 19.170 @ 17.32a
                    Trim: Aft 0.063/51.960,  Heel: zero
Part-------------------------------Weight(MT)----LCG-----TCG-----VCG
FIXED WEIGHT                        2,840.30  14.130f  0.000  52.435
                Load-----SpGr-----Weight(MT)----LCG-----TCG-----VCG------RefHt
BWT1.C         0.190    1.025        783.77  34.639f  0.000   3.040     -6.122
BWT2.S         0.472    1.025      1,947.06  17.321a 30.000s  7.552    -15.083
BWT3.P         0.472    1.025      1,947.06  17.321a 30.000p  7.552    -15.083
  Total Tanks--------->            4,677.89   8.615a  0.000   6.796
  Total Weight-------->            7,518.19   0.022a  0.000  24.038
                                   Displ(MT)----LCB-----TCB-----VCB
HULL                   1.025      7,518.18   0.038a  0.000   9.574    -19.149
-------------------------------------------------------------------------------
```

**Figure 4.5:** Loading condition (operation).

Few key points of operation loading condition are listed below:

- Draft 19.1 m, no trim, no heel
- Total weight of the platform is 7518.2 ton with COG at (0.022a, 0.000, 24.038) m
- Displacement 7518.2 ton with COB at (0.038a, 0.000, 9.574) m

A summary of stability criteria for operation condition is presented in Figure 4.6. There are three (3) columns in the figure. Left column lists the stability criterion to be evaluated, middle column presents the regulatory requirements and the right column shows the value obtained from stability calculation. LIM (1) indicates the value of first intercept, $\theta_1$ (point $P_1$ in Figure 4.2) where heeling moment and righting moments are in equilibrium. LIM (2) is a measure of area ratio, $k$ as indicated in Figure 4.2. LIM (3) and LIM (4) are not regulatory requirements but ensure the completeness of stability criteria. A detail stability report of operation condition can be viewed in Appendix A.

```
LIM--------------------STABILITY CRITERION------------Min/Max--------Attained
(1) Absolute Angle at Equilibrium                 <    10.00  deg     8.65 P
(2) Abs Area Ratio from 0 deg to RAzero or Flood  >    1.300         1.479 P
(3) Angle from Equilibrium to Flood               >     0.00  deg      LARGE
(4)  GM Upright                                   >    0.500   m.   16.880 P
```

**Figure 4.6:** Summary of stability criteria (operation).

### 4.9.2 Load case - 2 (free-floating)

Free-floating condition can be an example of floating out from dock after construction. This loading condition can also be used for transit from construction site to its operational area in North Sea.

Figure 4.7 presents the free-floating loading condition. It is different from the operation condition in terms of ballast distribution. The amount of total ballast water is 2318.3 ton which is distributed equally into the aft two tanks. BWT2.S and BWT.3P each has 28.1% of ballast water whereas BWT1.C has no ballast.

```
                    WEIGHT and DISPLACEMENT STATUS
              Baseline draft: 13.132 @ 34.64f, 13.142 @ 17.32a
                     Trim: Aft 0.010/51.960,  Heel: zero
Part-----------------------------Weight(MT)----LCG-----TCG-----VCG
FIXED WEIGHT                       2,840.30  14.130f  0.000  52.435
                Load-----SpGr-----Weight(MT)----LCG-----TCG-----VCG------RefHt
BWT2.S         0.281    1.025      1,159.16  17.321a 30.000s  4.496     -8.989
BWT3.P         0.281    1.025      1,159.16  17.321a 30.000p  4.496     -8.989
  Total Tanks--------->            2,318.32  17.321a  0.000   4.496
  Total Weight-------->            5,158.62   0.004a  0.000  30.891
                                   Displ(MT)----LCB-----TCB-----VCB
HULL                   1.025      5,158.62   0.009a  0.000   6.569    -13.139
--------------------------------------------------------------------------------
```

**Figure 4.7:** Loading condition (free-floating).

Few key points of free-floating loading condition are listed as follows:

- Draft 13.140 m, no trim, no heel
- Total weight of the platform is 5158.6 ton with COG at (0.004a, 0.000, 30.891) m
- Displacement 5158.6 ton with COB at (0.009a, 0.000, 6.569) m

A summary of stability criteria similar to operation case is shown in Figure 4.8. Large amount of margin is reserved. A detail Stability report for free-floating condition is attached in Appendix A.

```
LIM--------------------STABILITY CRITERION------------Min/Max--------Attained
(1) Absolute Angle at Equilibrium                  <    10.00  deg     2.45 P
(2) Abs Area Ratio from 0 deg to RAzero or Flood   >    1.300         7.089 P
(3) Angle from Equilibrium to Flood                >     0.00  deg      LARGE
(4)  GM Upright                                    >    0.500   m.   21.611 P
```

**Figure 4.8:** Summary of stability criteria (free-floating).

# Chapter 5

# Hydrodynamic analysis

Before start with the hydrodynamic analysis, an investigation has been made to understand the influence of the design parameters on the rigid body motions of the platform. After studying similar concepts, for example, 5MW NREL WindFloat [1], it is understood that natural period in heave, $T_{n3}$ may fall within wave frequency range.

The heave natural period of a platform can be written in the form of Equation 5.1. Where $M$ is the mass of the platform including turbine and ballast, $A_{33}$ is added mass in heave due to heave motion, $\varrho_w$ represents density of water and $A_w$ is the total water plane area of the platform.

$$T_{n3} = 2\pi\left(\frac{(M + A_{33})}{\varrho_w g A_w}\right)^{\frac{1}{2}} = 2\pi\left(\frac{(1 + c_1)M}{\varrho_w g A_w}\right)^{\frac{1}{2}} \tag{5.1}$$

In order to get a heave natural period outside the wave frequency range ($T_{n3} > 20s$), the required displacement (or mass) of the platform can be obtained from Equation 5.2. Where $n$ represents the number of columns in the platform and $c_1$ ($A_{33} = c_1 M$) is the factor of added mass. Thus, for a particular value of $c_1$, it is possible to obtain a definite relationship ($M \propto D^2$) between column diameter and required displacement.

$$\begin{aligned} M &= \frac{\varrho_w g A_w}{4\pi^2} \cdot \frac{(T_{n3})^2}{(1 + c_1)} \\ &= \frac{\varrho_w g (n \cdot \frac{\pi D^2}{4})}{4\pi^2} \cdot \frac{(T_{n3})^2}{(1 + c_1)} \\ &= n \cdot \frac{\varrho_w g}{16\pi} \cdot \frac{(T_{n3})^2}{(1 + c_1)} \cdot D^2 \end{aligned} \tag{5.2}$$

It is also found that the value of $c_1$ strongly depends upon the shape and dimension of heave plates (for detail see section 5.3). There are two (2) types of heave plate can be found. It can either be circular or polygonal. Roddier et al. [1] used a hexagonal type of heave plate for a generic 5MW WindFloat design. The edge length of heave plate is 1.5 times of column diameter, $D$. Effects of column diameter, column height and heave plates on the rigid body motions of the platform are discussed in detail in section 5.1, section 5.2 and section 5.3 respectively.

## 5.1 Column diameter and displacement

Equation 5.2 is pictured in Figure 5.1, shows the relationship between the column diameter and displacement of the platform in order to keep the heave natural period outside the wave period range ($3s \sim 20s$). For a series of column diameter from 10 m to 15 m, required minimum displacements are computed separately with hexagonal heave plate and circular heave plate.

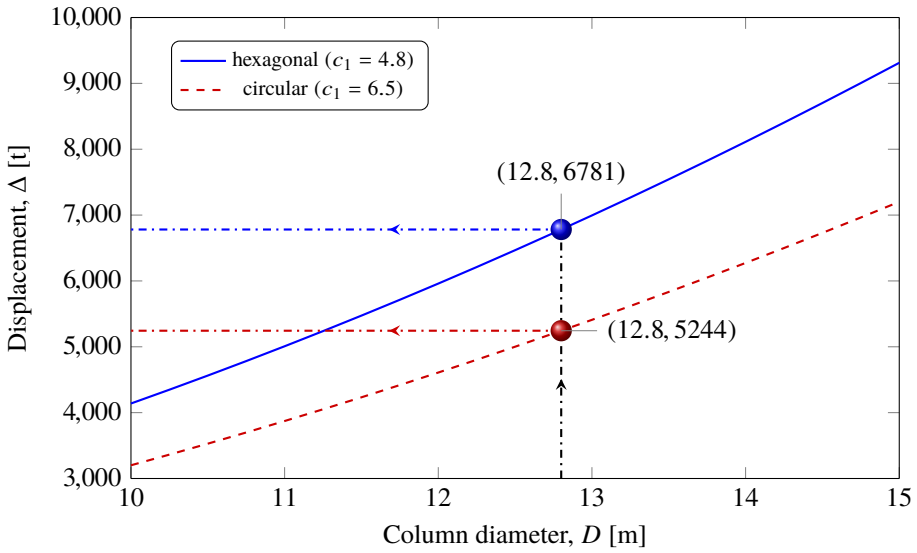


**Figure 5.1:** Relationship between column diameter and displacement for favourable motions in heave with different heave plates.

Using Figure 5.1 it is possible to find out the minimum displacement of the platform which can shift the heave natural period ($T_{n3}$) outside the wave frequency range for a particular column diameter. For example, with a column diameter of 12.8 $m$, the minimum required displacement with circular heave plate, $\Delta_{cir} \geq 5244\ t$ and for hexagonal heave plate, $\Delta_{hex} \geq 6781\ t$. This information will narrow down the search field during initial design work and can save significant time. Figure 5.1 also shows the possibility to achieve same heave natural period with lower displacement by using circular heave plate.

## 5.2 Column height

For a particular heave plate, column diameter, $D$ and displacement, $\Delta$ are estimated based on Figure 5.1. Next, it is straightforward to calculate column height, $H$ using Equation 5.3 where $f$ indicates freeboard of the platform.

$$Column\ height = Draft + Freeboard$$

$$H = \frac{\Delta}{TPC} + f \tag{5.3}$$

## 5.3 Heave plate

Heave plates are found to be an important component during the design of the platform. They are designed to shift the heave natural frequency of the platform outside the wave frequency range

without significant increase in displacement or reduction in column diameter. They can help to achieve favourable motion characteristics of the platform by damping the motion especially in heave.

The heave plates provide additional hydrodynamic inertia to the platform due to the fact that they can displace large amount of water as the platform moves vertically. In addition, vortices are created along the edge of the plates, generate large damping forces that further impede the motion of the platform.

The drag coefficients of various submerged horizontal plates have been measured by Prislin et al. [24]. They recommend a $C_d$ value between 5 and 10 for a square plate when analyzing results of model tests. But some differences are expected here, because viscous effects from the plate will arise from motions of the plate as well as the kinematics of the waves. Furthermore, interactions may occur between vortex- shedding and potential flow affecting the combined loading on the plate.

Figure 5.2 presents a comparison of added mass in heave ($A_{33}$) for hexagonal and circular heave plate of same external dimension. It is found that for a particular column diameter, circular heave plates can provide 35% more added mass in heave than the hexagonal heave plates. Hydrodynamic analysis of a similar 5MW WindFloat by Roddier et al. [1] suggests that the added mass in heave is four (4) times larger than its total mass, M which is a close agreement to our findings.

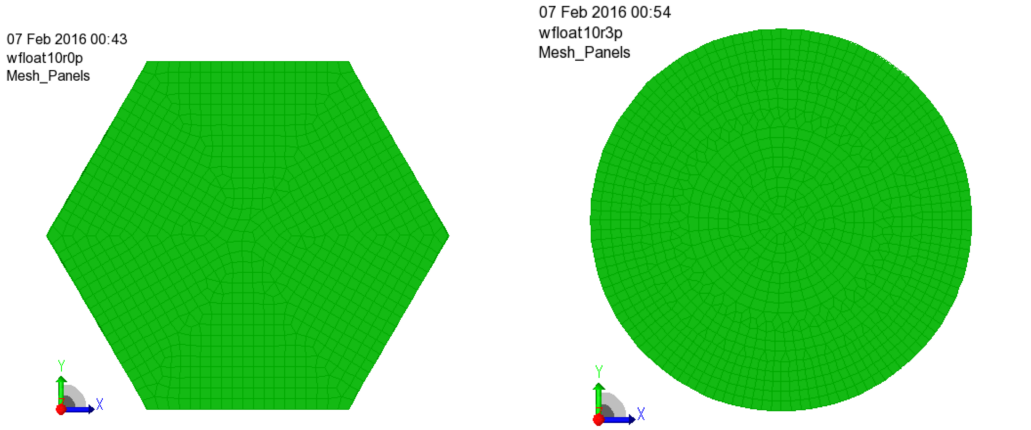


(a) Hexagonal heave plate, ($A_{33} = 4.8M$; $c_1 = 4.8$)

(b) Circular heave plate, ($A_{33} = 6.5M$; $c_1 = 6.5$)

**Figure 5.2:** Comparison of added mass in heave between hexagonal and circular heave plate.

A hexagonal type of heave plate is used during hydrodynamic analysis to find the natural periods of rigid body motion of the platform. Hexagonal heave plates are easy to fabricate, have smaller footprint which make them more economical than the circular type. For this reason, hexagonal heave plates are considered for rest of the analysis.

## 5.4 Frequency domain hydrodynamic analysis

For frequency domain hydrodynamic analysis, DNV-GL Wadam [25] is used. Wadam stands for Wave Analysis by Diffraction and Morison Theory. Wadam uses Morison equation for slender structures and 3D potential theory for large volume structures. If a body is composed of

both slender and large volume structures, Morison's equation and potential theory can be used altogether. For example, bracing of a semi-submersible can be considered as slender structures whereas columns are large volume structures, responsible for wave diffraction.

The objective of the frequency domain hydrodynamic analysis are listed as follows:

- First order wave exciting forces and moments.
- Second order mean (wave) drift forces from the results of first order calculations using Newman's approximation.
- Hydrodynamic added mass and damping coefficients.
- Linear stiffness (hydrostatic stiffness) matrix.
- Natural periods of rigid body motions of the platform.

The frequency domain hydrodynamic analysis is performed without the mooring lines. Forces and moments are taken into account in terms of transfer functions.

Sesam GeniE is used as a pre-processing tool to create a panel model (see section 5.6) and mass model (see section 5.7) of the platform. Panel model accounts for the hydrodynamic loads and mass model accounts for global mass distribution and inertia of the platform. HydroD module is a graphical user interface (GUI) and responsible for running the hydrodynamic analysis using Wadam as a solver. Hydrodynamic analysis schematic using Wadam is presented in Figure 5.3.

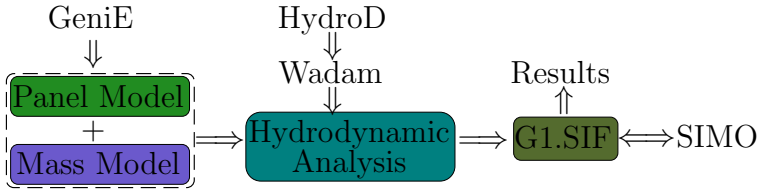


**Figure 5.3:** Hydrodynamic calculations flowchart.

## 5.5 Hydrodynamic coordinate system

The oscillatory translational ($\eta_1,\ \eta_2,\ \eta_3$) and rotational motions ($\eta_4,\ \eta_5,\ \eta_6$) of the platform are defined in an inertial earth-fixed coordinate system. By inertial reference frame we mean the coordinate system has no acceleration and Newton's second law of motion, $\vec{\mathbf{F}} = m\vec{\mathbf{a}}$ is valid without modifications.

The $(x, y)$ plane lies in the still water level, above (or below) the centre of gravity of the platform. The positive $x-$axis is along the direction of wave propagation and positive $z-$axis is in upward direction.

The global hydrodynamic coordinate system is shown in Figure 5.4. Point $O$ represents the origin of the coordinate system, $x_g$ and $z_g$ pointed toward the $x$ and $z$ axis direction.

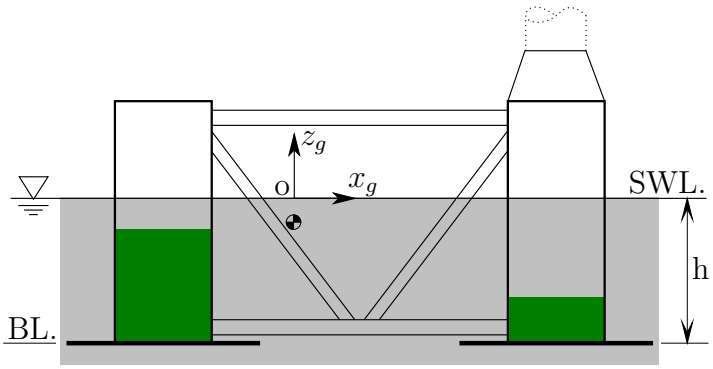


**Figure 5.4:** Hydrodynamic coordinate system.

## 5.6 Panel model

The panel model is used to calculate the hydrodynamic loads and responses from potential theory. The basic part of a panel model consists of quadrilateral or triangular panels representing the wet surfaces of a body. It may describe either the entire wet surface or it may take advantage of either one or two planes of symmetry of the wet surfaces. Figure 5.5 represent panel model of the platform with $x - z$ plane of symmetry.

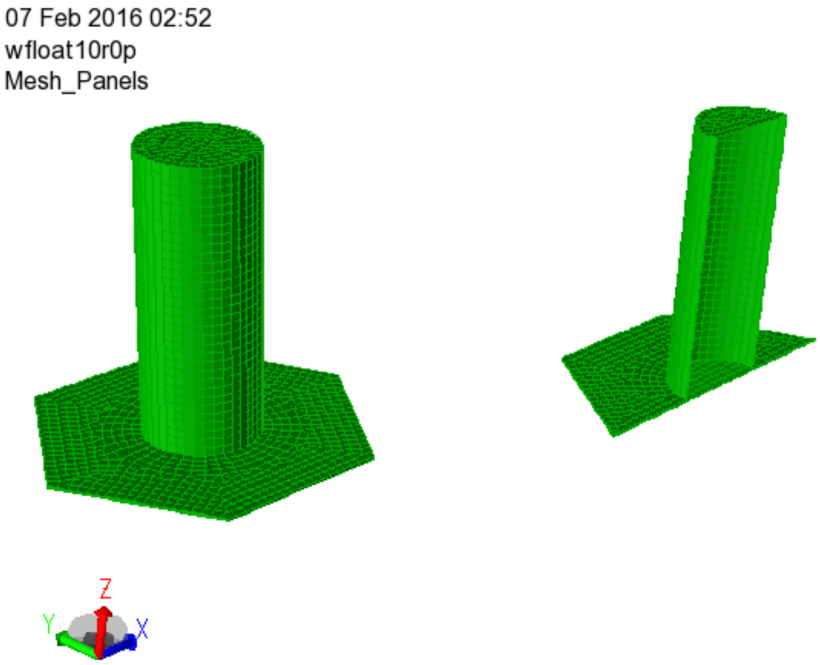


**Figure 5.5:** Panel model of the platform (PS shown, SB symmetric).

## 5.7 Mass model

Global mass information in Wadam also known as mass model is required for analysis of floating structures. The mass model can be used for both hydrostatic and stability calculations and in the equations of motion. There are two methods available in Wadam to establish the global mass matrices:

- Direct input of a global mass matrix ($6 \times 6$)
- Assembling of a global mass matrix from a mass model (no utilisation of symmetry planes)

Figure 5.6 presents the global mass model of the platform. The floating platform is modelled using a equivalent plate thickness, $t_{eq}$ of 30 mm. The tower is modified (reduced 19.5 m from bottom) to keep the hub at its design height [2] of 119 m. It is modelled using beam elements of tubular cross sections. The blades are modelled as point mass in such a way that it yields the same mass distribution as the DTU 10MW turbine blades. These point masses are connected to each other by mass less beam elements. Ballast are also modelled as solid beam element having a material density equal to the density of sea water. The free surface effect of the tanks were neglected in hydrodynamic analysis. But the free surfaces effects are taken into account in stability analysis with GHS software package. See Appendix A for detail stability analysis.

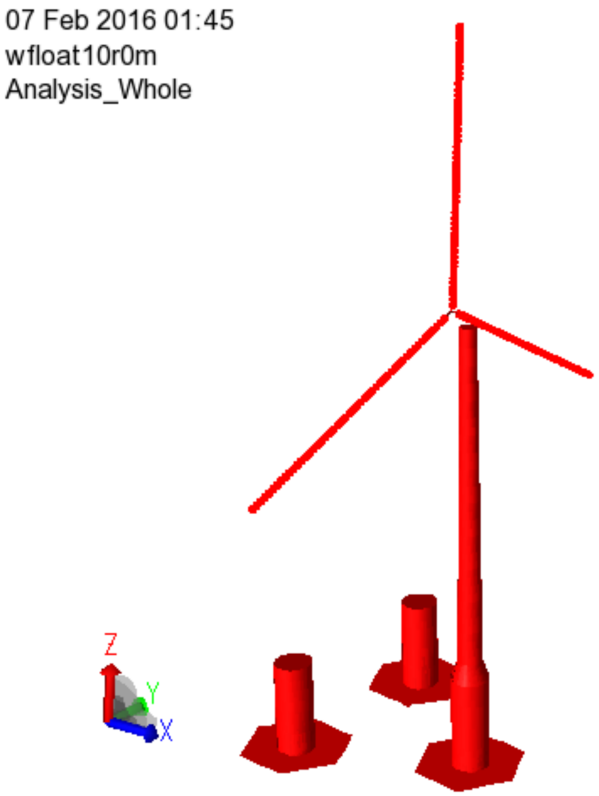


**Figure 5.6:** Mass model of the supporting platform including the DTU 10MW RWT and hexagonal heave plate.

## 5.8 Results

### 5.8.1 Natural periods of rigid body motions

Natural periods of rigid body motions of the platform in heave, roll and pitch are listed in Table 5.1. Moreover, a comparison has been made among the 5MW WindFloat [1], scaled and 10MW semi-submersible floater.

It is possible to verify the natural periods of rigid body motions using Equation 5.4.

$$T_{ni} = 2\pi\left(\frac{(M + A_{ii})}{C_{ii}}\right)^{\frac{1}{2}} \tag{5.4}$$

For heave motion, Mass, $M_{33} = 7518.2e + 03$ kg, added mass in heave, $A_{33} = 4.8M_{33}$ and $C_{33} = \varrho_w g A_w = 3.834e + 06$ N/m (see Figure 5.7) will give a heave natural period of 21.2s.

**Table 5.1:** Comparison of a 5MW, scaled and 10MW WindFloat motion characteristics ($sf = \sqrt{2}$).

| Motion | 5MW WFloat | Scaled | 10MW Semi |
|---|---|---|---|
| Heave, $T_{n3}$ $[s]$ | 19.9 | 23.7 | 21.7 |
| Roll, $T_{n4}$ $[s]$ | 43.3 | 51.5 | 37.9 |
| Pitch, $T_{n5}$ $[s]$ | 43.2 | 51.4 | 38.4 |

The natural periods in the horizontal plane (surge, sway and yaw) is determined by decay tests using the detailed numerical model in SRA (see section 8.1).

### 5.8.2 Hydrostatic stiffness matrix

The hydrostatic stiffness matrix, **K** specifies how the net weight, buoyancy force and moments varies as the vessel experiences heave, roll and pitch motion relative to its datum configuration.

There are two (2) effects which contribute to the **K**. Firstly, *water plane area effects*, account for the change in load due to the change in submerged volume of the vessel as it heaves, rolls and pitches. Secondly, *moment arm effects* refer to the change in moment caused by relative movement of the vessel's centre of gravity and centre of buoyancy as it rolls and pitches. The hydrostatic stiffness matrix is only applicable for small changes in the vessel's position and rotation.

The hydrostatic stiffness matrix from frequency domain analysis in Wadam is presented in Figure 5.7. The hydrostatic restoring coefficient for pitch motion, $C_{55} = 1.138e + 09$ kg m$^2$ $s^{-2}$

$$\mathbf{K} = \begin{array}{c} \begin{matrix} \text{surge} & \text{sway} & \text{heave} & \text{roll} & \text{pitch} & \text{yaw} \end{matrix} \\ \begin{pmatrix} 0 & 0 & 0 & 0 & 0 & 0 \\ 0 & 0 & 0 & 0 & 0 & 0 \\ 0 & 0 & 3.834e+06 & 0 & -371 & 0 \\ 0 & 0 & 0 & 1.138e+09 & 0 & -1.636e+06 \\ 0 & 0 & -371 & 0 & 1.138e+09 & 368.1 \\ 0 & 0 & 0 & 0 & 0 & 0 \end{pmatrix} \end{array} \begin{matrix} \text{surge} \\ \text{sway} \\ \text{heave} \\ \text{roll} \\ \text{pitch} \\ \text{yaw} \end{matrix}$$

**Figure 5.7:** Hydrostatic stiffness matrix.

It is possible to verify the static pitch inclination at rated thrust using $C_{55}$ highlighted in Figure 5.7. The total heeling moment at rated thrust from Equation 4.2 is 195355 kNm. Thus, static pitch inclination

$$(\eta_5)_{static} = \left(\frac{1.95355e+08}{1.138e+09}\right) \cdot \left(\frac{180}{\pi}\right)$$
$$= 9.8^{\circ} \leq 10^{\circ} \tag{5.5}$$

The result of static pitch inclination from hydrodynamic analysis (see Equation 5.5) is closer to what we have obtained ($8.7^{\circ}$) earlier from stability analysis in operation condition (see Figure 4.6). This indicates the correctness of hydrostatic stiffness matrix which will later be used for coupled dynamic Analysis in SRA.

# Chapter 6

# Numerical modelling in SRA

A convenient way to start with the numerical modelling using Simo-Riflex-AeroDyn (SRA) may begin with the output of a frequency domain hydrodynamic analysis program like Wadam or Wamit. Simo is used to model the platform as a rigid body. Hydrostatic stiffness matrix and force transfer functions are directly imported to Simo from pressure panel analysis in Wadam. Riflex is a structural analysis software for slender marine structures. It is used for modelling flexible element like turbine blades, tower and mooring lines. Aerodynamic loads are calculated using NREL AeroDyn [7] (see subsection 1.3.1) which uses either BEM or GDW theory depending upon the wind speed. It can calculate the tower drag forces including the shadow effect. A typical overview of numerical modelling in SRA is shown in Figure 6.1.

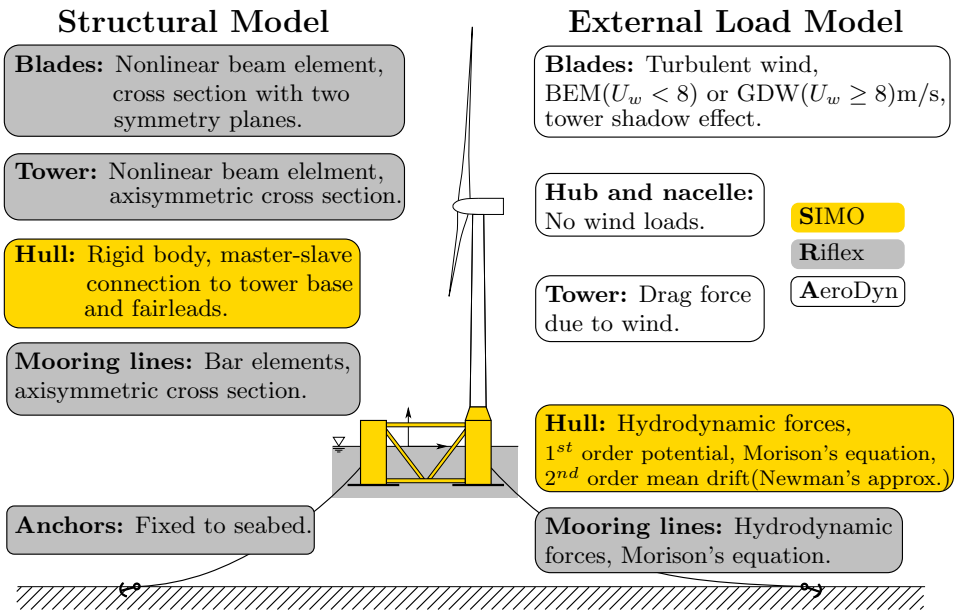


**Figure 6.1:** Modelling overview in SRA.

## 6.1 Simo-Riflex coupled modelling

A general approach to build a coupled Simo-Riflex model for floating wind turbine has been developed by Kvittem, M. and Luan, C. [4, pp. 175-177]. A summary of the modelling procedure is given below:

1. Mass and inertia of the platform are calculated using Sesam GeniE.
2. Hydrodynamic panel method analysis is done in Wadam with mass model (platform including ballast and turbine) and panel model (platform only).
3. Output from Wadam, **G1.SIF** is imported to Simo.
4. In Simo, inside the system description file ("sys-*.dat") following properties are updated.
   (a) Mass and inertia of the platform (see subsection 6.1.1)
   (b) Centre of gravity
   (c) Add specified force (see subsection 6.1.2)
   (d) Modify restoring coefficient obtained from Wadam analysis (see subsection 6.1.3)

### 6.1.1 Platform mass and inertia distribution

GeniE calculates the mass and inertia of a body about it's COG. During coupled dynamic analysis, the global coordinate system is placed at SWL. So, a transformation of platform's mass and inertia are required about the global coordinate system. The COG location of the platform is also updated about the global coordinate system. The mass and inertia properties of tower, turbine and mooring lines are taken care by Riflex.

From physics it is known to us that the inertia of a body is minimum about an axis passing through its COG. So, transformation to the global coordinate system will increase the inertia of the platform. The transformation of mass and inertia properties of the platform is done using parallel axis theorem (see Equation 6.1).

$$(I_{xx})_O = I_{xx} + m(y_G^2 + z_G^2) \tag{6.1a}$$
$$(I_{yy})_O = I_{yy} + m(z_G^2 + x_G^2) \tag{6.1b}$$
$$(I_{zz})_O = I_{zz} + m(x_G^2 + y_G^2) \tag{6.1c}$$
$$(I_{xy})_O = (I_{yx})_O = I_{xy} + mx_G y_G \tag{6.1d}$$
$$(I_{xz})_O = (I_{zx})_O = I_{xz} + mx_G z_G \tag{6.1e}$$
$$(I_{yz})_O = (I_{zy})_O = I_{yz} + my_G z_G \tag{6.1f}$$

Where **O** represents the origin of the global coordinate system, $m$ and **G** $(x_G, y_G, z_G)$ are the mass and COG of the platform.

### 6.1.2 Buoyancy as specified force

Simo assumes the rigid body as neutrally buoyant. In other words, Simo does not account for the buoyancy force automatically from the values imported from Wadam. This is why the buoyancy is given as a specified force at the COB $(x_B, y_B, z_B)$ of the platform. As buoyancy is given as a specified force, the hydrostatic stiffness (linear stiffness matrix in Wadam) shall also be adjusted accordingly. Adjustment of hydrostatic stiffness matrix is described in subsection 6.1.3.

### 6.1.3 Modification of hydrostatic stiffness

Hydrostatic stiffness and its effect on the platform motion is described earlier in chapter 5, subsection 5.8.2. The hydrostatic stiffness matrix obtained from Wadam already contains the complete mass and buoyancy distribution. Thus, modification of platform mass, inertia and addition of buoyancy shall be adjusted according to Equation 6.2 [4, pp. 175-177].

$$C(4,4)^{new} = C(4,4)^{wadam} - \varrho_w g \forall z_b - (-mgz_G) \tag{6.2a}$$
$$C(5,5)^{new} = C(5,5)^{wadam} - \varrho_w g \forall z_b - (-mgz_G) \tag{6.2b}$$
$$C(4,6)^{new} = C(4,6)^{wadam} + \varrho_w g \forall x_b - (mgx_G) \tag{6.2c}$$
$$C(5,6)^{new} = C(5,6)^{wadam} + \varrho_w g \forall y_b - (mgy_G) \tag{6.2d}$$

### 6.1.4 Hydrodynamic modelling in Simo-Riflex

For coupled time domain simulation, the hydrodynamics are modelled as follows:

- First order potential flow added mass, radiation damping and excitation on the hull
- No additional linear damping on the hull
- Viscous (quadratic) damping on the columns ($C_D = 1.0$)
- Viscous (quadratic) damping on the heave plates ($C_D = 2C_q\varrho_w A^{proj} = 7.5$) [15]
- Morison forces on the mooring lines
  - Chain: $C_D = 2.4, C_a = 1$ linear damping 1.15
  - Polyester rope: Chain: $C_D = 1.6, C_a = 1$ linear damping 1.15

### 6.1.5 Retardation function

The non-linearity of the system is taken into account by solving the equation of motion in time domain. Thus, equation of motion in frequency domain is transformed into time domain. During transformation, an impulse response function is introduced into the equation of motion. It is often termed as 'memory function'. It accounts for the frequency dependent added mass and linear damping of the system in time domain.

The retardation function is approximated by the numerical solution of the integral described by Equation 6.3

$$h_{ij}(\tau) = -\frac{2}{\pi}\int_0^\infty (B_{ij}(\omega) - B_{ij}(\infty))\cos(\omega\tau)d\omega \tag{6.3}$$

Retardation function for surge (1,1) and heave (3,3) are shown in Figure 6.2. Similar plots for pitch (5,5) and yaw (6,6) are presented in Figure 6.3. It is observed that amplitudes for rotational motions are about 1000 times larger than amplitudes in translational motion.

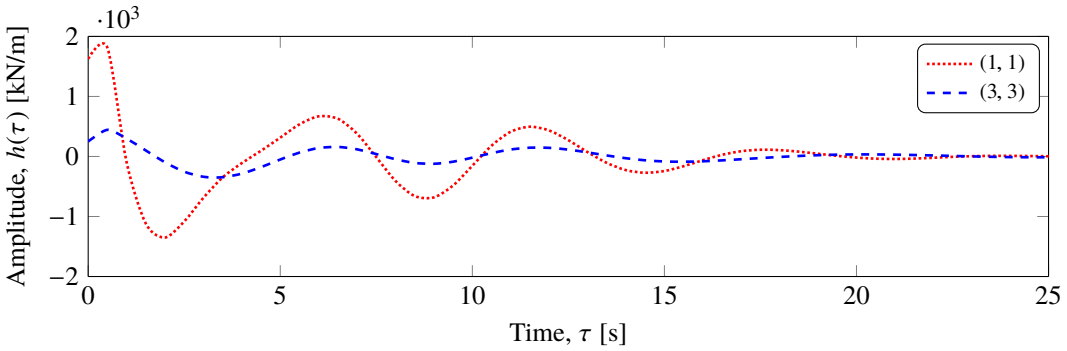


**Figure 6.2:** Retardation function for surge and heave.

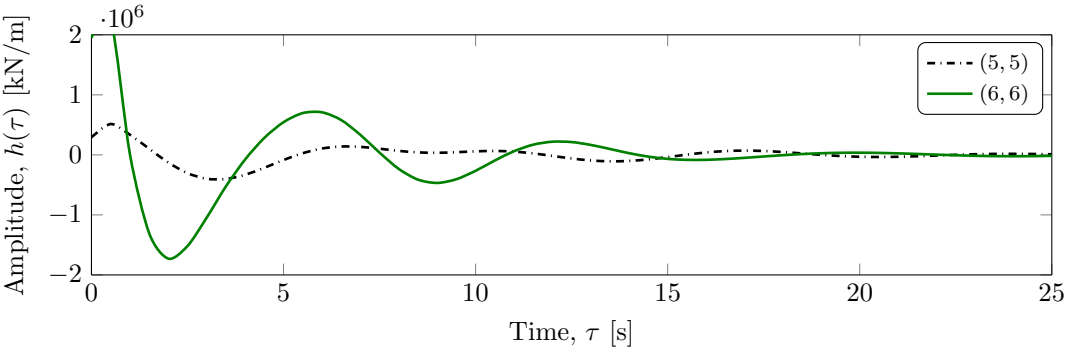


**Figure 6.3:** Retardation function for pitch and yaw.

## 6.2 Aerodynamic modelling

Aerodynamic modelling of the DTU 10MW RWT is done by NREL AeroDyn v12.5. AeroDyn is an element-level wind turbine aerodynamic analysis routine which can calculate aerodynamic load on blade elements at a given location and time using the input provided by its user. It may also provides a straightforward interface to various dynamic codes in order to perform a fully coupled dynamic analysis.

A typical scheme for calculating aerodynamic load using AeroDyn is shown in Figure 6.4.

## 6.3 Input into AeroDyn

AeroDyn calculates the aerodynamic loads on wind turbine blade elements based on velocities and positions provided by dynamic analysis routines and simulated wind inputs. To be more

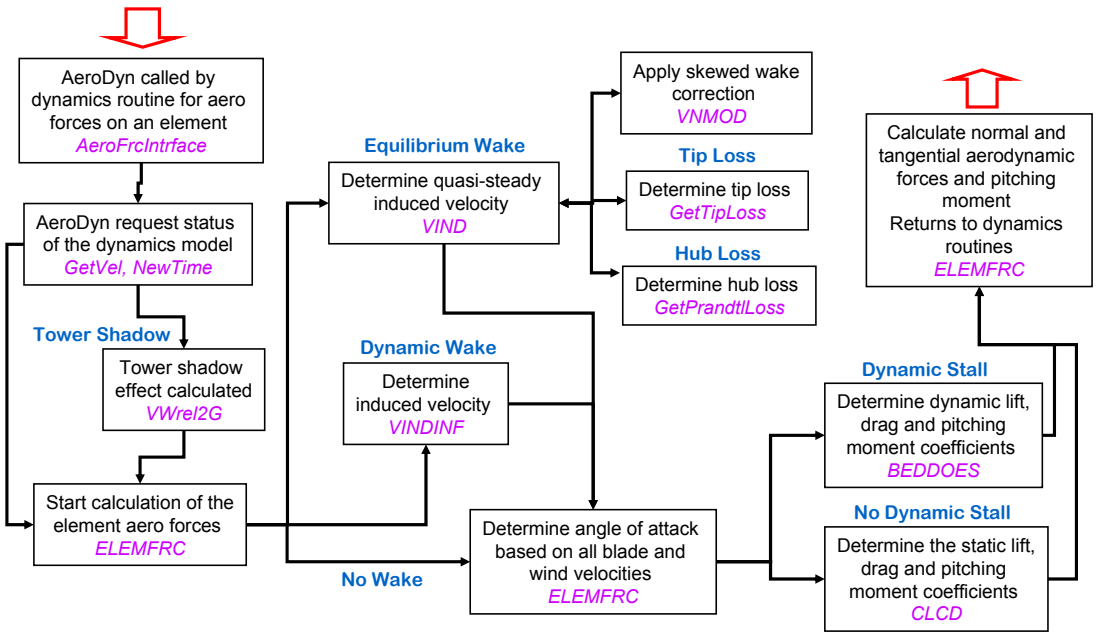


**Figure 6.4:** Typical scheme for calculating normal and tangential load on a blade element using AeroDyn. *(Aerodyn presentation slide, Jason Jonkman and Pat Moriarty)*

specific, AeroDyn requires information on the status of a wind turbine from the dynamics analysis routine and returns the aerodynamic loads for each blade element to the dynamics routines.

### 6.3.1 Aerodynamic coefficients

Aerodynamic coefficients ($C_l, C_d$ and $C_m$) are usually obtained from wind tunnel tests. But for the case of 10MW DTU RWT, aerodynamic coefficients are the result of 2D CFD calculations for AOA $[-32° : +32°]$. Coefficients for AOA $[\pm 45° : \pm 180°]$ are generated based on flat plate approximation of airfoil section and coefficients for AOA within $[\pm\ 32° : \pm\ 45°]$ are interpolated values from CFD calculation and flat plate approximation.

### 6.3.2 Location of airfoil sections

Table 6.1 shows the location of airfoil sections along blade's pitch axis based on their relative thickness. NACA0015 airfoil section is used for closing blade tip for $r/R > 0.99$.

### 6.3.3 Discretization of blade

Discretization of each blade is done using 26 blade elements for integration of the aerodynamic forces. Blade elements have smaller length in region with high aerodynamic gradients which is normally around the blade tip.

Distributed aerodynamic properties of turbine blades, for instance, twist and chord values at nodes shown in Table 6.2 are re-calculated using the cubic spline interpolation function fitted through the DTU 10MW blade planform properties [2].

**Table 6.1:** Location of airfoil sections along blade span.

| airfoil section | input file | $t/c$ | rotor span |
|---|---|---|---|
| cylinder | cylinder.dat | 100 % | 2.8 m |
| FFA-W3-600 | ffa-w3-600.dat | 60 % | 17.1 m |
| FFA-W3-480 | ffa-w3-480.dat | 48 % | 20.8 m |
| FFA-W3-360 | ffa-w3-360.dat | 36 % | 28.1 m |
| FFA-W3-301 | ffa-w3-301.dat | 30.1 % | 36.3 m |
| FFA-W3-241 | ffa-w3-241.dat | 24.1 % | 63.7 m |
| NACA0015[(a)] | | | 88.3 m |

[(a)] used for closing blade tip ($\frac{r}{R} > 0.99$)

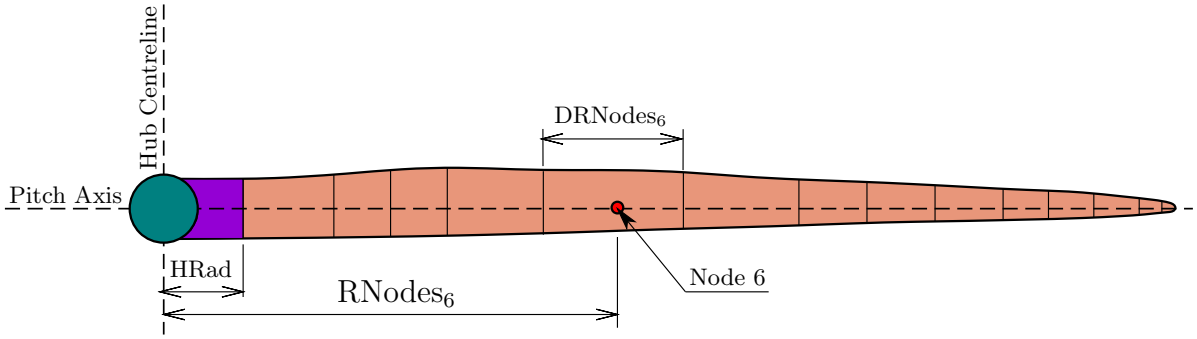


**Figure 6.5:** Blade layout and element discretization [26]

### 6.3.4 Wind file

In order to run a simulation using AeroDyn, a wind input file is required. There are two (2) types of wind input files.

- hub-height (HH) wind files. HH wind files can be generated using IECwind.
- full-field (FF) turbulence files, a simulated full-field wind data that represent all three components of the wind vector varying in space and time. Two files, one binary wind data file (*.wnd) and one summary file (*.sum), must be in the specific form generated by the NREL program Turbsim.

## 6.4 Output from AeroDyn

AeroDyn creates only one output file, the element file, which is optional. Other output files are controlled by the dynamics routines. The element file is a tab-delimited time-series file containing wind and aerodynamic data for the elements selected in the “aerodyn.ipt” file.

## 6.5 Simulation schematic

A coupled dynamic simulation work-flow using Simo-Riflex-AeroDyn is shown in Figure 6.6 and a list of files required to run dynamic analysis in SRA Table 6.3.

**Table 6.2:** Distributed blade aerodynamic properties.

| Node | RNodes [m] | AeroTwst [deg] | DRNodes [m] | Chord [m] | Airfoil Table [-] |
|---|---|---|---|---|---|
| 1 | 4.300000 | 14.500000 | 3.000000 | 5.380000 | ffa-w3-Cyl |
| 2 | 7.300000 | 14.500000 | 3.000000 | 5.380000 | ffa-w3-Cyl |
| 3 | 9.300020 | 14.499410 | 1.000040 | 5.392083 | ffa-w3-Cyl |
| 4 | 10.650275 | 14.451589 | 1.700470 | 5.435962 | ffa-w3-Cyl |
| 5 | 12.351255 | 14.249685 | 1.701490 | 5.526866 | ffa-w3-Cyl |
| 6 | 14.103300 | 13.819985 | 1.802600 | 5.648624 | ffa-w3-Cyl |
| 7 | 15.505550 | 13.272131 | 1.001900 | 5.756729 | ffa-w3-Cyl |
| 8 | 16.908250 | 12.525999 | 1.803500 | 5.866075 | ffa-w3-Cyl |
| 9 | 19.412550 | 10.925934 | 3.205100 | 6.040336 | ffa-w3-600 |
| 10 | 22.616450 | 9.066472 | 3.202700 | 6.174607 | ffa-w3-480 |
| 11 | 25.818350 | 7.844984 | 3.201100 | 6.204512 | ffa-w3-480 |
| 12 | 29.019100 | 7.042235 | 3.200400 | 6.148891 | ffa-w3-360 |
| 13 | 32.219350 | 6.401402 | 3.200100 | 6.025425 | ffa-w3-360 |
| 14 | 35.419550 | 5.801489 | 3.200300 | 5.849905 | ffa-w3-360 |
| 15 | 40.020050 | 4.959678 | 6.000700 | 5.537415 | ffa-w3-301 |
| 16 | 46.221050 | 3.755047 | 6.401300 | 5.051513 | ffa-w3-301 |
| 17 | 52.622450 | 2.412591 | 6.401500 | 4.507604 | ffa-w3-301 |
| 18 | 59.023850 | 1.109606 | 6.401300 | 3.957483 | ffa-w3-301 |
| 19 | 65.425000 | -0.056212 | 6.401000 | 3.424737 | ffa-w3-241 |
| 20 | 71.825800 | -1.095113 | 6.400600 | 2.923096 | ffa-w3-241 |
| 21 | 78.426350 | -2.058340 | 6.800500 | 2.450441 | ffa-w3-241 |
| 22 | 82.576650 | -2.619175 | 1.500100 | 2.142015 | ffa-w3-241 |
| 23 | 84.076900 | -2.814934 | 1.500400 | 1.996255 | ffa-w3-241 |
| 24 | 85.577250 | -3.007481 | 1.500300 | 1.817980 | ffa-w3-241 |
| 25 | 87.077550 | -3.197100 | 1.500300 | 1.583291 | ffa-w3-241 |
| 26 | 88.496600 | -3.374032 | 1.337800 | 1.155488 | ffa-w3-241 |

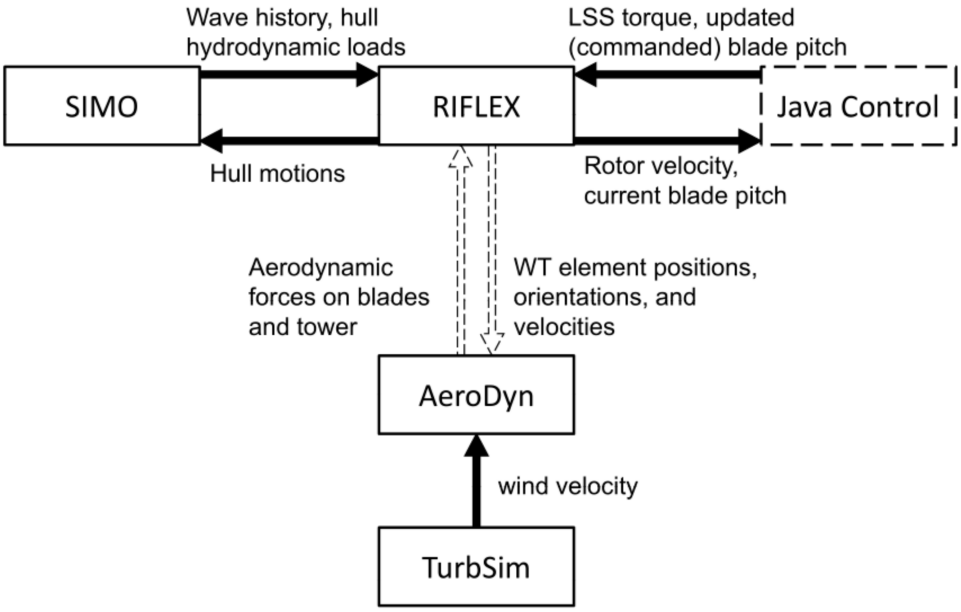


**Figure 6.6:** Dynamic simulation in Simo-Riflex-AeroDyn (SRA) [27]

**Table 6.3:** Required file to run SRA simulation and their functions.

| File name | Function |
|---|---|
| start_dos | Start a DOS shell |
| RunSRAlog.bat | Run simulation and crate a log file |
| aerodyn.ipt | AeroDyn input file |
| AD_DLL_inputs | AeroDyn dynamic link library |
| AirfoilLibrary.dat | Airfoil data file |
| DTU10MW.jar | Turbine control file |
| Controllinput.txt | Input to control file |
| sys_Semi.dat | System description file in SIMO |
| Semi_inpmod.inp | Riflex input file (FEM) |
| Semi_stamod.inp | Simo static analysis input file |
| Semi_dynmod.inp | Dynamic analysis parameters, procedure and force response storage |
| DYN_Semi.MAC | Simo macro file for dynamic solution |
| S2X-Semi.MAC | Output configuration file |
| STA-Semi.MAC | Simo macro file for static solution |

# Chapter 7

# Mooring system design

Stationkeeping and motion control is one of the most important aspect of marine operations. Mooring system is used as a means to control the offset of a platform due to combined actions of wind, wave and current. It reduces platform's movement by introducing mooring stiffness (both linear and non-linear) into the equation of motion (see Equation 2.34). Linear stiffness of a catenary mooring line is a function of it's weight in water, water depth at site and pretension in the line. On the other hand, the non-linear stiffness, often refer to geometric stiffness is a result of change in geometry of the mooring lines.

## 7.1 Catenary mooring system

Catenary mooring equations are due to O'Brien and Francis [28]. However, a detail analysis of a catenary mooring system is described by Faltinsen [21].

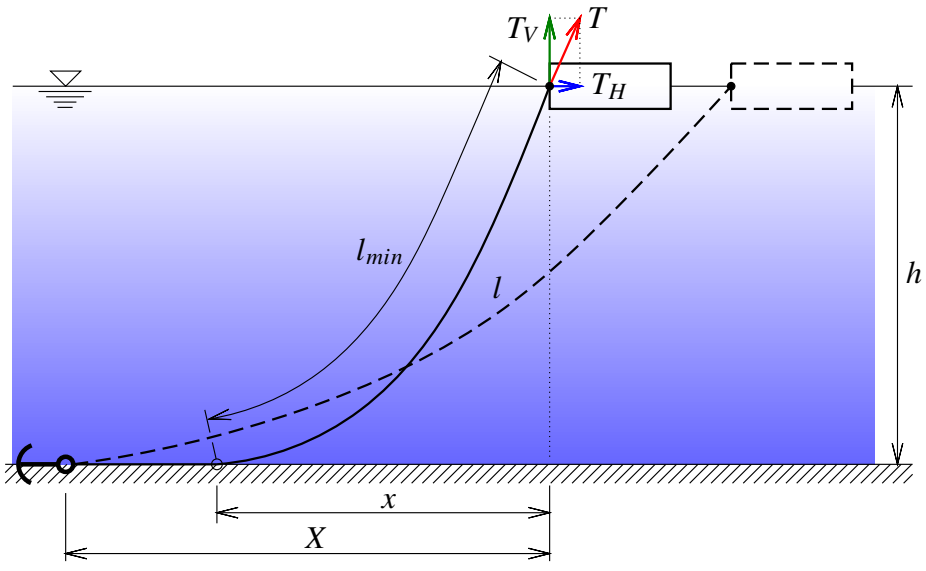


**Figure 7.1:** Illustration of line characteristics of a catenary mooring system.

A typical catenary moored barge structure is shown in Figure 7.1. $h$ is the depth from fairlead to seabed, $x$ is the horizontal scope and $X$ is the horizontal distance from fairlead to anchor

touchdown point. $l$ is the total length of mooring line and $l_{min}$ is hanging length in water. Key equations of a catenary mooring system with elasticity are as follows:

Horizontal force for a given fairlead tension, $T$:

$$T_H = AE\sqrt{\left(\frac{T}{AE}+1\right)^2 - \frac{2wh}{AE}} - AE \tag{7.1}$$

Minimum line length required (or suspended length for a given fairlead tension) for gravity anchor:

$$l_{min} = \left(\frac{1}{w}\right)\sqrt{T^2 - T_H^2} \tag{7.2}$$

Vertical force at the fairlead:

$$T_V = wl_{min} \tag{7.3}$$

Horizontal scope (length in plan view from fairlead to touchdown point):

$$x = \left(\frac{T_H}{w}\right)\sinh^{-1}\left(\frac{wl_{min}}{T_H}\right) + \frac{T_H l_{min}}{AE} \tag{7.4}$$

Anchor locations can be found using Equation 7.5.

$$X = l - l_{min} + x \tag{7.5}$$

## 7.2 Mooring configuration

Many different mooring configurations are possible which can arise from the operational requirements and cost drives. A catenary mooring system can be a combination of steel chain and rope or the chain alone. Often, polyester rope is used between chain segment to reduce the weight of the mooring system so that the platform can carry more payload. A catenary spread mooring system with three (3) lines is selected for the rest of the analysis.

A typical arrangement of a catenary spread moored semi-submersible platform is shown in Figure 7.2. $(x_i, y_i, z_i)$, $(i = 1 \cdots 3)$ are the coordinates of the fairlead location, $T_H$ is horizontal tension in mooring lines and $R$ represent the radius to anchors from fairleads. Table 7.1 presents various configuration data of mooring lines which are required for preliminary design.

## 7.3 Preliminary design of mooring system

For preliminary design of the mooring system, only linear static analysis is performed. During preliminary design of a catenary mooring system, it is assumed that following parameters are known and used as input for designing the mooring system.

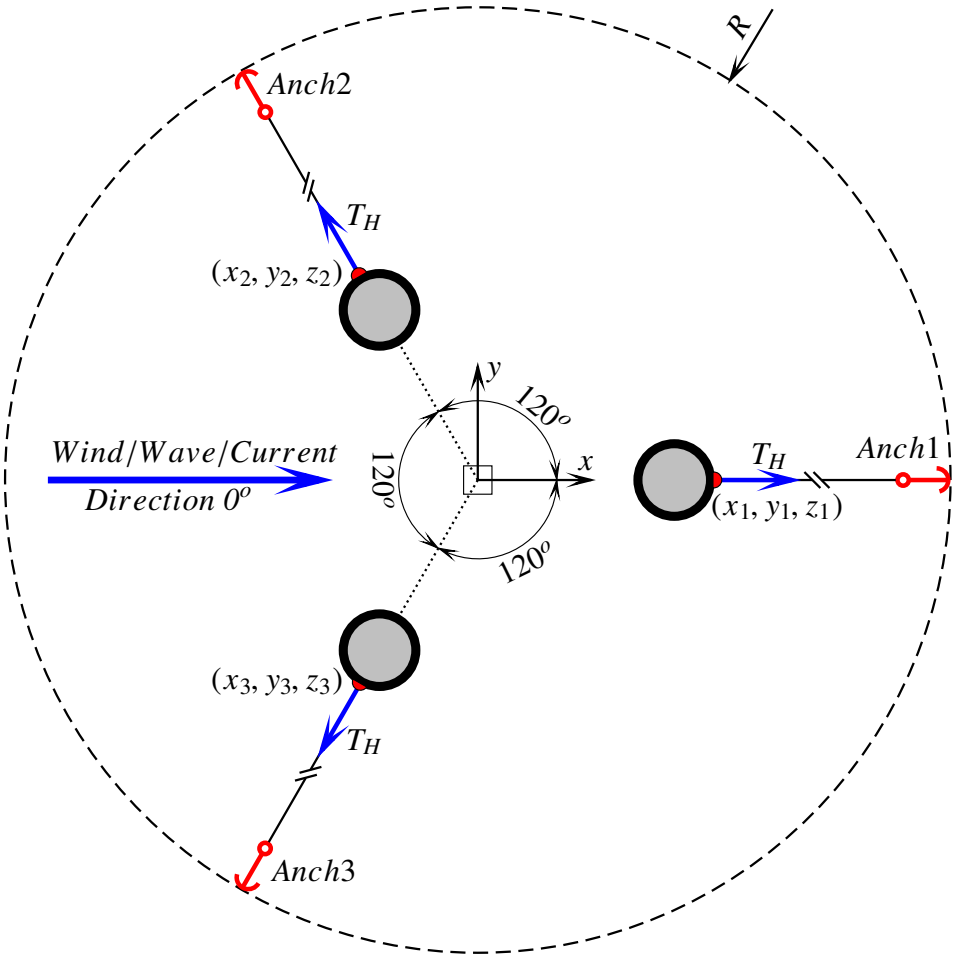


**Figure 7.2:** Mooring arrangement of 10MW semi-submersible platform (top view).

**Table 7.1:** Mooring configuration.

| | | |
|---|---|---|
| Number of mooring lines | 3 | [-] |
| Angle between adjacent mooring lines | 120 | [deg] |
| Water depth at site | 200 | [m] |
| Depth from fairlead to seabed | 181.5 | [m] |
| Radius to anchors from platform centre | 902.2 | [m] |
| Radius to fairleads from platform centre | 41.04 | [m] |
| Unstretched mooring line length | 861.2 | [m] |
| Mooring line angle at fairlead | 43 | [deg] |
| Pretension in mooring lines | 1020 | [kN] |

- line weight in water, $w$
- axial stiffness, $EA$
- water depth at site, $h$

Empirical analysis suggests that the horizontal length of mooring lines from anchor to fairlead position is usually 5-20 time of water depth in site location.

## 7.4 Design requirements

The main purpose of mooring system design is to satisfy following requirements:

### 7.4.1 Stiffness requirement

Stiffness of the mooring system shall be sufficient to limit the horizontal offset of the platform within allowable limit. In addition to that, it should not excite the slow-drift motion (difference-frequency) of the platform.

### 7.4.2 Strength requirement

Strength of the mooring lines shall be adequate to resist the maximum designed tension for the mooring lines. In other words, tension in the mooring lines shall have a lower value (accounts proper factor of safety) than the breaking strength of the mooring chain.

## 7.5 Chain properties

For a catenary mooring system, stiffnesses are due to the tension in mooring lines and arises from their weight in water. As tension in the lines may very within broad range, geometric stiffness is important and shall be taken into account properly. On the other hand, bending stiffness of mooring chain is considered negligible. Hydrodynamic and mechanical properties of studless R4 type mooring chain are listed in Table 7.2.

**Table 7.2:** Mooring chain properties.

| | | |
|---|---|---|
| Chain type | studless R4 | |
| Chain diameter | 153 | [mm] |
| Mass/Length | 466 | [kg/m] |
| Axial stiffness | 2.00E+06 | [kN] |
| Bending stiffness | 0 | [kN] |
| Minimum breaking loads | 2.04E+04 | [kN] |
| Normal drag coefficient | 2.4 | [-] |
| Axial drag coefficient | 1.15 | [-] |
| Normal added mass coefficient | 1 | [-] |
| Axial added mass coefficient | 0.5 | [-] |
| Friction coefficient | 0.4~0.8 | [-] |

## 7.6 Catenary mooring design algorithm

Freely hanging catenary is much more suitable for applying an computer algorithm. A computer program has been written to solve Equation 7.1 to Equation 7.5 in order to obtain the design parameters for the mooring system. Mooring chain properties are taken from Table 7.2. It is also possible to design the preliminary mooring system without considering the elastic properties of the mooring lines.

1. Assume a tension $T$ ($> wh$) in the mooring line and solve for $T_H$ using Equation 7.1
2. Use $T$ and $T_H$ obtained previously in Equation 7.2 and get $l_{min}$
3. Determine vertical force $T_V$ using Equation 7.3
4. Solve Equation 7.4 to obtain the value of horizontal scope $x$
5. Finally solve Equation 7.5 to get $X$ which requires few iterations.

As the fairlead positions are known, we only need to know the length of a mooring line $l$ and anchor touchdown point in sea bed $X$. The value of $l$ is 902.2 m and $X$ is 872.1 m. Mooring line angles and static tension values are shown in Table 7.1.

# Chapter 8

# Coupled dynamic analysis

Coupled dynamic analysis is performed to predict the response of the floating wind turbine system in a stochastic environment composed of wind and wave. It also accounts for the non-linearity in wave loading on the submerged floater and the aerodynamic loading on the rotor.

Simo-Riflex-AeroDyn (SRA) is used for the coupled dynamic analysis. SRA combines the power of SIMO in hydrodynamics, Riflex takes advantage of non-linear FEM and AeroDyn accounts for the aerodynamics of turbine blades using BEM. An effective guideline to perform coupled dynamic analysis using SRA is described in detail by Bachynski [27].

Coupled time domain simulations are performed as decay test, constant wind test and turbulent wind test. Decay test is for determining the period of resonance in horizontal plane and the damping in the system. Constant wind test to analyze the performance of the rotor and turbulent wind tests are done to investigate the floater and turbine response during operation at site.

## 8.1 Free decay test

Free decay tests are performed for system identification. Natural periods of the platform in horizontal plane (surge, sway and yaw) are determined by decay tests using the detailed numerical model in SRA. Moreover, natural periods in heave, roll and pitch can be verified with the frequency domain results from Wadam.

During decay tests, an excitation (force or moment) is applied on the platform in it's centre of gravity for a shorter period ($200 \sim 300s$) of time. The applied excitation is a combination of ramp (constant derivative) and constant force or moment. Next, the platform is released to perform a free oscillation. The motion of the platform will die out with time due to the presence of damping (both linear and quadratic) in the system.

The decaying motion of the platform is recorded as a time series. This time series can further be processed to find out the logarithmic decrement, $\delta$ using Equation 8.1

$$\delta = \frac{1}{n} \ln \frac{\eta_0}{\eta_n} \tag{8.1}$$

The logarithmic decrement is used to calculate the damping ratio, $\zeta$ from the Equation 8.2

$$\zeta = \frac{1}{\sqrt{1 + (\frac{2\pi}{\delta})^2}} \tag{8.2}$$

Finally, the damping ratio can be used to determine the natural period of oscillation, $T_n$ of the platform for a particular motion using Equation 8.3. Where $T_d$ is the damped period of oscillation and usually measured from experiment.

$$\begin{aligned} T_d &= \frac{2\pi}{\omega_d} = \frac{2\pi}{\omega_n \sqrt{1-\zeta^2}} = \frac{T_n}{\sqrt{1-\zeta^2}} \\ T_n &= T_d \sqrt{1-\zeta^2} \end{aligned} \tag{8.3}$$

During simulation, no environmental forces (wind, wave and current) are applied on the system and the turbine is kept parked to ensure that no aerodynamic or hydrodynamic forces acted on the platform during decay tests.

Time history of decay tests in surge, heave, pitch and yaw are presented in Figure 8.1. Transient motions of the platform at the beginning of simulation were skipped during calculation. Mean natural periods in surge, heave, pitch and yaw are listed in Table 8.1. It can be seen that the mean natural periods are in close agreement with typical offshore semi-submersible platform.

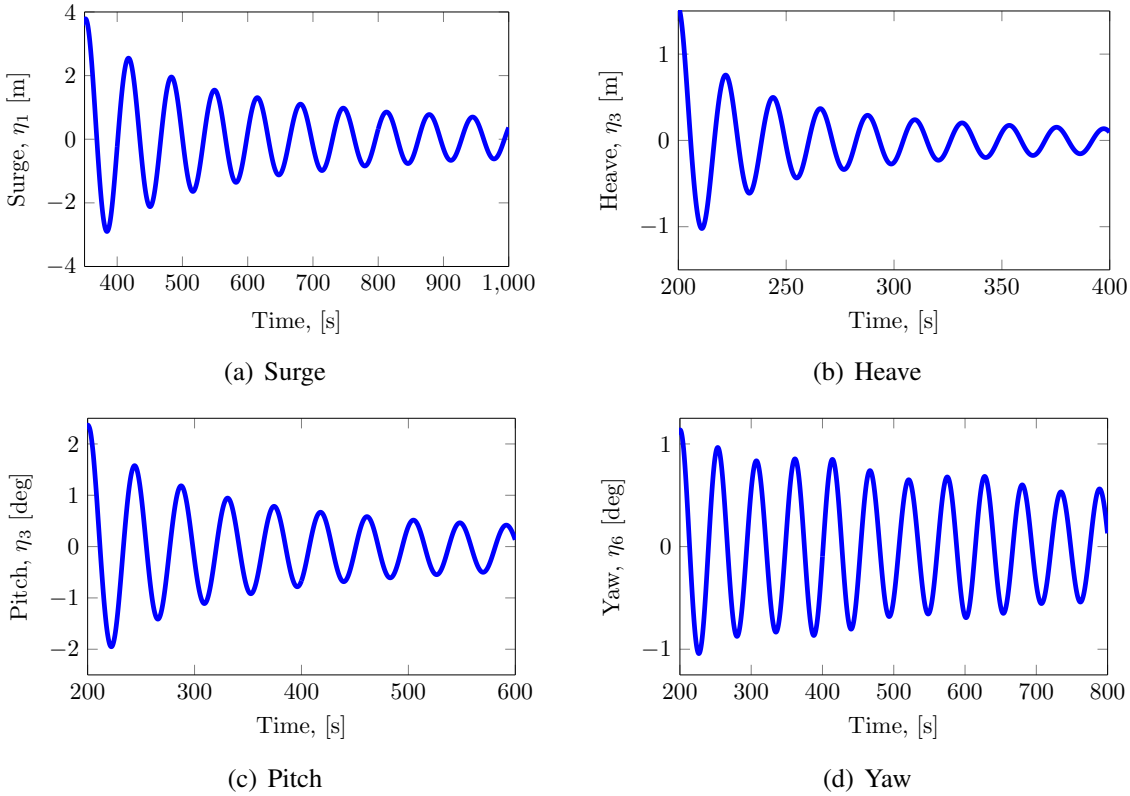


(a) Surge (b) Heave

(c) Pitch (d) Yaw

**Figure 8.1:** Platform response in decay test.

A comparison can be made between the frequency domain eigenperiods for 10MW semi-submersible platform (see Table 5.1) and the natural periods obtained from decay test (Table 8.1). It shall be noted that the frequency domain analysis in Wadam does not include the mooring lines. It is seen that for heave and pitch motion, the natural period from decay test are a bit higher (for pitch) than that obtained from frequency domain results. The reason is the increased mass and pretension in the mooring lines.

**Table 8.1:** Decay test results.

| Motion | $t_0$ | $\eta_0$ | $t_n$ | $\eta_n$ | n | $\delta$ | $\zeta$ | $T_d$ | $T_n$ |
|---|---|---|---|---|---|---|---|---|---|
| Surge | 417.4 | 2.5480 | 944.6 | 0.6979 | 8 | 0.162 | 0.026 | 65.900 | 65.878 |
| Heave | 221.9 | 0.7566 | 397.2 | 0.1355 | 8 | 0.215 | 0.034 | 21.913 | 21.900 |
| Pitch | 243.9 | 1.5764 | 589.6 | 0.3997 | 8 | 0.172 | 0.027 | 43.213 | 43.196 |
| Yaw | 253.1 | 0.9651 | 680.2 | 0.6009 | 8 | 0.059 | 0.009 | 53.388 | 53.385 |

## 8.2 Constant wind test

The purpose of constant wind test is to study the mean offsets of the platform in surge, sway and yaw which help to design an effective mooring system to restrict platform's motion within allowable limit. This test is also considered as a means to test the performance of the turbine including controller.

During constant wind simulations, a constant uniform wind field is applied perpendicular to the rotor plane for at least $800s$ and the turbine was fully operational. By fully operational we mean the turbine can rotate about it's axis and blade pitch can be adjusted by the controller depending upon wind speed to maximize power output. No wave force is applied during constant wind simulations.

**Table 8.2:** Platform motions and turbine characteristics as a function of wind speed from SRA simulation.

| wind speed $[m/s]$ | Surge $[m]$ | Pitch $[deg]$ | Rot. speed $[rad/s]$ | Thrust $[kN]$ | Torque $[kNm]$ | M. Power $[kW]$ | Bl. pitch $[deg]$ |
|---|---|---|---|---|---|---|---|
| 4 | 2.440 | 2.229 | 0.6280 | 296.6 | 248 | 156 | 0 |
| 6 | 4.236 | 3.890 | 0.6280 | 498.6 | 2116 | 1329 | 0 |
| 8 | 6.760 | 6.150 | 0.7012 | 774.6 | 4846 | 3398 | 0 |
| 10 | 11.026 | 10.096 | 0.8997 | 1245.7 | 7976 | 7174 | 0 |
| 11 | 13.187 | 12.129 | 1.0050 | 1488.5 | 9336 | 9385 | 0 |
| 12 | 15.030 | 9.813 | 1.0326 | 1229.2 | 10321 | 9402 | 3.646 |
| 14 | 7.394 | 7.642 | 0.9904 | 974.5 | 10178 | 10000 | 8.721 |
| 16 | 7.760 | 6.579 | 1.0102 | 746.4 | 9889 | 10000 | 12.180 |
| 18 | 7.203 | 6.000 | 1.0023 | 702.4 | 10003 | 10000 | 14.381 |
| 20 | 6.944 | 5.623 | 1.0038 | 645.1 | 9968 | 10000 | 16.567 |
| 22 | 6.753 | 5.418 | 1.0052 | 597.1 | 9952 | 10000 | 18.669 |
| 24 | 6.673 | 5.328 | 1.0055 | 564.8 | 9950 | 10000 | 20.582 |

### 8.2.1 Surge and pitch motion

Mean offset of the platform in surge and pitch are shown in Figure 8.2. Surge motion usually has longer period than pitch motion. It results from different frequency wave loads. The period of surge motion, $T_{n1}$ can be adjusted by changing the properties of the mooring system, for instance, weight of mooring lines, material properties and pretension from winch. On the other hand, pitch motion is related to the hydrostatic stiffness of platform. It depends upon the geometry of the platform and mass distribution.

Figure 8.2 (top) shows rapid increase of surge motion with the increase of wind speed until the rated wind speed is reached. After rated wind speed, surge motion reduces dramatically and remains almost constant for higher values of wind speed.

The pitch motion of the platform Figure 8.2 (bottom) also shows similar trend like surge motion but no drastic reduction is observed near rated wind speed.

The reason of higher platform response can be explained by the values of thrust around rated wind speed listed in Table 8.2. It is also noted that the maximum value of surge and pitch motion are about 12 m and 15° which result near rated wind speed.

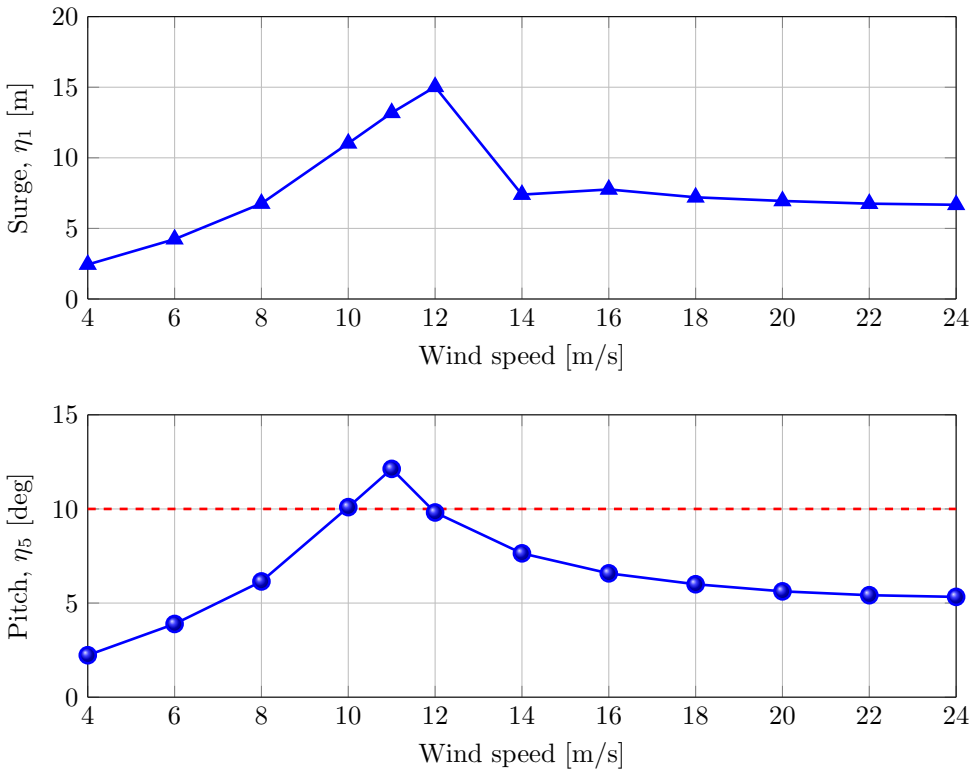


**Figure 8.2:** Mean offset of the platform in surge and pitch motion.

As the platform is designed to operate at a pitch angle lower than 10°, it is possible to control the extra inclination by adopting an active ballast system as described by Roddier [20]. The active ballast system keeps the rotor plane perpendicular to the wind field to maximize power output by exchanging the ballast between forward and aft tanks.

### 8.2.2 Power and thrust curve

Figure 8.3(a) and Figure 8.3(b) present a comparison of mean mechanical power and mean thrust between the DTU 10MW land-based turbine and floating turbine. Power and thrust values for land based turbine resulted from HAWCStab2 simulation which is based on BEM and taken from [2]. For the semi-submersible platform, values of power and thrust are obtained from constant wind simulation using SRA.

It is seen from Figure 8.3(a) that below rated wind speed, both the land-based and floating turbine maintain a close relationship. But at rated and above rated wind speeds, floating turbine cannot reach the rated value of 10MW. This happens because of pitch motion of the platform. Due to pitch motion, the rotor plane does not remain perpendicular to the wind direction but makes an angle of $\sim 7^{\circ}$, the same angle of pitch inclination.

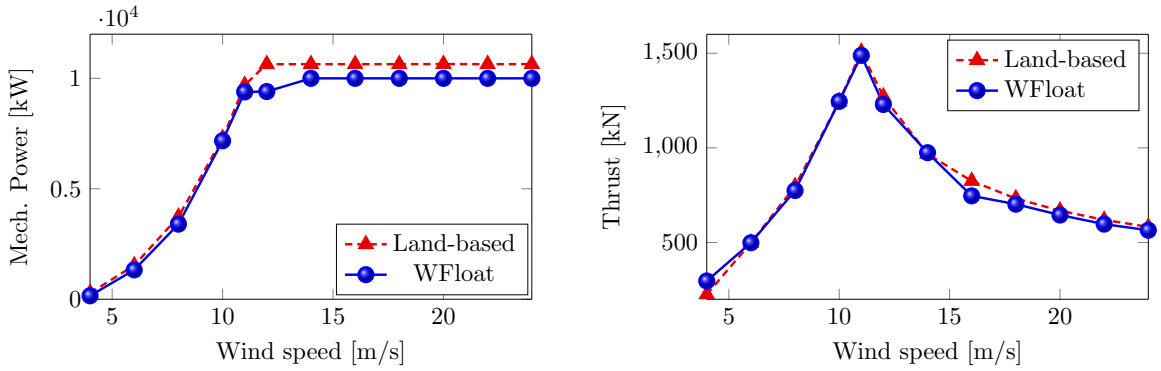


(a) Mech. Power

(b) Thrust

**Figure 8.3:** Comparison of thrust curve of the land-based and floating wind turbine.

It is possible to compare the generated power by multiplying the mechanical power with a generator efficiency. Bak et al. [2] suggested typical values for the DTU 10MW RWT is around 0.94.

### 8.2.3 Power and thrust coefficients

It is convenient to compare the rotor performance of land-based turbine with the floating one using power coefficient. Power and thrust coefficient are defined using Equation 8.4a and Equation 8.4b respectively.

$$C_P = \frac{\text{Rotor power}}{\text{Power in the wind}} = \frac{P}{\frac{1}{2}\varrho_a A U^3} \tag{8.4a}$$

$$C_T = \frac{\text{Thrust force}}{\text{Dynamic force}} = \frac{T}{\frac{1}{2}\varrho_a A U^2} \tag{8.4b}$$

Power coefficient can reach as maximum as to Betz limit ($16/27 = 0.5926$), the theoretical maximum value. But in reality it is not possible to reach Betz limit due to following unavoidable facts.

- rotation of the wake behind the rotor

- finite number of blades
- non-zero aerodynamic drag

Power and thrust coefficients are plotted as a function of wind speed in Figure 8.4(a) and Figure 8.4(b) respectively. Power coefficient curve shows that the floating turbine performance is better at and above rated wind speed though it is always less efficient than the land-based turbine due to it's pitch inclination.

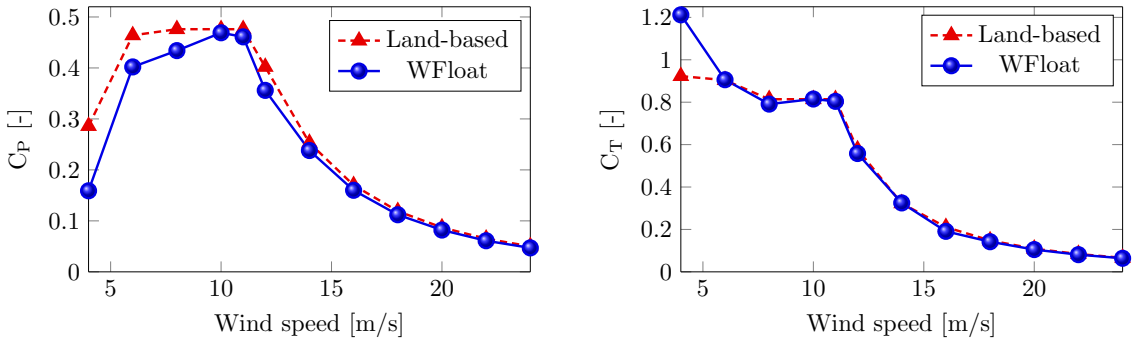


(a) Power coefficient

(b) Thrust coefficient

**Figure 8.4:** Comparison of power and thrust coefficient of the land-based and floating wind turbine.

For the case of thrust coefficient, land-based turbine and floating wind turbine have match. At very lower values of wind speed, for instance, at 4 m/s, thrust coefficient shows value greater than 1.0 which is unrealistic.

## 8.3 Turbulent wind test

Turbulent wind tests are performed to asses the platform and turbine responses, for example motions of the platform, mooring line tension, bending moment at tower base and out-plane bending moment at blade root. Moreover, turbine and controller performances are also checked for a specific site condition.

From a joint distribution of wind, wave and current, few combinations are chosen based on contour line method. Then one hour simulation is run for each sea states. During turbulent wind test following assumptions are made:

- unidirectional wind and waves are assumed along positive $x-$ axis.
- spatial variation of wind speeds are along positive $x-$ axis perpendicular to rotor plane.
- no current is assumed over the draft of the platform.

### 8.3.1 Site location

Figure 8.5 presents the potential locations of five (5) European offshore sites. NTM design load cases are studied only for Norway 5 (marked 14 on the map).


**Figure 8.5:** Site location for turbine installation.

### 8.3.2 Environmental conditions

The environmental conditions which are used to asses platform's characteristics are presented in Table 8.3. NTM DLC's are based on IEC 61400-3 standard [29]. OP1, OP2 and OP3 are based on power production mode (DLC 1) and EWM is based on parked (stand still or idling) condition,DLC 6. It is a no fault condition.

- OP1, below rated wind speed
- OP2, at rated wind speed
- OP3, above rated wind
- EWM, extreme wind speed model (50-yr recurrence)

**Table 8.3:** Environmental conditions for NTM and EWM design load case (DLC).

| Env. cond. | Wind speed [m/s] | $H_s$ [m] | $T_p$ [s] | Turb. Intensity [-] | Turbine status [-] |
|---|---|---|---|---|---|
| OP1 | 8 | 2.0 | 10.3 | 0.17 | operating |
| OP2 | 11.4 | 2.5 | 10.2 | 0.15 | operating |
| OP3 | 18 | 4.1 | 10.5 | 0.13 | operating |
| EWM | 40 | 15.6 | 14.5 | 0.11 | parked |

### 8.3.3 Platform motions

Platform motions in surge and pitch under turbulent wind condition (OP3) are plotted in Figure 8.6. Transient motions of the platform in the beginning of simulation are skipped in the plot. Maximum motions of the platform in surge and pitch are about 7 m and 10.5° respectively. Mean values of platform motions can be found from Table 8.4. Moreover, power spectrum investigation of platform motions are discussed in section 8.4.

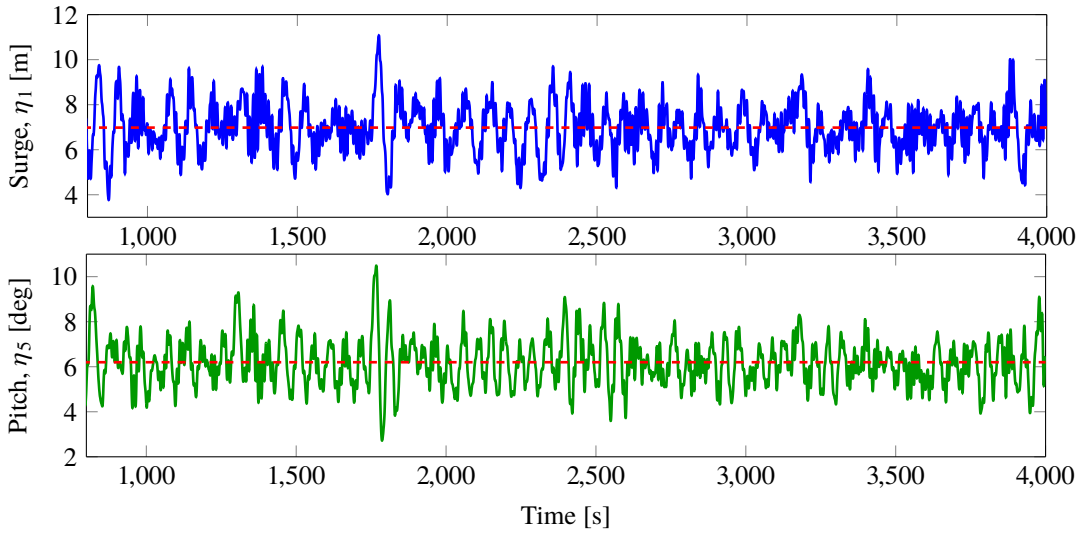


**Figure 8.6:** Platform motion history in surge (above) and pitch (below) under turbulent wind conditions (OP3).

Rotor and controller performance of the turbine under OP3 environmental condition is presented in Figure 8.7. The top sub-figure shows the turbulent wind speed, in the middle, variation of blade pitch, and generated power is shown in the bottom. It is worth noting that blade pitch is smoothly adjusted by the controller with the variation in wind speed to produce constant power. The rotor cannot produce rated power (10MW) because the relative wind velocity experienced by turbine blades are lower than it should be due to pitch inclination of the platform.

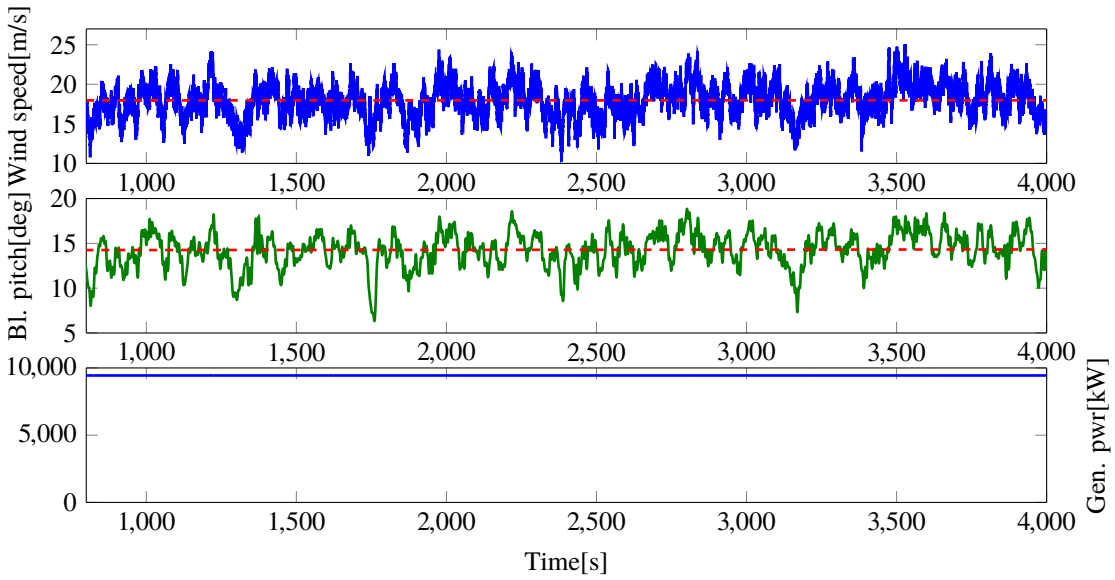


**Figure 8.7:** Rotor and controller performance in terms of generated power and blade pitch in turbulent wind conditions (OP3).

**Table 8.4:** Results of turbulent wind test.

| Env. cond. | Mean surge [m] | Mean pitch [deg] | Rotor speed [rad/s] | Thrust [kN] | Torque [kNm] | Gen. Pwr [kW] | Bl. pitch [deg] |
|---|---|---|---|---|---|---|---|
| OP1 | 6.639 | 6.1 | 0.68 | 733 | 3990 | 2849 | 0 |
| OP2 | 11.263 | 10.4 | 0.97 | 1332 | 10431 | 9049 | 4.2 |
| OP3 | 6.982 | 6.2 | 1.01 | 712 | 10001 | 9440 | 12.2 |
| EWM | 10.176 | 4.1 | 0 | 218 | 0 | 0 | 0 |

## 8.4 Power spectrum analysis

The response spectrum provides a convenient and practical way to summarize the frequency content and their energy density in a given time history of platform response. A time history of a signal, for example, surge motion of the platform, can be considered as a superposition of large numbers of sinusoidal waves which may have difference in frequency, amplitude and phase.

A continuous time series, $y(t)-$can be transformed into frequency domain using Fourier transformation:

$$\tilde{y}(\omega) = \int_{-\infty}^{\infty} y(t)\, e^{-i\omega t}\, dt \tag{8.5}$$

Again, for a single frequency regular wave, energy content is proportional to the amplitude squared:

$$\mathbf{P}(\omega) \propto |\tilde{y}(\omega)|^2 \tag{8.6}$$

Frequency domain investigations are carried out to identify the frequency of most energetic wave component in the signal. Moreover, a check has been made to see if there is any resonance between platform response and excitations from wind and wave.

For spectral analysis, WAFO [30] (Wave Analysis for Fatigue and Oceanography) is used exclusively. It is a toolbox of Matlab routines for statistical analysis and simulation of random waves and random loads.

## 8.5 Response spectra

Response spectra are plotted for the platform responses and turbine responses. Platform responses include spectrum of surge, heave, pitch and yaw motions. In addition to that mooring line spectrum is also plotted. Similarly, turbine responses include spectrum of blade root out-plane bending moment and tower base bending moment.

### 8.5.1 Platform response spectra

Figure 8.8 presents the platform response spectra for OP3 environmental condition. It is our objective to investigate the frequency band under which most of the energy of each spectrum lies. Moreover, the influence of environment (wind and wave) is also examined.

At the beginning, wind and wave spectrum are plotted so that they can be used to compare

each response spectrum and help to identify the source of most energetic response. The peak frequency of wind and wave are approximately 0.1 and 0.6 ($2\pi/10.5 = 0.5983$) rad/s respectively.

Form Figure 8.8, it is clear that except heave spectrum, other spectra show their peak frequency more or less near to wind frequency range. Although surge (Figure 8.8(b)), pitch (Figure 8.8(d)) and mooring (Figure 8.8(f)) line tension spectra show peak near wave frequency range but the influence is negligible compared to wind. On the other hand, heave spectrum, (Figure 8.8(c)) shows strong correlation with wave spectrum.

### 8.5.2 Turbine response spectra

Turbine response spectra are plotted for environmental condition OP2 and EWM. OP2 is operation condition at rated wind speed and EWM describes extreme environmental condition with 50 yr recurrence period. It is believed that they are the representative condition and can create maximum turbine responses.

Turbine responses in terms of blade root out-plane BM and tower base BM are summarized in Table 8.5. It is found that in OP2 condition wave has no resonance. On the other hand, in EWM condition tower base BM is completely excited by wave frequency but blade root BM is excited by both wind (relatively larger) and wave.

**Table 8.5:** Turbine response for OP2 and EWM environment condition.

| Item | OP2 | EWM |
|---|---|---|
| Environment | $H_s$ = 2.5 m, $\omega_p$ = 0.616 rad/s, $U_w$ = 11.4 m/s | $H_s$ = 15.6 m, $\omega_p$ = 0.433 rad/s $U_w$ = 40 m/s |
| Blade root BM (out-plane) | Excited by wind and 1P freq. | Excited by wind and wave |
| Tower base BM | Excited by wind | Excited by wave |

## 8.6 Statistical response characteristics

In order to obtain statistical properties (mean, standard deviation) of platform and turbine responses, several time domain simulations are performed for each environmental condition described in Table 8.3. Next, platform responses are averaged to get the mean value of four (4) simulations.

### 8.6.1 Platform statistical response

Statistical response of the platform are presented in Figure 8.11 for (*a*) surge, (*b*) pitch and (*c*) mooring line tension. Standard deviations are plotted as error bar on top of mean values.

Platform response in surge and pitch show similar pattern with non-zero mean values. At rated wind speed, platform responses are characterized by large surge and pitch motions with high standard deviation. Maximum surge motion occurs at extreme wind condition, while pitch motion is highest at rated wind speed.

Mooring line tension follow identical pattern to surge motion of the floater. The tension is maximum at 40 m/s wind speed (EWM) when the platform experience highest horizontal offset from its mean position.

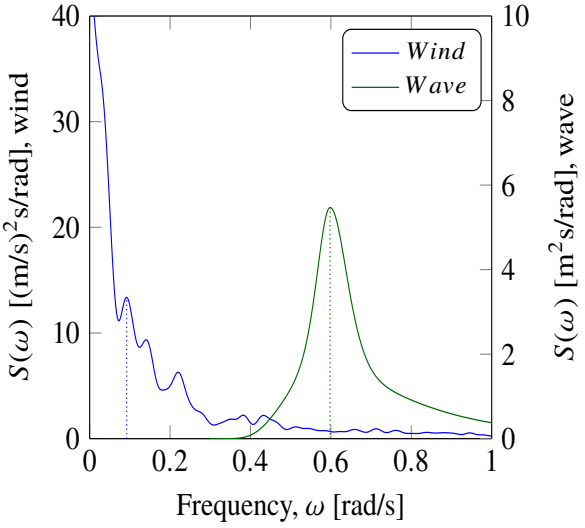


(a) Wind and wave spectra

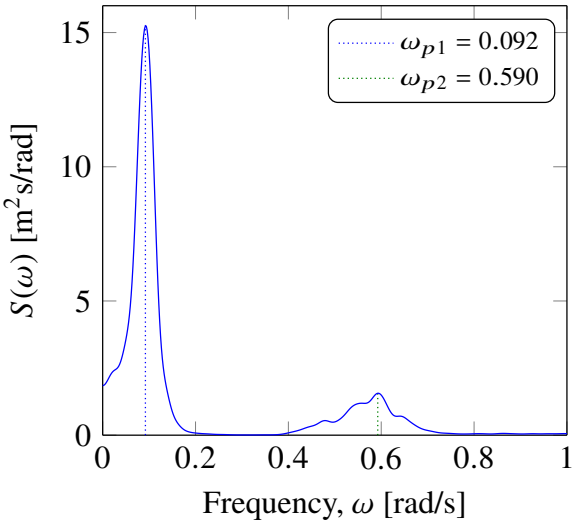


(b) Surge spectrum.

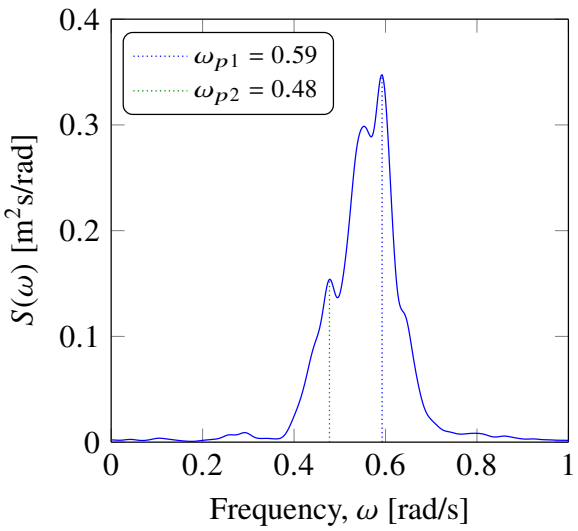


(c) Heave spectrum

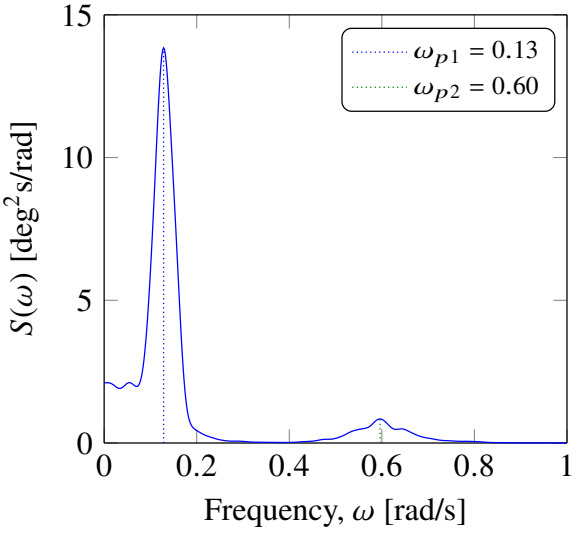


(d) Pitch spectrum

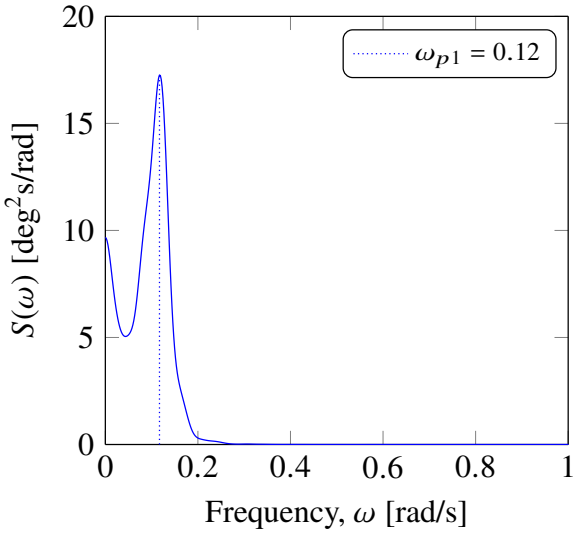


(e) Yaw spectrum

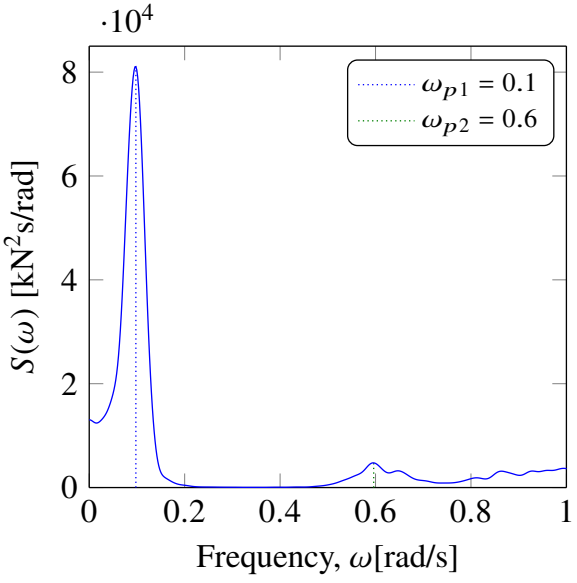


(f) Mooring line tension spectrum

**Figure 8.8:** Platform response (motion) spectra for NTM condition OP3.

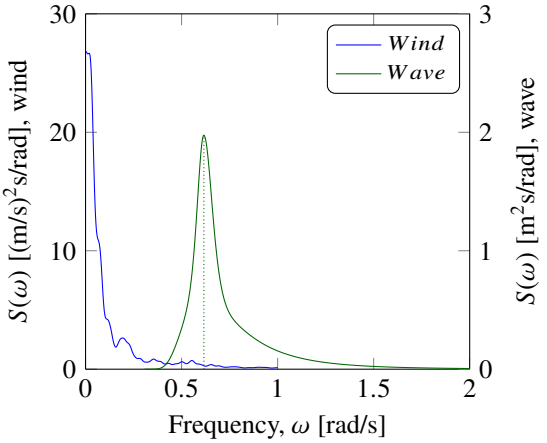


(a) Wind and wave spectra (OP2)

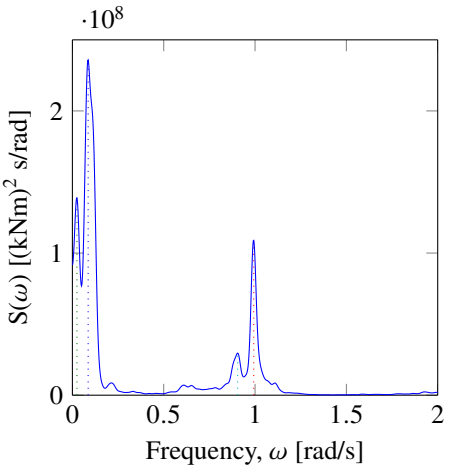


(b) Blade root out-plane BM

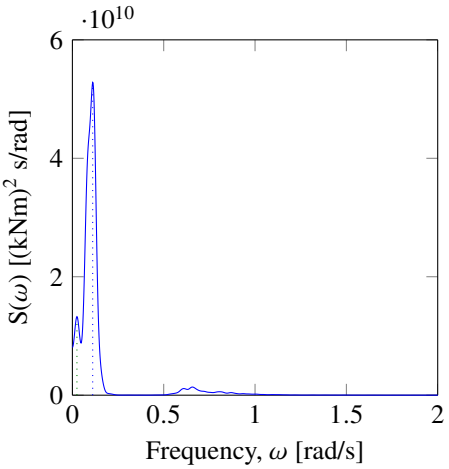


(c) Tower base BM

**Figure 8.9:** Turbine response spectra for OP2.

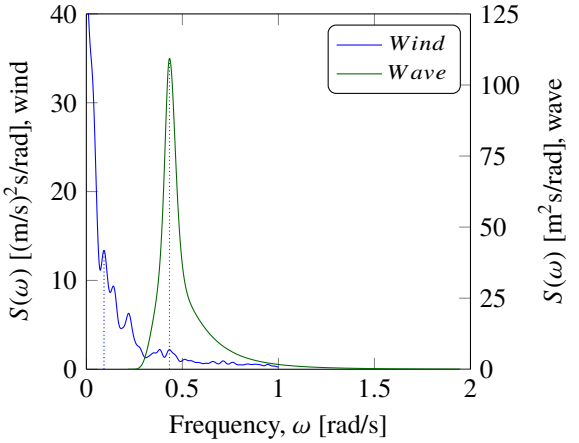


(a) Wind and wave spectra (EWM)

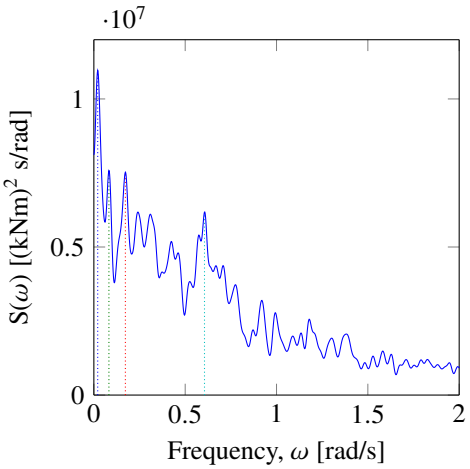


(b) Blade root outplace BM

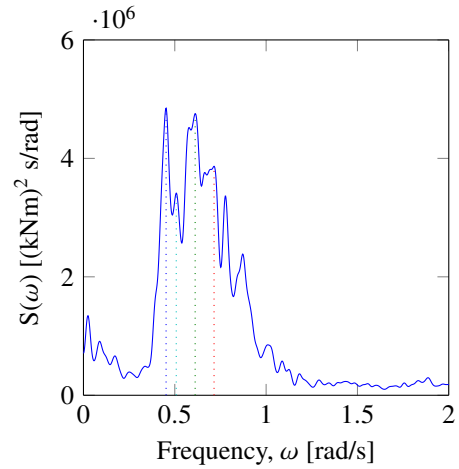


(c) Tower base BM

**Figure 8.10:** Turbine response spectra for EWM.

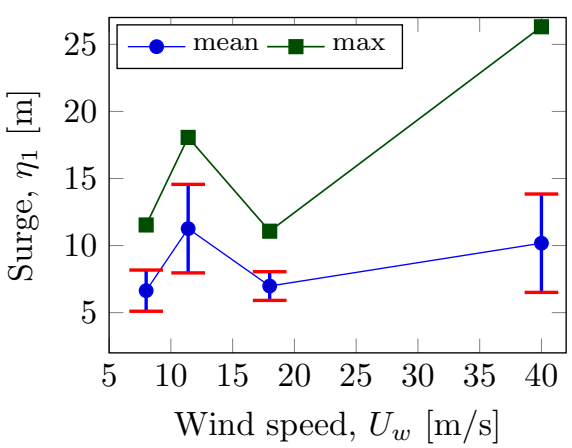


(a) Response in surge.

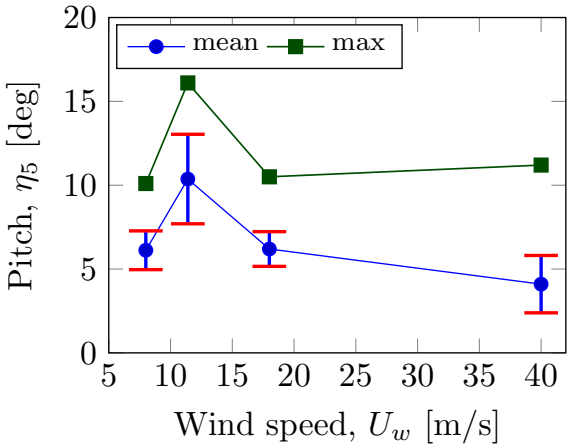


(b) Response in pitch.

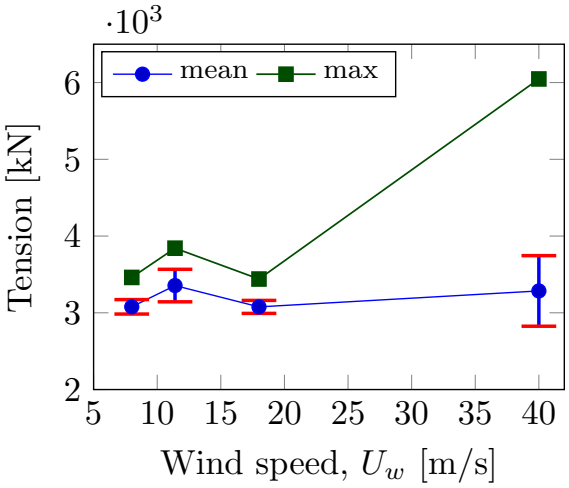


(c) Response of mooring lines.

**Figure 8.11:** Statistical properties of platform response.

As a conclusion, operational condition (OP2) with rated wind speed of 11.4 m/s is the most influential condition for pitch motion of the platform. On the other hand, EWM condition with 40 m/s wind speed is critical for surge motion and mooring line tension of the platform.

### 8.6.2 Turbine statistical response

Statistical properties of turbine responses are presented in Figure 8.12(a), blade root (out-plane) bending moment and Figure 8.12(b), tower base bending moment. Mean and maximum BM values at blade root shows similar pattern and have maximum at rated wind speed. For EWM (parked condition) with 40 m/s wind speed, BM values are lowest.

Mean and maximum tower base bending moments have peak value at rated wind speed. For parked condition, though the mean value is less than other conditions, but maximum tower bending moment are the highest.

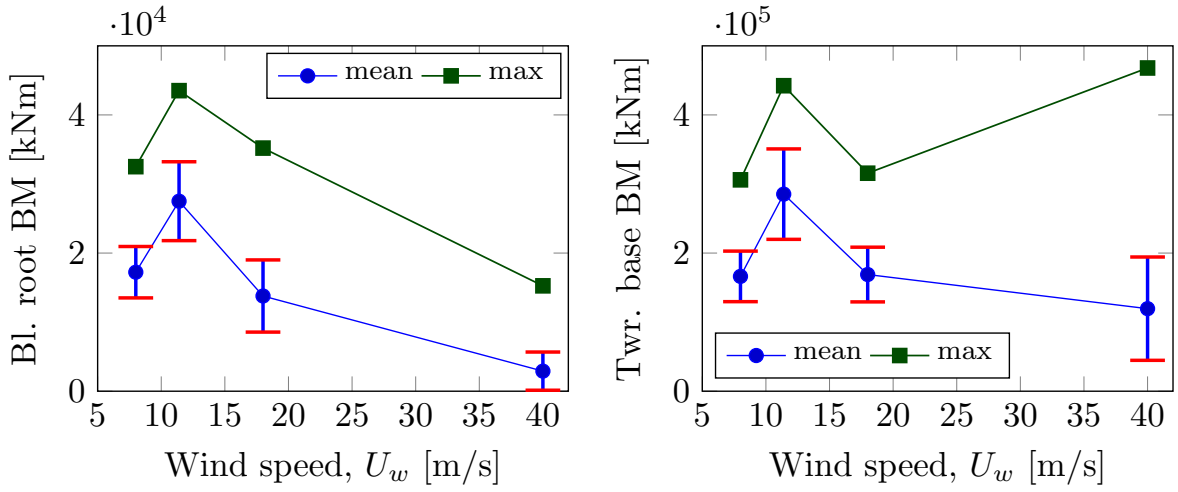


(a) Blade root BM

(b) Tower base BM.

**Figure 8.12:** Statistical properties of turbine response.

# Chapter 9

# Comparison of dynamic responses of Spar, Semi-submersible and TLP

SRA numerical models of the Spar, Semi-submersible and TLP platform are presented in Figure 9.1. A comparison of the design dimensions of three (3) concepts are also listed in Table 9.1. Spar is characterized by its highest draft (120 m) and designed water depth of 300 m while both the Semi-submersible and TLP platform are designed to operate in 200 m. lower than 40 m.

Spar has the highest accumulated mass of 13405 ton primarily achieved by high density ballast (concrete) which is almost double than the Semi-submersible and 1.5 times higher than TLP. Centre of mass (CM) location of Spar is 75 m below mean sea level indicates it's gravity stabilized characteristics. On the other hand, TLP has buoyancy ($\sim$ 85%) higher than it's weight which produces large tension in the tethers.

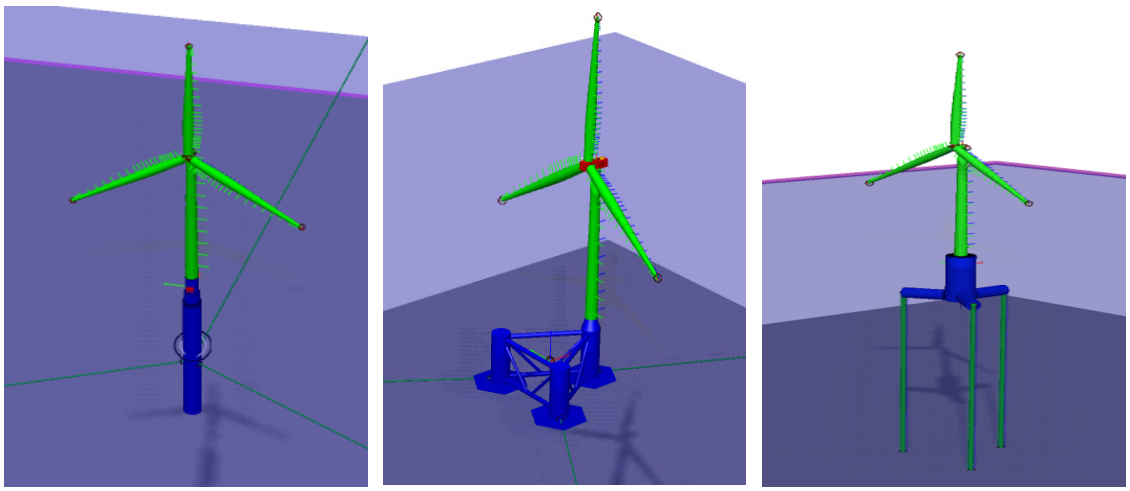

(a) Spar (b) Semi (c) TLP

**Figure 9.1:** Three (3) FOWT concepts: Spar, Semi-submersible and TLP.

Table 9.2 presents a comparison of the natural periods of rigid body motions of Spar, Semi and TLP. Spar has the largest natural period in surge and heave which is due to its large displacement

**Table 9.1:** Properties of the three floating platforms.

| Floater | Spar | Semi | TLP |
|---|---|---|---|
| Water depth [m] | 320 | 200 | 200 |
| Draft (operation) [m] | 120 | 19.2 | 35.3 |
| Column diameter [m] | 12 | 12.8 | 19.8 |
| Hull mass, including ballast and generator [t] | 13405 | 7520 | 9293 |
| CM location from SWL [m] | -74.5 | 4.9 | -9.8 |
| Displacement [$m^3$] | 13078 | 7337 | 17362 |
| COB from SWL [m] | -62.1 | -9.6 | -22.7 |

and lower stiffness than Semi and TLP. TLP has the highest eigenfrequency (lowest period) for heave and pitch motion because of its higher stiffness arises from the tension in tethers. But Spar exhibits smallest yaw period which is due to its small inertia in yaw motion.

**Table 9.2:** Natural periods of the three concepts obtained by decay test.

| Floater | Spar | Semi | TLP |
|---|---|---|---|
| Surge [s] | 103.3 | 65.9 | 45.2 |
| Heave [s] | 31.3 | 21.9 | 0.6 |
| Pitch [s] | 35.5 | 43.2 | 0.6 |
| Yaw [s] | 7.6 | 53.4 | 20.8 |

## 9.1 Comparison of platform response

Platform responses in terms of surge and pitch motion are plotted as a function of wind speed in Figure 9.2. Standard deviations are shown as error-bar on top of mean values to indicate the variation in the data.

### 9.1.1 Surge response

It is interesting to notice that the Spar and Semi show opposite response characteristics in surge and pitch motion. Spar is more sensitive to surge motion than pitch, while the opposite is true for the semi-submersible platform. High surge motion of Spar is due to it's low stiffness from mooring lines. Platforms (Spar and Semi) experiences highest surge motion at the rated wind speed with high standard deviation. Offset in surge for Spar is 1.5 times higher than the Semi-submersible. Response of TLP in surge compare to other platforms is considered negligible. At extreme wind speed (40 m/s), TLP shows a mean value of 2.7 m with a standard deviation 3.9 m.

### 9.1.2 Pitch response

Pitch response of the platform is considered more important than surge because it can change the angle between rotor plane and relative wind which is directly related to the power output from turbine. Platforms are designed to be operated for the value of pitch angle lower than $10^{\circ}$. At rated wind speed, Spar has a pitch angle of $6^{\circ}$ while the same for Semi-submersible is slightly above $10^{\circ}$ with a standard deviation of $2.7^{\circ}$. TLP is not affected from rotor thrust and environmental conditions with regard to pitch motion.

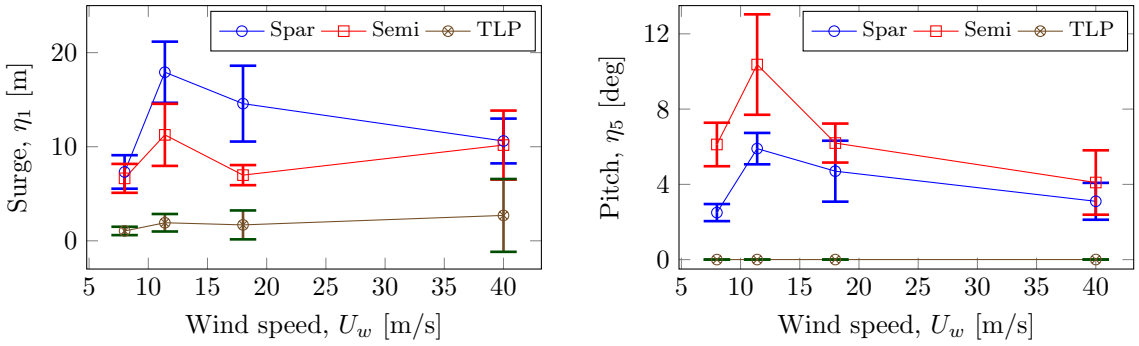


(a) Mean surge motion.

(b) Mean pitch motion.

**Figure 9.2:** Mean values of (*a*) surge and (*b*) pitch motions of the three HAWT concepts with error bar indicating the standard deviation.

## 9.2 Comparison of turbine response

Turbine responses, for example, blade root (out-plane) and tower base bending moments for the three concepts are compared using Figure 9.3 and Figure 9.4 respectively.

### 9.2.1 Blade root BM

From Figure 9.3, it is obvious that maximum values of blade root out-plane BM occurs for OP2 environmental condition which is characterized by the rated wind speed. Semi-submersible platform shows the highest blade root BM followed by Spar and TLP. Although, mean BM values for TLP is very low in comparison to Spar and Semi but large standard deviation (*sd*) indicates highly scattered data. For EWM condition, TLP shows highest blade root BM. EWM condition has a wind speed of 40 m/s and turbine blades are parked. As TLP has high stiffness in pitch than Spar and Semi, blade responses becomes stronger.

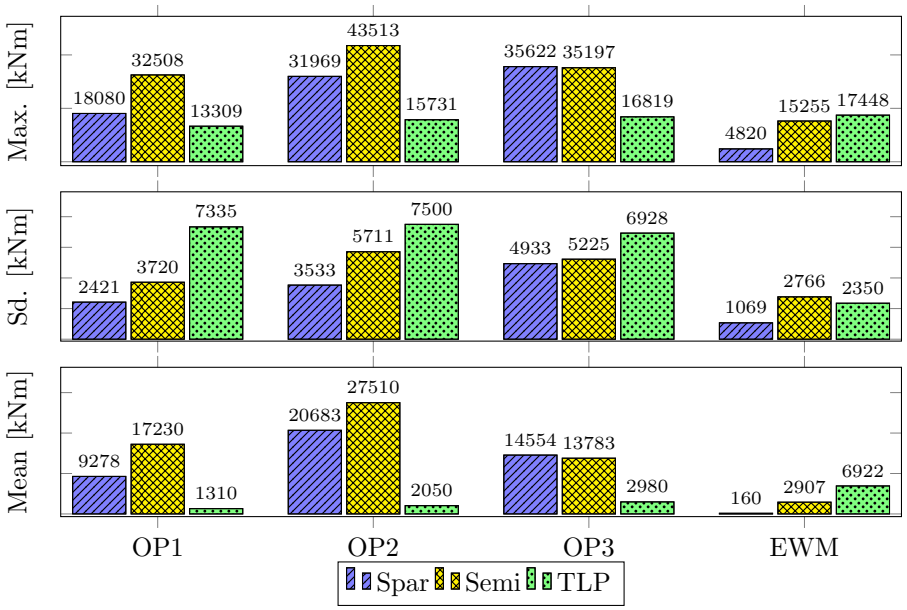


**Figure 9.3:** Comparison of blade root BM for the three concepts.

### 9.2.2 Tower base BM

Comparison of tower base BM of the three concepts are presented in Figure 9.4. Semi-submersible platform has the highest mean values of BM for all environmental conditions which is largest in OP2 environmental condition.

*sd* value of tower base BM of Spar shows an increasing pattern as we move from OP1 to EWM environmental condition with highest value in EWM environmental condition. Semi and TLP has ups and downs but have highest value for EWM condition.

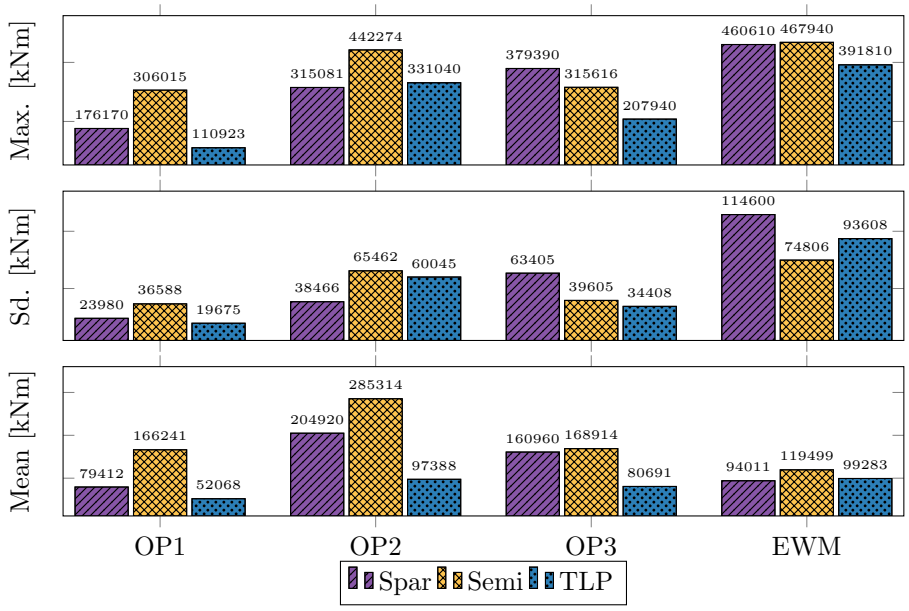


**Figure 9.4:** Comparison of tower base BM for the three concepts.

Although, semi-submersible platform has the highest tower base bending moment, $M_y$ = 467940 [kNm] for EWM condition, bending stress will have a value less than yield stress of the material.

Area moment of inertia of a pipe section can be written as:

$$I_y = \frac{\pi\left(D_o^4 - D_i^4\right)}{64} = \frac{\pi\left(7.85^4 - 7.77^4\right)}{64} = 7.5 \text{ m}^4$$

Thus, maximum bending stress (outer fibre) at tower base:

$$\sigma_b = \frac{M_y y}{I_y}$$
$$= \frac{\left(467940\text{kNm} \times \frac{7.85}{2}\right)}{7.5} = 245\ (< 250)\ \text{MPa}$$

Which is closer to the yield stress (250 MPa) of normal steel. Thus, it is advised to do a finite element calculation with refined mesh near tower base including the connection piece. Moreover, fatigue calculation shall be done in order to check the feasibility of higher strength steel.

# Chapter 10

# Conclusions and recommendations

This master thesis deals with the design, numerical modelling and analysis of a semi-submersible platform supporting the DTU 10MW RWT. The purpose of this study is to determine the principal dimensions of a floater by scaling NREL 5MW WindFloat and with initial design calculation. Later, initial dimensions are adjusted and verified using detail stability calculations, analysis of rigid body motions and finally by coupled time domain simulation for selected environmental conditions.

After careful investigation of platform and turbine responses, rotor performance, it can be concluded that the semi-submersible concept is capable of supporting the DTU 10MW or similar wind turbine identical to North sea environment. General conclusions from analysis are listed as follows:

## 10.1 Conclusions

1. During initial design, it is found that scaling always results with much higher dimensions. For example, scaled displacement of the floater is found 13125 ton but the final displacement obtained by detail stability calculation is 7520 ton. So it is advised to do a detail stability calculation with necessary stability requirements in combination with preliminary calculation of rigid body motions.

2. Natural period in heave is found to be critical for the design of the platform. Heave plates can shift the heave natural period away from wave frequency range. Although, circular heave plate is more effective than hexagonal type, preference is given to hexagonal type because they can be fabricated easily and thus become cheaper. Edge length of heave plate shall be around 1.5 times of column diameter.

3. Although, the mean pitch angle of the platform is slightly above the design value of $10^{\circ}$, it is possible solve the problem by two (2) ways. Firstly, designing an active ballast system similar to NREL 5MW WindFloat concept to minimize the pitch response and thus maximize power output. Secondly, raising the hydrostatic stiffness of the floater with higher values of column diameter or by increasing the distance between column centre. However, the later approach is not suggested because with increased column diameter, the platform will experience higher hydrodynamic loading. On the other hand, raised column spacing will increase bracing span which is not favourable from fatigue point of view.

With increased stiffness, the platform will be more stiffer and the period of rigid body motion will move towards wave frequency range.

4. operational condition (OP2) is the most important condition for the semi-submersible platform as large pitch motion occurs near rated wind speed which in turn affect the power production. On the other hand, at extreme wind condition (EWM), surge motion and mooring line tensions becomes higher and shows large variation.

5. Turbulent wind is able to excite platform responses in surge, pitch and yaw in addition to mooring line tension. Only heave response of the platform is dominated by wave frequency under operational conditions.

## 10.2 Recommendations

Due to limited scope and time, few topics have not studied or discussed in detail are recommended to broaden the understanding of the semi-submersible floating wind turbine.

1. The tower used in the coupled dynamic analysis is a modified version of the DTU 10MW RWT which is a land based turbine. It could be possible to redesign the tower and connection piece to be efficient in terms of weight and structural strength. Eigenvalue analysis of the tower can also be done to determine modified eigenfrequency of the tower.

2. Mooring weight shall be considered during initial design calculation which will result more realistic dimensions of the platform. At present condition, ballast is reduced to take the mooring weight into account which does not represent the case in reality.

3. It is possible to design an active ballast system which can reduce the pitch angle near rated wind speed as discussed earlier. Pump capacity, amount of ballast water to be transferred and the period of operation are of particular importance.

4. More load cases for additional environmental conditions shall be investigated to widen our understanding about the platform. Wind shear, wind-wave misalignment and few fault scenarios shall be studied.

5. Results of the coupled dynamic analysis can be cross checked using different dynamic simulation software like HAWC2 and if possible, a model test shall be sufficient.

6. Economic analysis on the cost of the platform can be done to determine the cost per kWh generation of electricity.

# Bibliography


[1] D. Roddier et al. 'A generic 5 MW WINDFLOAT for numerical tool validation & comparison against a generic spar'. In: *ASME 30th International Conference on Ocean, Offshore and Arctic Engineering, OMAE2011*. Rotterdam, Netherlands, June 2011.

[2] C Bak et al. 'Description of the DTU 10 MW reference wind turbine'. In: *DTU Wind Energy Report-I-0092* (2013).

[3] J Jonkman et al. 'Definition of a 5-MW Reference Wind Turbine for Off-shore System Development (National Renewable Energy Laboratory, CO)'. In: (2009).

[4] Marit Irene Kvittem. 'Modelling and response analysis for fatigue design of a semi-submersible wind turbine'. PhD thesis. Norwegian University of Science and Technology., 2014.

[5] Jason Mark Jonkman. *Dynamics modeling and loads analysis of an offshore floating wind turbine*. ProQuest, 2007.

[6] BJ Jonkman and JM Jonkman. 'Addendum to the user's guides for FAST, A2AD, and AeroDyn released March 2010-February 2013'. In: *National Renewable Energy Laboratory: Golden, Colorado* (2013).

[7] Patrick J Moriarty and A Craig Hansen. *AeroDyn theory manual*. Citeseer, 2005.

[8] JM Jonkman, A Robertson and GJ Hayman. 'HydroDyn user's guide and theory manual'. In: *National Renewable Energy Laboratory* (2014).

[9] Torben J Larsen and Anders Melchior Hansen. *How 2 HAWC2, the user's manual*. Tech. rep. Risø National Laboratory, 2007.

[10] Bonnie J Jonkman. *TurbSim user's guide: Version 1.50*. 2009.

[11] 'SIMO - Theory Manual Version 4.0 rev. 1'. In: *MT51 F93-0184, MARINTEK* (2012).

[12] IJ Fylling et al. 'Riflex theory manual'. In: *SINTEF report no. STF70 F* 95219 (1995), p. 53.

[13] Martin OL Hansen. *Aerodynamics of wind turbines*. Routledge, 2015.

[14] Tony Burton, ed. *Wind energy: handbook*. Chichester ; New York: J. Wiley, 2001.

[15] Erin Bachynski. *Lecture notes on TMR4505: Integrated Dynamic Analysis of Wind Turbines.* Department of Marine Technology, NTNU, 2015.

[16] Marilena Greco. *Lecture notes on TMR4215: Sea Loads*. Department of Marine Technology, NTNU, 2012.

[17] Line Roald et al. 'The effect of second-order hydrodynamics on floating offshore wind turbines'. In: *Energy Procedia* 35 (2013), pp. 253–264.

[18] T Duarte, AJNA Sarmento and Jason Jonkman. 'Effects of second-order hydrodynamic forces on floating offshore wind turbines'. In: *AIAA SciTech* (2014).

[19] Arvid Naess and Torgeir Moan. *Stochastic dynamics of marine structures*. Cambridge University Press, 2012.

[20] Dominique Roddier et al. 'WindFloat: A floating foundation for offshore wind turbines'. In: *Journal of Renewable and Sustainable Energy* 2.3 (2010), p. 033104.

[21] Odd Faltinsen. *Sea loads on ships and offshore structures*. Vol. 1. Cambridge university press, 1993.

[22] Qiang Wang. 'Design of a Steel Pontoon-type Semi-submersible Floater Supporting the DTU 10MW Reference Turbine'. M.Sc. thesis. Trondheim, Norway: Delft University of Technology, Norwegian University of Science and Technology, 13th June 2014. 172 pp.

[23] *DNVGL-OS-C301: Stability and watertight integrity*. Offshore Standard. DNV GL, 2015.

[24] I Prislin, RD Blevins and JE Halkyard. 'Viscous damping and added mass of solid square plates'. In: (1998).

[25] Det Norske Veritas. 'Wave analysis by diffraction and morison theory (Wadam)'. In: *SESAM Users Manual, Det Norske Veritas (DNV): Hvik, Norway* (1994).

[26] Jason M Jonkman and Marshall L Buhl Jr. 'FAST user's guide'. In: (2005).

[27] Erin Elizabeth Bachynski. 'Design and dynamic analysis of tension leg platform wind turbines'. PhD thesis. Norwegian University of Science and Technology, Mar. 2014.

[28] W Terence O'Brien and AS Francis. 'Cable movements under two-dimensional loads'. In: *Journal of the Structural Division* 90.3 (1964), pp. 89–124.

[29] International Electrotechnical Commission et al. 'IEC 61400-3'. In: *Wind Turbines-Part* 3 (2009).

[30] Pär Andreas Brodtkorb et al. 'WAFO-a Matlab toolbox for analysis of random waves and loads'. In: *The Tenth International Offshore and Polar Engineering Conference*. International Society of Offshore and Polar Engineers. 2000.

# Appendix A

# Stability Load Cases

06/13/16 10:49:26 Page 1
GHS 12.00 **10MW WINDFLOAT DTU RWT**

**Load Case - 1**
**(Operation Condition)**

WEIGHT and DISPLACEMENT STATUS
Baseline draft: 19.107 @ 34.64f, 19.170 @ 17.32a
Trim: Aft 0.063/51.960, Heel: zero

| Part | | | Weight(MT) | LCG | TCG | VCG | |
|---|---|---|---|---|---|---|---|
| FIXED WEIGHT | | | 2,840.30 | 14.130f | 0.000 | 52.435 | |
| | Load | SpGr | Weight(MT) | LCG | TCG | VCG | RefHt |
| BWT1.C | 0.190 | 1.025 | 783.77 | 34.639f | 0.000 | 3.040 | -6.122 |
| BWT2.S | 0.472 | 1.025 | 1,947.06 | 17.321a | 30.000s | 7.552 | -15.083 |
| BWT3.P | 0.472 | 1.025 | 1,947.06 | 17.321a | 30.000p | 7.552 | -15.083 |
| Total Tanks---------> | | | 4,677.89 | 8.615a | 0.000 | 6.796 | |
| Total Weight--------> | | | 7,518.19 | 0.022a | 0.000 | 24.038 | |
| | | | Displ(MT) | LCB | TCB | VCB | |
| HULL | | 1.025 | 7,518.18 | 0.038a | 0.000 | 9.574 | -19.149 |
| Righting Arms: | | | | 0.001f | 0.000 | | |

Distances in METERS.

HYDROSTATIC PROPERTIES
Trim: Aft 0.063/51.960, No Heel, VCG = 24.038

| LCF Draft | Displacement Weight(MT) | Buoyancy-Ctr. LCB | VCB | Weight/ cm | LCF | Moment/ cm trim | GML | GMT |
|---|---|---|---|---|---|---|---|---|
| 19.149 | 7,518.18 | 0.038a | 9.574 | 3.93 | 0.000 | 24.42 | 16.878 | 16.878 |

Distances in METERS. Specific Gravity = 1.025. Moment in m.-MT.
Trim is per 51.96m.
Draft is from Baseline. True Free Surface included.

Condition Graphic - Draft: 19.107 @ 34.640f, 19.170 @ 17.320a Heel: zero

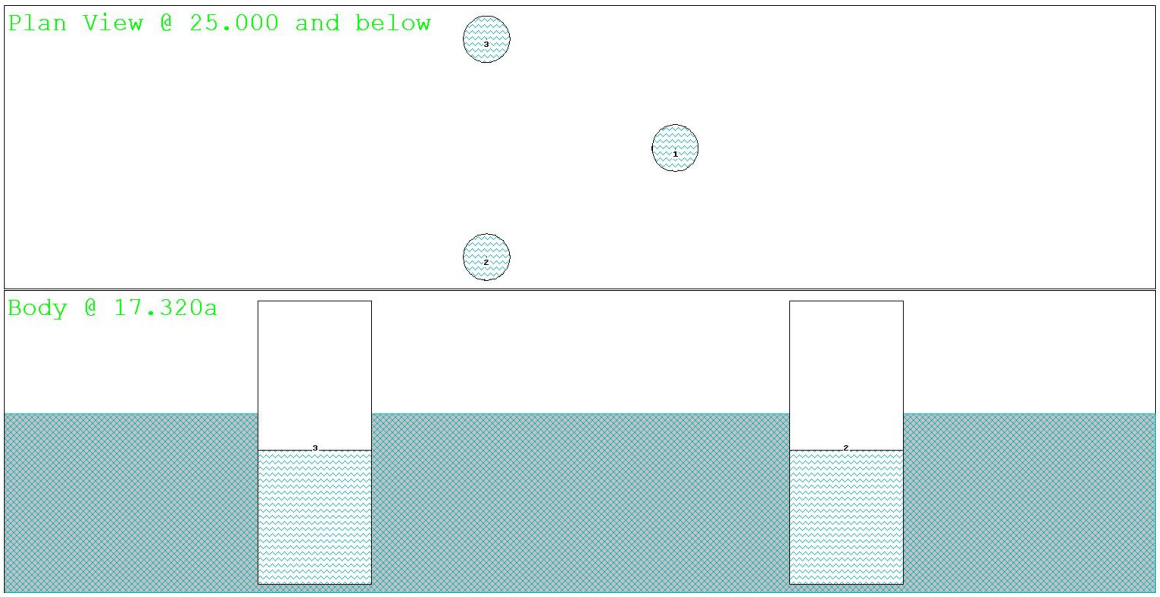


Tanks
1 BWT1.C..19% SEA WATER 2 BWT2.S..47% SEA WATER 3 BWT3.P..47% SEA WATER

HEELING MOMENT specification
Heeling Moment
19,659.79f m.-MT
Constant heeling moment forward----------> 19,659.79

RESIDUAL RIGHTING ARMS vs HEEL ANGLE
Fixed CG: LCG = 14.130f TCG = 0.000 VCG = 52.435

Inclination axis rotated Fwd 90.00 degrees

| Origin Depth | Degrees of Trim | Heel | Displacement Weight(MT) | Residual Arms in Trim | in Heel---> | Area | Flood Pt Height |
|---|---|---|---|---|---|---|---|
| 19.149 | 0.00 | 0.07a | 7,518.08 | 0.000 | -2.614 | 0.0000 | |
| 19.149 | 0.00 | 0.07f | 7,518.08 | 0.000 | -2.571 | -0.0065 | 13.715(1) |
| 19.149 | 0.00 | 0.93f | 7,519.07 | 0.000 | -2.319 | -0.0430 | 13.288(1) |
| 19.140 | 0.00 | 1.93f | 7,518.93 | 0.000 | -2.024 | -0.0809 | 12.789(1) |
| 19.124 | 0.00 | 2.93f | 7,518.17 | 0.000 | -1.728 | -0.1137 | 12.288(1) |
| 19.104 | 0.00 | 3.93f | 7,518.15 | 0.000 | -1.431 | -0.1412 | 11.782(1) |
| 19.078 | 0.00 | 4.93f | 7,518.14 | 0.000 | -1.132 | -0.1636 | 11.271(1) |
| 19.046 | 0.00 | 5.93f | 7,518.10 | 0.000 | -0.832 | -0.1808 | 10.757(1) |
| 19.009 | 0.00 | 6.93f | 7,518.06 | 0.000 | -0.529 | -0.1926 | 10.240(1) |
| 18.965 | 0.00 | 7.93f | 7,518.00 | 0.000 | -0.223 | -0.1992 | 9.720(1) |
| 18.931 | 0.00 | 8.65f | 7,518.29 | 0.000 | 0.000 | -0.2006 | 9.343(1) |
| 18.916 | 0.00 | 8.93f | 7,518.11 | 0.000 | 0.087 | -0.2004 | 16.274(2) |
| 18.861 | 0.00 | 9.93f | 7,517.82 | 0.000 | 0.400 | -0.1961 | 16.533(2) |
| 18.800 | 0.00 | 10.93f | 7,517.71 | 0.000 | 0.718 | -0.1864 | 16.787(2) |
| 18.734 | 0.00 | 11.93f | 7,517.57 | 0.000 | 1.040 | -0.1710 | 17.036(2) |
| 18.661 | 0.00 | 12.93f | 7,517.41 | 0.000 | 1.368 | -0.1500 | 17.280(2) |
| 18.583 | 0.00 | 13.93f | 7,517.21 | 0.000 | 1.702 | -0.1232 | 17.519(2) |
| 18.499 | 0.00 | 14.93f | 7,516.99 | 0.000 | 2.042 | -0.0905 | 17.753(2) |
| 18.132 | 0.00 | 19.93f | 7,517.86 | 0.000 | 3.565 | 0.1552 | 18.702(2) |
| 18.161 | 0.00 | 20.71f | 7,518.03 | 0.000 | 3.605 | 0.2038 | 18.738(2) |
| 18.644 | 0.00 | 23.87f | 7,518.17 | 0.000 | 2.979 | 0.3901 | 0.002(1) |
| 18.838 | 0.00 | 24.93f | 7,518.18 | 0.000 | 2.679 | 0.4423 | 18.297(2) |
| 19.668 | 0.00 | 29.93f | 7,518.19 | 0.000 | 1.239 | 0.6136 | 17.486(2) |
| 20.252 | 0.00 | 34.14f | 7,518.27 | 0.000 | 0.000 | 0.6593 | 16.699(2) |

Distances in METERS.----Specific Gravity = 1.025.----------Area in m.-Rad.

Note: The Center of Gravity shown above is for the Fixed Weight of 2840.30 MT. As the tank load centers shift with heel and trim, the total Center of Gravity varies. The righting arms shown above include the effect of the C.G. variation.

Note: The Residual Righting Arms shown above are in excess of the overturning arms derived from these moments (in m.-MT):
Stbd heeling moment = 19659.79

| Critical Points | | LCP | TCP | VCP | |
|---|---|---|---|---|---|
| (1) | Air vent opening in col1 | TIGHT 28.266f | 0.000 | 32.900 | BWT1.C |
| (2) | Air vent opening in col2 | FLOOD 17.321a | 23.625s | 32.900 | |

06/13/16 10:49:26 Page 3
GHS 12.00 **10MW WINDFLOAT DTU RWT**

| LIM | STABILITY CRITERION | Min/Max | | Attained |
|---|---|---|---|---|
| (1) | Absolute Angle at Equilibrium | < 10.00 | deg | 8.65 P |
| (2) | Abs Area Ratio from 0 deg to RAzero or Flood | > 1.300 | | 1.479 P |
| (3) | Angle from Equilibrium to Flood | > 0.00 | deg | LARGE |
| (4) | GM Upright | > 0.500 | m. | 16.880 P |

Relative angles measured from 0.069

06/13/16 10:49:26 Page 4
GHS 12.00 **10MW WINDFLOAT DTU RWT**

Inclination Axis rotated fwd -90.00 degrees

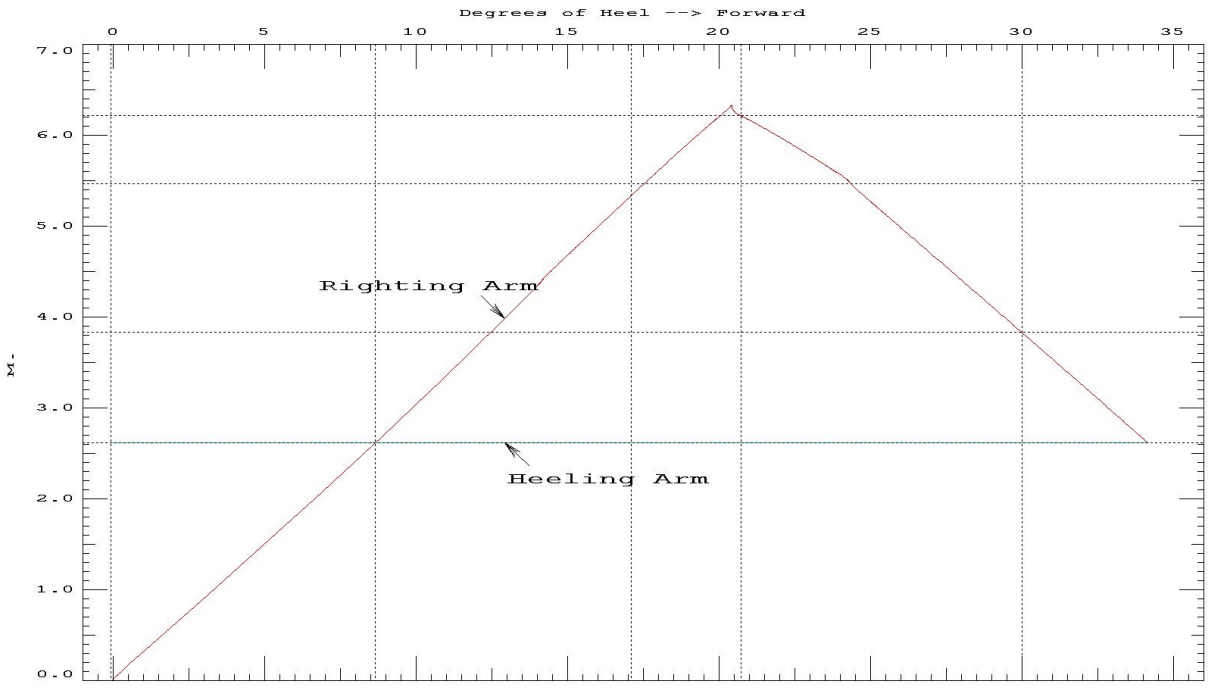


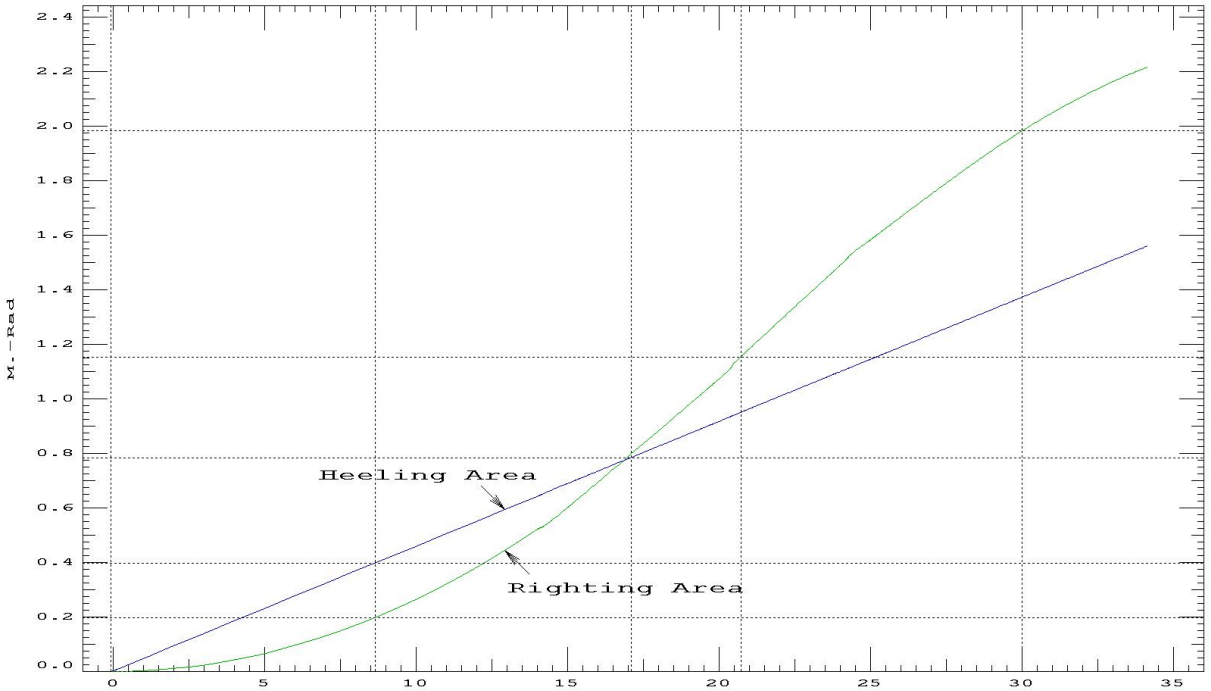

06/13/16 10:41:11 Page 1
GHS 12.00 **10MW WINDFLOAT DTU RWT**

**Load Case - 2**
**(Free Floating Condition)**

WEIGHT and DISPLACEMENT STATUS
Baseline draft: 13.132 @ 34.64f, 13.142 @ 17.32a
Trim: Aft 0.010/51.960, Heel: zero

| Part | | | Weight(MT) | LCG | TCG | VCG | |
|---|---|---|---|---|---|---|---|
| FIXED WEIGHT | | | 2,840.30 | 14.130f | 0.000 | 52.435 | |
| | Load | SpGr | Weight(MT) | LCG | TCG | VCG | RefHt |
| BWT2.S | 0.281 | 1.025 | 1,159.16 | 17.321a | 30.000s | 4.496 | -8.989 |
| BWT3.P | 0.281 | 1.025 | 1,159.16 | 17.321a | 30.000p | 4.496 | -8.989 |
| Total Tanks---------> | | | 2,318.32 | 17.321a | 0.000 | 4.496 | |
| Total Weight--------> | | | 5,158.62 | 0.004a | 0.000 | 30.891 | |
| | | | Displ(MT) | LCB | TCB | VCB | |
| HULL | | 1.025 | 5,158.62 | 0.009a | 0.000 | 6.569 | -13.139 |
| Righting Arms: | | | | 0.000 | 0.000 | | |

Distances in METERS.

HYDROSTATIC PROPERTIES
Trim: Aft 0.010/51.960, No Heel, VCG = 30.891

| LCF Draft | Displacement Weight(MT) | Buoyancy-Ctr. LCB | VCB | Weight/ cm | Moment/ LCF | cm trim | GML | GMT |
|---|---|---|---|---|---|---|---|---|
| 13.139 | 5,158.62 | 0.009a | 6.569 | 3.93 | 0.000 | 21.45 | 21.610 | 21.610 |

Distances in METERS. Specific Gravity = 1.025. Moment in m.-MT.
Trim is per 51.96m.
Draft is from Baseline. True Free Surface included.

Condition Graphic - Draft: 13.132 @ 34.640f, 13.142 @ 17.320a Heel: zero

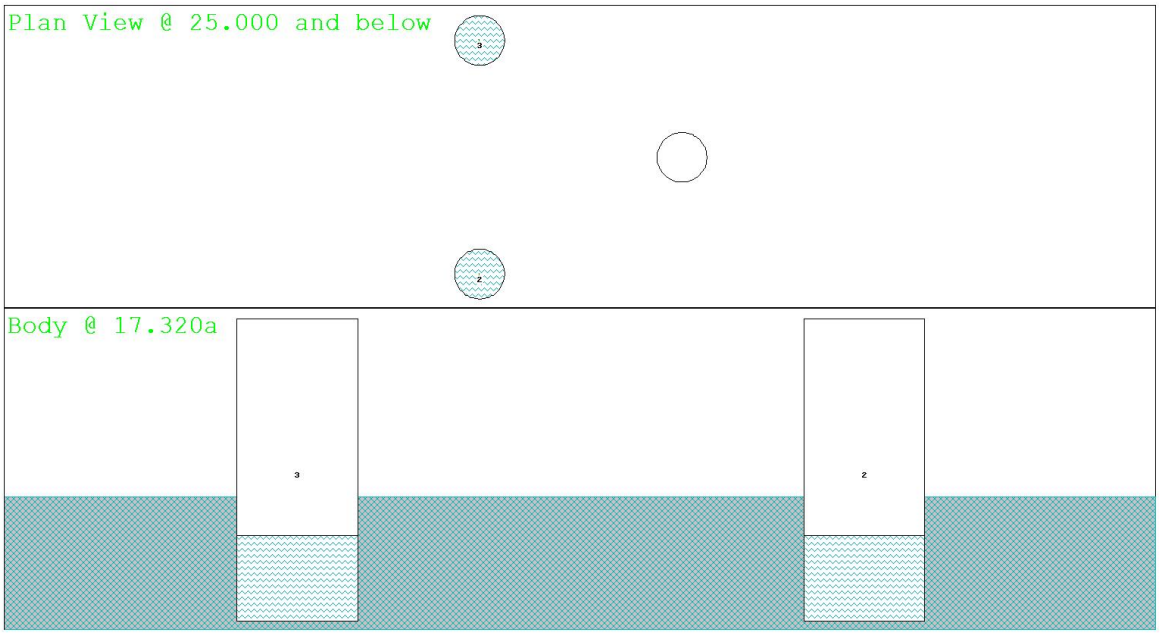


Tanks
2 BWT2.S..28% SEA WATER Intact 3 BWT3.P..28% SEA WATER Intact

HEELING MOMENT specification
Heeling Moment
4,800.08f m.-MT
Constant heeling moment forward----------> 4,800.08

RESIDUAL RIGHTING ARMS vs HEEL ANGLE
Fixed CG: LCG = 14.130f TCG = 0.000 VCG = 52.435

Inclination axis rotated Fwd 90.00 degrees

| Origin Depth | Degrees of Trim | Heel | Displacement Weight(MT) | Residual Arms in Trim | in Heel | Area | Flood Pt Height |
|---|---|---|---|---|---|---|---|
| 13.139 | 0.00 | 0.01a | 5,158.62 | 0.000 | -0.930 | 0.0000 | |
| 13.139 | 0.00 | 0.01f | 5,158.62 | 0.000 | -0.922 | -0.0004 | 19.756(1) |
| 13.139 | 0.00 | 0.99f | 5,159.39 | 0.000 | -0.553 | -0.0129 | 19.268(1) |
| 13.132 | 0.00 | 1.99f | 5,159.17 | 0.000 | -0.175 | -0.0193 | 18.767(1) |
| 13.127 | 0.00 | 2.45f | 5,158.62 | 0.000 | 0.000 | -0.0200 | 18.534(1) |
| 13.121 | 0.00 | 2.99f | 5,158.61 | 0.000 | 0.204 | -0.0191 | 20.637(2) |
| 13.107 | 0.00 | 3.99f | 5,158.60 | 0.000 | 0.585 | -0.0122 | 20.918(2) |
| 13.089 | 0.00 | 4.99f | 5,158.59 | 0.000 | 0.968 | 0.0014 | 21.193(2) |
| 13.067 | 0.00 | 5.99f | 5,158.56 | 0.000 | 1.355 | 0.0216 | 21.461(2) |
| 13.041 | 0.00 | 6.99f | 5,158.54 | 0.000 | 1.745 | 0.0487 | 21.722(2) |
| 13.011 | 0.00 | 7.99f | 5,158.50 | 0.000 | 2.140 | 0.0826 | 21.977(2) |
| 12.977 | 0.00 | 8.99f | 5,158.44 | 0.000 | 2.540 | 0.1234 | 22.225(2) |
| 12.939 | 0.00 | 9.99f | 5,158.39 | 0.000 | 2.946 | 0.1713 | 22.467(2) |
| 12.897 | 0.00 | 10.99f | 5,158.31 | 0.000 | 3.358 | 0.2263 | 22.701(2) |
| 12.851 | 0.00 | 11.99f | 5,158.22 | 0.000 | 3.778 | 0.2886 | 22.929(2) |
| 12.801 | 0.00 | 12.99f | 5,158.10 | 0.000 | 4.206 | 0.3583 | 23.150(2) |
| 12.748 | 0.00 | 13.99f | 5,157.97 | 0.000 | 4.643 | 0.4355 | 23.364(2) |
| 12.690 | 0.00 | 14.99f | 5,157.82 | 0.000 | 5.090 | 0.5204 | 23.570(2) |
| 12.347 | 0.00 | 19.99f | 5,158.62 | 0.000 | 7.499 | 1.0677 | 24.492(2) |
| 11.909 | 0.00 | 24.99f | 5,158.65 | 0.000 | 10.308 | 1.8418 | 25.228(2) |
| 11.828 | 0.00 | 28.99f | 5,158.55 | 0.000 | 11.711 | 2.6141 | 25.344(2) |
| 11.938 | 0.00 | 29.99f | 5,158.60 | 0.000 | 11.619 | 2.8184 | 25.215(2) |
| 12.462 | 0.00 | 32.64f | 5,158.59 | 0.000 | 10.550 | 3.3305 | -0.000(1) |
| 12.959 | 0.00 | 34.99f | 5,158.18 | 0.000 | 9.382 | 3.7397 | 23.927(2) |
| 13.918 | 0.00 | 39.99f | 5,158.61 | 0.000 | 6.825 | 4.4477 | 22.420(2) |
| 14.733 | 0.00 | 44.99f | 5,159.44 | 0.000 | 4.184 | 4.9286 | 20.781(2) |
| 15.387 | 0.00 | 49.99f | 5,158.31 | 0.000 | 1.486 | 5.1764 | 19.032(2) |
| 15.673 | 0.00 | 52.69f | 5,157.99 | 0.000 | 0.000 | 5.2115 | 18.045(2) |

Distances in METERS.----Specific Gravity = 1.025.----------Area in m.-Rad.

Note: The Center of Gravity shown above is for the Fixed Weight of 2840.30 MT. As the tank load centers shift with heel and trim, the total Center of Gravity varies. The righting arms shown above include the effect of the C.G. variation.

Note: The Residual Righting Arms shown above are in excess of the overturning arms derived from these moments (in m.-MT):
Stbd heeling moment = 4800.08

| Critical Points | | LCP | TCP | VCP | |
|---|---|---|---|---|---|
| (1) Air vent opening in col1 | TIGHT | 28.266f | 0.000 | 32.900 | BWT1.C |
| (2) Air vent opening in col2 | FLOOD | 17.321a | 23.625s | 32.900 | |

| LIM | STABILITY CRITERION | Min/Max | | Attained |
|---|---|---|---|---|
| (1) | Absolute Angle at Equilibrium | < 10.00 | deg | 2.45 P |
| (2) | Abs Area Ratio from 0 deg to RAzero or Flood | > 1.300 | | 7.089 P |
| (3) | Angle from Equilibrium to Flood | > 0.00 | deg | LARGE |
| (4) | GM Upright | > 0.500 | m. | 21.611 P |

Relative angles measured from 0.011

06/13/16 10:41:11 Page 4
GHS 12.00 **10MW WINDFLOAT DTU RWT**

Inclination Axis rotated fwd -90.00 degrees